

6-13-1985

# Geochemistry of Alteration and Mineralization of the Wind River Gold Prospect, Skamania County, Washington

Krista I. McGowan  
*Portland State University*

Follow this and additional works at: [https://pdxscholar.library.pdx.edu/open\\_access\\_etds](https://pdxscholar.library.pdx.edu/open_access_etds)



Part of the [Geochemistry Commons](#), and the [Geology Commons](#)

Let us know how access to this document benefits you.

---

## Recommended Citation


McGowan, Krista I., "Geochemistry of Alteration and Mineralization of the Wind River Gold Prospect, Skamania County, Washington" (1985). *Dissertations and Theses*. Paper 3586.  
<https://doi.org/10.15760/etd.5469>

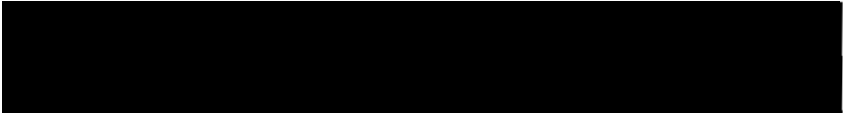
This Thesis is brought to you for free and open access. It has been accepted for inclusion in Dissertations and Theses by an authorized administrator of PDXScholar. Please contact us if we can make this document more accessible: [pdxscholar@pdx.edu](mailto:pdxscholar@pdx.edu).

AN ABSTRACT OF THE THESIS OF Krista I. McGowan for the Master of Sciences in Geology presented June 13, 1985.

Title: Geochemistry of Alteration and Mineralization of the Wind River Gold Prospect, Skamania County, Washington.

APPROVED BY MEMBERS OF THE THESIS COMMITTEE:

  
Michael L. Cummings, Chairman

  
Marvin H. Beeson

  
Ansel G. Johnson

The Wind River gold prospect is located in T5N, R7E of Skamania County, Washington, and is an epithermal gold-quartz vein system hosted in volcanic rocks of the Ohanapecosh Formation, a late Eocene to middle Oligocene unit of calcalkaline chemical composition. Andesitic pyroclastic rocks of the Ohanapecosh Formation are the host of

mineralization in the study area, and form the lowest of several stratigraphic subunits. These pyroclastic rocks are overlain by two sequences of lava flows which cap the ridges and are folded by an anticlinal warp over the length of Paradise Ridge, plunging gently to the southeast. Toward the west, the number of flows decreases and the proportion of intercalated pyroclastic rocks increases. Numerous dikes cut the pyroclastic rocks at the Wind River prospect. Geochemical data show these dikes to have been feeders for the overlying lava flows. Differing degrees of alteration of the dikes relative to the most intensely altered pyroclastic rocks which they cut indicates a complex history of overlapping hydrothermal and volcanic activity at the prospect.

Three associations of hydrothermal alteration have been recognized in the study area and represent expression of the hydrothermal system at differing lateral and vertical distances from the center of activity. The lava flow sequences overlying the pyroclastic rocks acted as a limited permeability barrier on the system, and hydrothermal activity was controlled mainly by structures.

The main system alteration, Type 3, is found at the Wind River prospect, and is controlled by the northeast-trending No. 5 structure. The alteration is zoned and grades from a chlorite-smectite zone as the least altered to a smectite zone with decreasing chlorite and increasing illite toward a more intensely altered zone of calcite-Fe-carbonate-illite-kaolinite-quartz. The inner zone is of illite-kaolinite-quartz, and includes the No. 5 structure, which consists of discontinuous stringers of fine-grained, sulfide-rich quartz in a clay matrix.

Geochemical anomalies of Au, Ag, As, Sb, W, and Hg are associated with the No. 5 structure, but the highest concentrations of Au, Ag, and Sb are found in the large, structurally-controlled quartz veins which cut the alteration zones and which were formed late in the history of the system.

Type 2 alteration is found at higher elevations than the main system and affects lavas and tuffs along the crest of Paradise Ridge to the west and northwest of the prospect. This alteration was produced by boiling and/or fluid mixing in permeable horizons in the upper part of the system. Kaolinite, illite, and poorly crystalline or amorphous clays are common alteration minerals in all rock types. Tuffs are more pervasively altered than lava flows, and silicification is most prevalent in tuffs. Geochemical anomalies of both As and Sb are found in these zones.

Restricted "leaks" from the system produced Type 1 "rootless zone" alteration peripheral to the main system. These zones are characterized by localized, quartz-cemented breccias which may contain calcite, and which lack obvious structural controls. Alteration of wallrock and breccia clasts is weak to moderate. Geochemical anomalies of Sb were detected in these zones.

Any possible association of the Wind River prospect with a porphyry copper type system at depth cannot be proven with currently available data. Minimum depths of formation of 300 to 600 m and fluid temperatures of 220<sup>o</sup> to 259<sup>o</sup> C are too shallow and too low, respectively, to fit accepted models of porphyry copper system metallogenesis in the Cascade Range of Washington and Oregon. The Wind

River prospect appears to be related to an episode of metallogenesis different from, and later than, that responsible for the porphyry copper systems in the Cascades.

GEOCHEMISTRY OF ALTERATION AND MINERALIZATION OF THE WIND RIVER  
GOLD PROSPECT, SKAMANIA COUNTY, WASHINGTON

by

KRISTA I. McGOWAN

A thesis submitted in partial fulfillment of the  
requirements for the degree of

MASTER OF SCIENCE  
in  
GEOLOGY

Portland State University

1985

TO THE OFFICE OF GRADUATE STUDIES AND RESEARCH:

The members of the Committee approve the thesis of Krista I. McGowan presented June 13, 1985.



Michael L. Cummings, Chairman



Marvin H. Beeson



Ansel G. Johnson

APPROVED:



Paul E. Hammond, Head, Department of Geology



James F. Heath, Dean of Graduate Studies and Research



## ACKNOWLEDGMENTS

I would like to thank the Washington Department of Natural Resources Division of Geology and Earth Resources and Mr. Milton Mitchek of the Wind River Mining Co. for partial funding of field studies for this project, and the Wind River Mining Co. and subsequently, Youngquist Mining Co. for access to the property.

Thanks are due especially to M. Mestrovich for field help, also to R. Swanson, J. Dernbach, J. Bull for surveying assistance. Special thanks to K. Wilson and to B. Lill for helping with lab work when I needed to be in two places at once. C. Burke and D. E. Pierson of the Portland State University Geology Department provided logistical support on numerous occasions.

Valuable discussions have been had with M. Beeson, M. Cummings, P. Hammond, R. Miller, B. Phillips, R. VanAtta. Finally, I would like to thank the members of my thesis committee, M. Beeson, M. Cummings, A. Johnson, for reviewing drafts of the thesis.



## TABLE OF CONTENTS

	PAGE
ACKNOWLEDGMENTS . . . . .	iii
LIST OF FIGURES . . . . .	vii
LIST OF TABLES . . . . .	xi
LIST OF PLATES . . . . .	xi
INTRODUCTION . . . . .	1
Purpose and scope . . . . .	4
Methods . . . . .	4
Location and access . . . . .	5
Relief and topography . . . . .	5
Previous work . . . . .	6
Mining history . . . . .	8
REGIONAL GEOLOGY . . . . .	9
Introduction . . . . .	9
Stratigraphy . . . . .	10
Structure . . . . .	13
Volcanic and tectonic history . . . . .	16
Economic Geology-General . . . . .	16
Economic Geology-St. Helens and Washougal	

Mining Districts . . . . . 21

WIND RIVER PROSPECT AREA . . . . . 25

    Introduction . . . . . 25

    Stratigraphy . . . . . 25

    Intrusions . . . . . 31

    Structure . . . . . 36

HYDROTHERMAL ALTERATION . . . . . 38

    Introduction . . . . . 38

    Hydrothermal alteration at the Wind River  
    Prospect . . . . . 40

    Veins . . . . . 47

    Fluid inclusions . . . . . 49

GEOCHEMISTRY . . . . . 52

    Introduction . . . . . 52

    Andesites . . . . . 52

    Dikes . . . . . 56

    Lavas and dikes . . . . . 67

    Types 1 and 2 alteration . . . . . 67

    Tuffs . . . . . 67

    No. 5 structure . . . . . 71

    No. 2 vein . . . . . 71

DISCUSSION AND CONCLUSIONS . . . . . 85

SUMMARY . . . . . 114

REFERENCES . . . . . 118

APPENDIX . . . . . 125

    Sample preparation . . . . . 125

Chondrite values used for normalization of rare earth elements . . . . .	127
Samples in which Ag, Hg, and W were detected . . . . .	128
INAA data . . . . .	129

## LIST OF FIGURES

FIGURE	PAGE
1. General geology of the Cascade Range in Washington and Oregon and location of the study area . . . . .	2
2. Stratigraphic relations in the southern Washington Cascades . . . . .	11
3. Regional structural features of the Washington Cascades . . . . .	14
4. Summary of volcanic and tectonic events in the Pacific Northwest from 55 to 17 Ma . . . . .	17
5. Classification of Cascade porphyry systems . . . . .	19
6. Schematic diagram of a Cascade linear porphyry copper intrusion . . . . .	20
7. Location of the St. Helens and Washougal mining districts and distribution of metal deposits in these districts . . . . .	22
8. Generalized stratigraphy of the study area . . . . .	26
9. Laterally extensive subdivisions of the Ohanapecosh Formation in the study area . . . . .	28
10. Other subdivisions of the Ohanapecosh Formation . . . . .	29

11.	Distribution of tuff units T <sub>1</sub> to T <sub>4</sub> in the vicinity of the Wind River prospect . . . . .	32
12.	Description of tuff units T <sub>1</sub> to T <sub>4</sub> . . . . .	34
13.	Alteration mineralogies and textures noted in lithologic units at differing intensities . . . . .	42
14.	Fluid inclusion data . . . . .	50
15.	Depth vs. boiling curves . . . . .	51
16.	Th vs. Hf for A <sub>1</sub> and A <sub>2</sub> andesites . . . . .	54
17.	Co vs. Hf and Co vs. Ta for A <sub>1</sub> and A <sub>2</sub> andesites . . . . .	55
18.	Chondrite-normalized REE plots for A <sub>1</sub> and A <sub>2</sub> andesites . . . . .	57
19.	Th vs. Hf and Th vs. Ta for D <sub>1</sub> , D <sub>2</sub> , and D <sub>3</sub> dikes . . . . .	60
20.	Co vs. Th and Co vs. Hf for D <sub>1</sub> , D <sub>2</sub> , and D <sub>3</sub> dikes . . . . .	62
21.	Co vs. Fe <sub>2</sub> O <sub>3</sub> and Sc vs. Fe <sub>2</sub> O <sub>3</sub> for D <sub>1</sub> dikes . . . . .	63
22.	Chondrite-normalized REE plot for D <sub>3</sub> dikes and for weakly, moderately, and strongly altered D <sub>2</sub> dike samples . . . . .	64
23.	Chondrite-normalized REE plot for weakly and moderately altered D <sub>1</sub> dikes . . . . .	65
24.	Chondrite-normalized REE plot for strongly altered D <sub>1</sub> dikes and range of REE values for D <sub>1</sub> dikes regardless of alteration . . . . .	66
25.	La/Sm vs. Th for A <sub>1</sub> and A <sub>2</sub> lavas and D <sub>1</sub> , D <sub>2</sub> , and D <sub>3</sub> dikes . . . . .	68
26.	Chondrite-normalized REE plot for altered T <sub>3</sub> and T <sub>4</sub> tuffs . . . . .	69

27. Chondrite-normalized REE plot for altered T<sub>4</sub> tuffs from the top switchback of the exploratory roadcut . . . . . 70
28. Chondrite-normalized REE plot for samples from the No. 5 structure . . . . . 72
29. Sketch of the No. 2 vein and wallrock zones in the adit at station C . . . . . 73
30. Chondrite-normalized REE plot for samples from the footwall of the No. 2 vein in the adit at station C . . . . . 77
31. Chondrite-normalized REE plot for samples from the hanging wall of the No. 2 vein in the adit at station C . . . . . 78
32. Sketch of the No. 2 vein and wallrock zones in the adit past station G . . . . . 80
33. Chondrite-normalized REE plot for samples from the footwall of the No. 2 vein in the adit past station G . . . . . 81
34. Chondrite-normalized REE plot for samples from the hanging wall of the No. 2 vein in the adit past station G . . . . . 82
35. Sketch of the Nos. 2 and 2A veins and wallrock zones on the exploratory roadcut . . . . . 83
36. Comparison of REE patterns for A<sub>1</sub> andesites and D<sub>1</sub> dikes, and for A<sub>2</sub> andesites and D<sub>3</sub> dikes . . . . . 90
37. The stability of Ca-Al silicates in equilibrium with

chalcedony and calcite as a function of CO <sub>2</sub> fugacity and temperature . . . . .	98
38. Schematic cross-section of a geothermal system of the Braodlands type . . . . .	99
39. Summary of models for epithermal precious metal deposits . . . . .	109
40. Cross-section of fluid flow patterns and lateral alteration zoning in the stacked-cell convection model of open-vein deposition . . . . .	110
41. Development of the Wind River hydrothermal system through time . . . . .	112

LIST OF TABLES

TABLE	PAGE
I. Trace element values for A <sub>1</sub> and A <sub>2</sub> andesites . . . . .	53
II. Trace element values for D <sub>2</sub> and D <sub>3</sub> dikes . . . . .	58
III. Trace element values for D <sub>1</sub> dikes . . . . .	59
IV. Trace element values for samples from the adit . . . . .	74

LIST OF PLATES

PLATE

1. Regional geology of the Wind River gold prospect
2. Map of the exploratory roadcut at the Wind River prospect at a scale of 1:1200
3. Map of the Wind River prospect adit at a scale of 1:120



## INTRODUCTION

The Cascade Range in the Wind River area of southern Washington is composed of extensive deposits of Tertiary lavas and pyroclastic rocks of calcalkaline chemical composition (Wise, 1961, 1970). These rocks have been intruded by a variety of gabbroic to dioritic dikes, sills, and plugs. In addition, the area is located among three large, andesitic Quaternary stratovolcanoes, Mt. Adams, Mt. St. Helens, and Mt. Hood (Fig. 1).

The thick, pre-Columbia River Basalt section in the Wind River area is divided into the Ohanapecosh, Stevens Ridge, and Eagle Creek Formations. The Wind River prospect is hosted in rocks of the Ohanapecosh Formation, a middle Eocene to late Oligocene sequence of interstratified andesitic and basaltic lava flows, pyroclastic rocks, and volcanoclastic rocks. Lava flows are most abundant and form resistant outcrops in that part of the Wind River area in which the prospect is located (Wise, 1970).

Mineralization in the southern Cascade Range of Washington is considered to be of the porphyry copper type (Grant, 1969, 1982; Moen, 1977). Deposits located in the nearby St. Helens and Washougal districts of southern Washington are porphyry copper type systems and consist of base metal sulfides hosted in quartz veins associated with

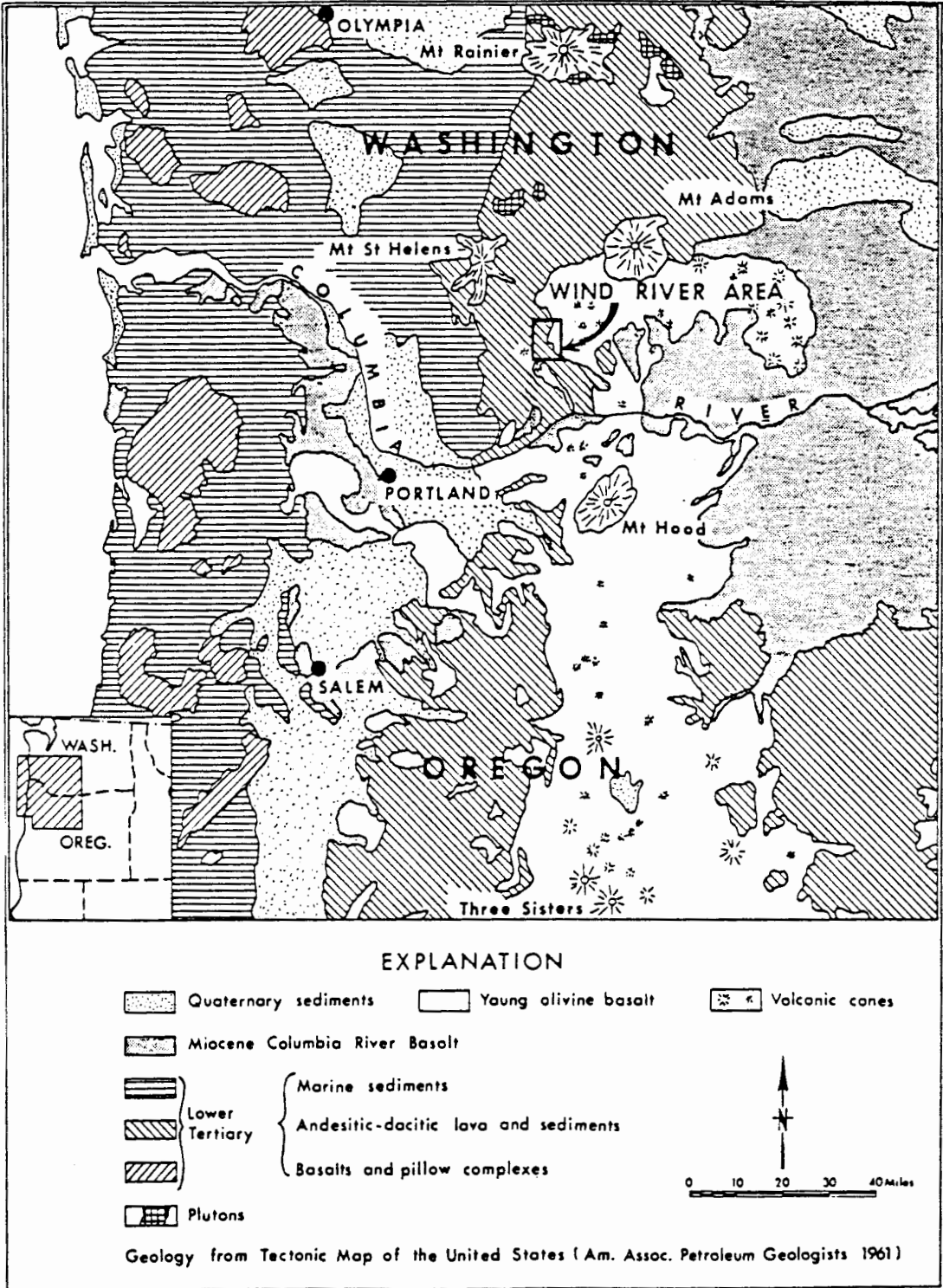


Figure 1. General geology of the Cascade Range in Washington and Oregon and location of the study area (modified from Wise, 1970).

high-level intrusions of granodioritic to quartz dioritic composition (Moen, 1977; Grant, 1969, 1982). Small amounts of gold and silver occur associated with base metal deposits in both districts.

Alteration at porphyry copper deposits of the southwestern United States was described in the classic works of Lowell and Guilbert (1970) and Rose (1970) as having a core of potassic alteration centered on a porphyritic intrusion, surrounded by a zone of sericitic alteration, and grading outward to a propylitic alteration zone. Alteration associated with Cascade porphyry deposits exhibits similar patterns (Brooks and Ramp, 1968; Callaghan and Buddington, 1938; Grant, 1969, 1982), but due to strong structural control, many of these systems are elongate along major structures ("linear porphyry copper deposits"), and zoning of alteration shows greater vertical than lateral extent (Grant, 1969, 1982).

The Wind River gold prospect is an epithermal gold-quartz vein system hosted in andesitic pyroclastic rocks of the Ohanapecosh Formation in Skamania County, Washington. It differs from other mineralization in the Cascade Range in that it is a gold-quartz vein system with little or no associated base metal mineralization, and does not fit with a porphyry-related model of metallogenesis.

Although the amount of ore produced from the Wind River prospect has been relatively minor, the deposit has produced the most gold of the southwestern Washington districts. The prospect is developed by approximately 146 m of adit, and vertical exposure of 270 m is available along an exploratory roadcut zigzagging up the hill above the development adit (Plate 2).

## PURPOSE AND SCOPE

The Wind River prospect is anomalous in terms of accepted models of metallogenesis in the Cascades. The purpose of the study is to define the alteration and mineralization history of the deposit in order to compare the Wind River prospect to systems more typical of the Cascades, and to develop models that may be used in further exploration for similar deposits in the Cascade Range. Specific goals of the study are to: 1) define the alteration mineralogy, 2) determine the zoning patterns in alteration mineralogy and selected metal concentrations in the system, 3) determine the relations among host structures and veins, 4) define in a preliminary manner the composition of ore solutions and temperatures of formation, and, 5) define the volcanic stratigraphy in the vicinity of the prospect.

The scope of the study is to determine relations among structure, alteration, and mineralization at the prospect. Alteration zones away from the prospect were noted in reconnaissance. The examination of stratigraphy and structures within the study area was related to controls on distribution of mineralization rather than correlation to regional patterns.

## METHODS

Field work was conducted during the summers of 1983 and 1984. Reconnaissance mapping was done during July-September, 1983. Mapping of the prospect and vicinity was done during June-August 1984. Mapping control points along the exploratory roadcut on the property were established by a transit survey; subsequent mapping of the roadcut and

prospect adit were done by alidade and plane table. Mapping of the adit on a scale of 1:120 (1"=10') and of the exploratory roadcut at a scale of 1:1200 (1"=100') was undertaken to define alteration patterns and identify possible variations in the hydrothermal system.

Geologic mapping away from the prospect was to establish possible structural controls on alteration and mineralization, possible relations of mineralization to intrusions, and to relate these to the tectonic setting of the region.

Laboratory analysis included examination of selected samples by: 1) transmitted light microscopy, 2) x-ray diffraction study of clay minerals, 3) fluid inclusion study of quartz vein and quartz-cemented breccia samples, and 4) trace element analysis by instrumental neutron activation analysis (INAA).

#### LOCATION AND ACCESS

The study area is located in T5N, R7E in Skamania County, Washington, and consists of approximately 34 square kilometers. Access from Washington state highway 14 on the north side of the Columbia River is by state route 8C (Wind River Highway), which intersects highway 14 east of the town of Stevenson and runs northwest to Government Mineral Springs. Two paved Forest Service roads, USFS 30 and USFS 64, go through the study area. A number of logging roads and hiking trails provide access to more remote parts of the area.

#### RELIEF AND TOPOGRAPHY

The study area is rugged and well-forested. Elevations range from approximately 335 to 490 m along the Wind River to 1220 m at the top of

Termination Point, approximately 1.4 km north of the study area. Local relief is seldom greater than 610 m.

The Wind River valley in the study area is a wide, U-shaped valley indicative of recent glaciation. North and east of the study area, swamps, lakes, and diverted streams are the result of recent volcanism. Streams in the area are aligned along three dominant trends: N40° to 50° W, N to N20° E, and approximately east-west. At least one change of direction from one of the dominant trends to another somewhere along their lengths is common.

Since the area is well-forested, access to outcrop is mainly provided by road cuts, logging roads, and along stream channels. Some exposures are also found on the steeper portions of ridge slopes, but on the whole, outcrop is sparse.

#### PREVIOUS WORK

The earliest work in the Wind River area was by Williams (1916) and Chaney (1918) who named the main stratigraphic units exposed in the south wall of the Columbia River Gorge south of the study area. They defined the Eagle Creek Formation to include all sedimentary rocks and intercalated lavas underlying the Columbia River Basalt. Allen (1932) did reconnaissance mapping north and south of the Columbia River Gorge in an area which extended 13-15 km on either side and grouped all rocks older than the Columbia River Basalt into the Warrendale Formation (Eagle Creek Formation has chronologic precedence). These rocks have also been called the Skamania series (Felts, 1939a,b; Trimble, 1963). Wise (1961,1970) indicated that A. C. Waters reconnoitered the area

north of the Columbia River in 1955-1956, and recognized a major unconformity within the Eagle Creek Formation. Waters observed that two periods of folding had deformed the pre-Pliocene rocks, and that the Quaternary olivine basalt in the Wind River valley came from a vent on Trout Creek Hill, and had once dammed the Columbia River. In the Washougal mining district of southwestern Washington, the Skamania series rocks of Felts (1939a) and Trimble (1963) have been informally divided into the Skamania Formation and the underlying East Fork Formation (Schreiner, 1979). Shepard (1979) has correlated the East Fork Formation with the Ohanapecosh Formation of Fiske and others (1963) and Wise (1970).

Wise (1961) mapped the Wind River 15' quadrangle, and parts of the Lookout Mountain, Willard, Bonneville Dam, and Hood River 15' quadrangles as part of a doctoral dissertation. He divided the pre-Columbia River Basalt section into the Weigle and Eagle Creek Formations. The informally named Weigle Formation was later correlated (Wise, 1970) with the Ohanapecosh Formation of Fiske and others (1963). More recently a third unit, the Stevens Ridge Formation has been described in the area (Hammond, 1974, 1980; Hammond and others, 1977). The Stevens Ridge Formation comprises a widespread stratigraphic marker in the southern Cascade Range of Washington.

Economic geology of the Cascade Range in southern Washington has been studied by Grant (1969, 1982). Similar studies in the Cascade Range of Oregon have been done by Callaghan and Buddington (1938) and Brooks and Ramp (1968). The St. Helens and Washougal mining districts of southwestern Washington are discussed by Moen (1977). The geology

and mineralization of the Silver Star stock in the Washougal district has been studied more recently by Shepard (1979). Berri and Korosec (1983) mapped along the Wind River valley south of Trout Creek Hill as part of a geothermal investigation. The mineral resource potential of the Indian Heaven roadless area to the east of the study area has also recently been investigated (Church and others, 1983a,b). Polivka (1984) studied the Quaternary volcanology of the West Crater-Soda Peaks area to the southwest of the study area.

#### MINING HISTORY

The Wind River prospect is discussed briefly by Moen (1977) in his report on the St. Helens and Washougal mining districts of Washington, where the history of the prospect up to 1977 is described. During the early 1900's, the area underwent prospecting for lode and placer gold deposits, mining claims were staked, but no important discoveries were made. During this time, the St. Helens and Washougal districts were established. In 1956, the Wind River Mining Co. obtained rights to 21 quartz lode claims and explored them for gold (Moen, 1977). Although the Wind River prospect is the only mining property in the area, old adits and prospect pits attest to past exploration activities. Up to 1977, 831 tons of gold ore had been shipped from the mine (Moen, 1977) representing approximately 90% of the total metal production of southwestern Washington during that same period. Poor recovery rates and low gold content of the siliceous ore have forced repeated cessation of activity and the property has changed hands many times. Currently the property is being worked by Youngquist Mining Co.



## REGIONAL GEOLOGY

### INTRODUCTION

The Washington Cascades have been divided into northern and southern geologic provinces separated by a transitional subprovince (Grant, 1982). The north Cascade province consists of a pre-Tertiary metamorphic-plutonic crystalline core separated by fault boundaries on the east and west from dominantly pre-Tertiary continental and marine rocks. The pre-Tertiary metamorphic rocks have been intruded by late Cretaceous to Tertiary calcalkaline plutonic rocks.

A transitional subprovince in which tectonic slices of northern Cascade crystalline rocks are juxtaposed against the Tertiary volcanic section separates the north from the south-central province. This south-central province is composed of unmetamorphosed early to middle Tertiary volcanic rocks and subordinate sedimentary rocks. This province in Washington, together with the Oregon Cascade Range has been referred to as the 'volcanic Cascade Range' and as the 'southern Cascade Range' (Hammond, 1979). Rocks of the volcanic Cascades have been stratigraphically divided into the informally named Western Cascade Group (Hammond and others, 1977; Hammond, 1979) and the High Cascade Group (Peck and others, 1964; Hammond, 1979). These units are intruded

by Tertiary calcalkaline plutonic rocks.

The upper Cretaceous to Tertiary age Cascade intrusions form two belts extending south from the Canadian border. The western belt ends near Portland, Oregon, while the eastern belt continues south along the western slope of the Oregon Cascades. The projection of these two belts diverges to the south (Hammond, 1979). Ages of the plutons decrease to the south in both belts, but the western belt is slightly younger than the eastern belt. Plutons of the western belt were emplaced between 35 to 15 Ma, while plutons of the eastern belt in Washington were emplaced between 50 to 25 Ma.

The intrusions of these belts have a composite magmatic history. The main phase rocks are calcalkaline and predominantly granodioritic to quartz dioritic in bulk composition, but late-stage magmatic differentiates of quartz monzonite and granite are relatively common. Emplacement of these late intrusive rocks appears to have been partly controlled by development of structures transverse to the regional trend (Grant, 1969).

## STRATIGRAPHY

Regional stratigraphy of the Cascade Range in Washington has been correlated by Hammond and others (1977) and Hammond (1979), who assign pre-Pliocene rocks in the Cascades to the informally named Western Cascade Group. Stratigraphic relations of major formational units of the Western Cascade Group in southern Washington are summarized in Figure 2.

The Western Cascade Group has been divided into lower, middle, and upper members (Hammond, 1979). The lower and upper members contain

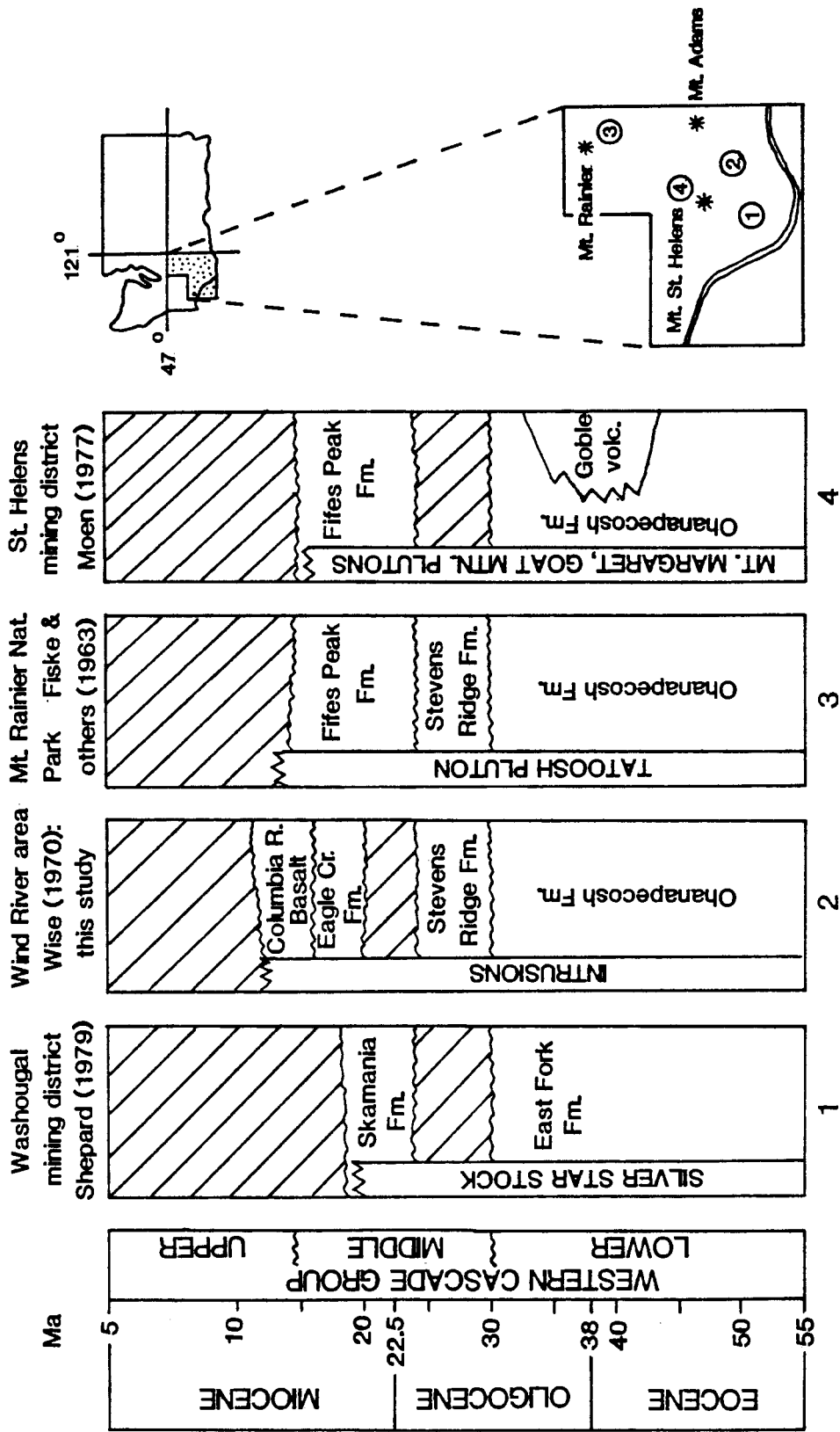


Figure 2. Stratigraphic relations in the southern Washington Cascades (ages and Western Cascade Group divisions from Hammond, 1979, other references indicated above individual stratigraphic columns).

interlayered lava flows, pyroclastic rocks, and volcanoclastic rocks, but the middle member is dominated by pyroclastic rocks (Hammond, 1979). Hydrothermal alteration is prevalent in deeper stratigraphic levels of the Western Cascade Group (Grant, 1969; Wise, 1961; Fiske and others, 1963; Peck and others, 1964), and coincides with two north-south trending belts of epizonal granodioritic to quartz dioritic plutons. Rocks of the Western Cascade Group are also intruded by numerous dike complexes thought to represent the roots of former volcanoes (Hammond, 1979). Presumably, these dike complexes have also contributed to the hydrothermal alteration.

The oldest rocks in the Wind River area were originally named the Weigle Formation (Wise, 1961) and later correlated with the Ohanapecosh Formation, a late Eocene to middle Oligocene unit first described at Mt. Rainier National Park by Fiske and others (1963), consisting of interstratified basaltic and andesitic lava flows, lahars, and pyroclastic rocks of andesitic to rhyodacitic composition. Fiske (1963) interpreted the environments of deposition as those of subaqueous and subaerial environments. Where there has been no repetition of units by faulting, the Ohanapecosh Formation in the Wind River area is nearly 5,800 m thick, and the base of the section is not exposed.

The Ohanapecosh Formation is unconformably overlain by the Stevens Ridge Formation, a distinctive unit consisting of light-colored interstratified dacitic to rhyodacitic ash flow tuffs with subordinate lahars, volcanoclastic rocks, and minor porphyritic lava flows (Fiske and others, 1963; Hammond, 1974, 1980; Hammond and others, 1977). South of the study area, the Stevens Ridge Formation is unconformably overlain

by the Eagle Creek Formation, a sequence of volcanic conglomerates, sandstones, and tuffs of early Miocene age (Wise, 1970). Also to the south of the study area, the flows of the Yakima Basalt Subgroup of the Columbia River Basalt Group overlie the Eagle Creek Formation. Quaternary olivine basalts erupted during the Pleistocene from vents located outside the study area are exposed in the eastern and northeastern part of the study area and occur as intracanyon flows along Falls Creek and Wind River in the south part of the study area.

## STRUCTURE

Regional structural features of Washington are shown in Figure 3. Major features are the Straight Creek fault, the Olympic-Wallowa lineament, and the Yakima folds. The Straight Creek fault extends from central Washington to Canada. Over much of its length, it separates relatively unmetamorphosed or weakly metamorphosed rocks on the west from the metamorphic core of the northern Cascades on the east. It has been recognized as a major structure with large right-lateral displacement (Misch, 1977; Davis and others, 1978). In central Washington, faults associated with the southern segment of the Straight Creek fault swing southeast into alignment with the Olympic-Wallowa lineament of Raisz (1945). The fundamental structure underlying this lineament is not known, but it is defined by northwest-trending topographic features extending from the Wallowa Mountains in eastern Oregon to the north side of the Olympic Mountains in Washington.

Two major fold patterns are found in rocks of the Western Cascade Group in Washington. An older group of northwest-trending folds whose

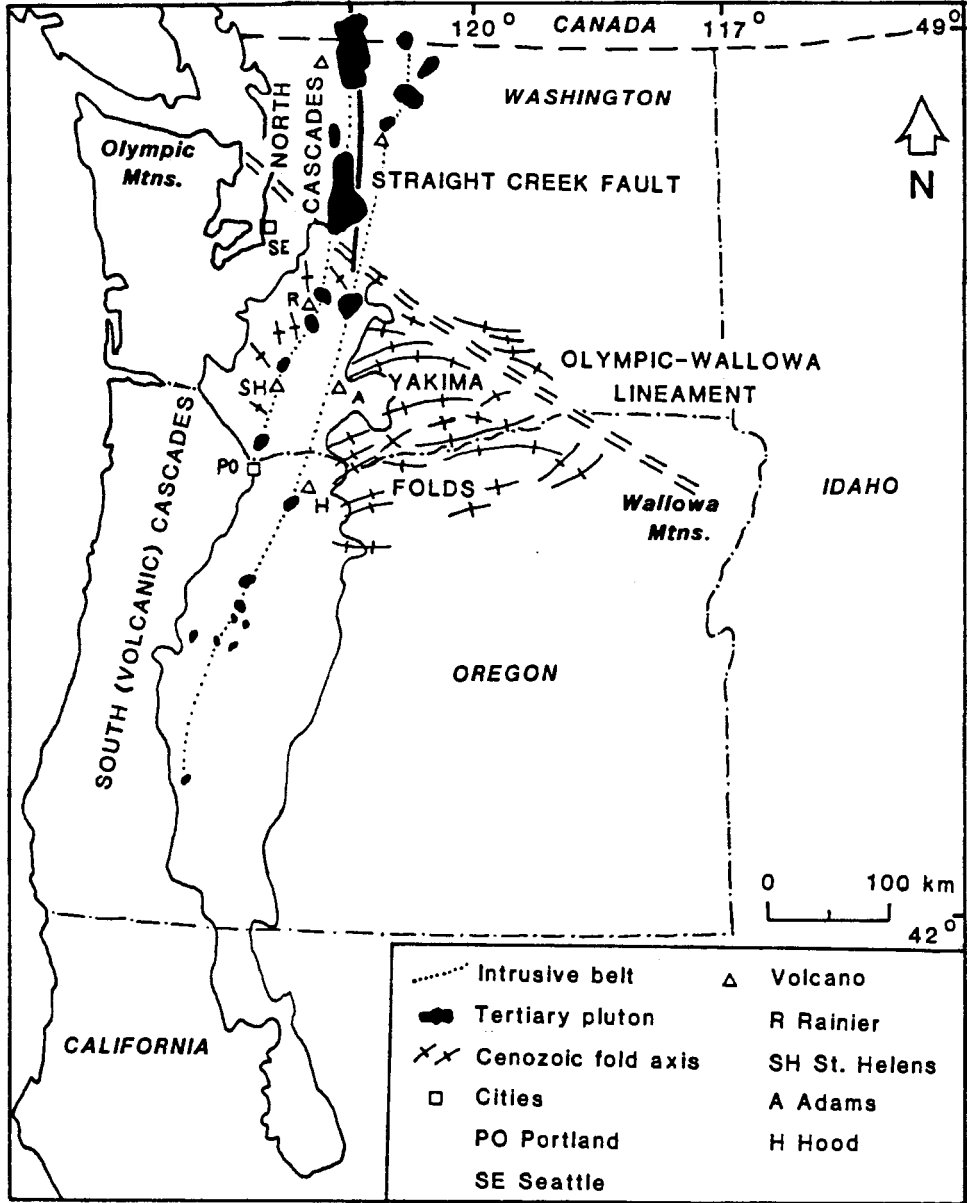


Figure 3. Regional structural features of the Washington Cascades (modified from Hammond, 1979).

limbs dip moderately at  $10^{\circ}$  to  $45^{\circ}$  are characteristic of the western slope of the Cascade Range in Washington. This fold pattern parallels the regional structural grain of the pre-Cenozoic terrain of the north Cascades (Hammond, 1979). Northwest-trending folds whose limbs dip in excess of  $45^{\circ}$  occur along the Olympic-Wallowa lineament on both sides of the Cascade Range.

A younger fold pattern characteristic of the Yakima fold system of the western Columbia Plateau (Newcomb, 1970) is superimposed on the older, northwest fold trend (Hammond, 1979), and has been found to extend into the Cascade Range (Beeson and others, 1982). The trend of these younger folds on the eastern flank of the Cascades shifts from dominantly northwest near the Olympic-Wallowa lineament to dominantly southwest near the Columbia River. Deformation of the Yakima folds is considered to have begun at approximately 12 Ma and ended at about 5 Ma (Hammond, 1979).

The principal fault directions in the southern Washington Cascades are northwest and north-south. The northwest fault trend parallels the older, northwest fold trend and the Olympic-Wallowa lineament, and is believed to have developed at the same time as the older fold trend (Hammond, 1979, 1980).

North-south faults occur in Washington between Mt. St. Helens and Mt. Rainier (Hammond, 1979). Other north-south structures are the Indian Heaven and King Mountain fissure zones located between Mt. St. Helens and Mt. Adams (Hammond, 1979, 1980). The approximate alignment of Soda Peak and Marble Mountain with Mt. St. Helens and the Goat Rocks volcanic complex with Spiral Butte are considered (Hammond, 1979, 1980)

to also indicate north-south structures. Immediately south of the Columbia River, north-south faults are developed in the Mt. Hood fault zone (Newcomb, 1969).

#### VOLCANIC AND TECTONIC HISTORY

The volcanic history of the Pacific Northwest has been episodic in nature. During the Eocene and Oligocene, volcanism was typically of intermediate silica content, and was distinct from Miocene and later basaltic and bimodal volcanism that is associated with later Cenozoic extensional tectonics (Lipman and others 1972; Christiansen and Lipman, 1972; Armstrong, 1978). Volcanic and tectonic history of the western Cordillera during the period 55 to 17 Ma is summarized in Figure 4.

The Ohanapecosh and Stevens Ridge Formations of the Wind River area are part of the thick Oligocene and lower Miocene sequence of intermediate to silicic pyroclastic rocks and lavas in the Cascade arc that has been correlated with the Basin and Range "ignimbrite flare-up" of 34 to 17 Ma (Lipman and others, 1971; Noble, 1972; Stewart and others, 1977). This episode of dominantly pyroclastic volcanism indicates emplacement of magmas at shallow depths in the crust, and implies significant extension within the arc (Hildreth, 1981).

#### ECONOMIC GEOLOGY-GENERAL

Although there are geologic differences between the north and the south-central Cascade Range in Washington, on the whole, the Cascades are metallogenically considered a copper province, with most major sulfide systems being classified as of the porphyry copper type (Grant, 1969, 1982). Due to strong structural controls, many Cascade porphyry



VOLCANIC EPISODE	TIME (Ma)	VOLCANIC EVENTS	TECTONICS	REFERENCES CITED
Cascade	19-17	Unconformity at 18 Ma. Deposition of upper Western Cascade Group rocks. Change from previous pyroclastic volcanism to more abundant pyroxene andesite and basalt flows.	Extension behind the arc.	Priest and others, 1982 Hammond, 1979 Peck and others, 1964
	36-17	Deposition of lower (Ohanapecosh) and middle (Stevens Ridge) Western Cascade Group-thick sequences of intermediate to silicic pyroclastic rocks. Dominant pyroclastic volcanism is correlative with Basin and Range "ignimbrite flare-up" of 34-17 Ma.	Change from earlier, compressional tectonics, related to a migrating flexure or an increasing dip angle of the subducted slab. Reduced horizontal compression allowed increased injection of magma into the crust, development of large, shallow magma chambers, and outbreak extensional-type volcanism.	Wells and others, 1984 Vance, 1982 Hammond, 1979 Stewart and others, 1977 Noble, 1972 Lipman and others, 1971 Fiske and others, 1963
	38-35	Regional unconformity	Subsidence in arc, back arc, and forearc environments.	Tabor and others, 1984 Wells and others, 1984 Gresens, 1982 Snively and Wagner, 1963
	44-35	Diminished volcanism parallel to new continental margin. Arc magmatism moves westward. Change from Challis volcanic axis occurred in a discrete step.	Accretion of Coast Range basement. Decrease in subduction rate to 40 km/Ma. Steepening of slab dip.	Vance, 1982 Priest and others, 1982 Lux, 1982 Hammond, 1979 Dickinson, 1979 Armstrong, 1978 Snyder and others, 1976
Challis	55-43	Predates Cascade arc volcanism. Occupies a NW-trending belt that is wide compared to the Cascade arc. Magmatic null in the western Cordillera. Arc magmatism moved inland and decreases in volume.	Shallowing of Farallon plate subduction angle. Rapid subduction rate of 150 km/Ma.	Vance, 1982 Dickinson, 1979 Buckovic, 1979 Armstrong, 1978 Davis, 1977 Snyder and others, 1976 Snively and Wagner, 1963

Figure 4. Summary of volcanic and tectonic events in the Pacific Northwest from 55 to 17 Ma.

copper deposits are linear. Alteration haloes show greater vertical than lateral zonation.

Grant (1982) has classified the Cascade porphyry systems on the basis of the depth of emplacement of their associated plutons. A summary of this classification is given in Figure 5. Most periods of metal deposition in the Washington Cascades are at least partly related to late Cretaceous to early Tertiary intrusive episodes (Grant, 1969) and appear to have occurred at approximately the same time or slightly later than emplacement of the associated intrusion (Grant, 1982). Major sulfide systems occur in the transitional subprovince or the south-central province rather than in the north Cascades, and they occur with intrusions that appear younger than their north Cascade equivalents.

The primary physical controls for distribution and concentration of sulfides appears to be a series of structural couples involving the intersection of transverse, northeast-trending structural belts that obliquely cut the northwest regional trend of the Cascades. Intensity of deformation along these transverse structures is an important factor in mineralization (Grant, 1969). The most favorable chemical environment is high in potassium and free silica. K-feldspar, secondary biotite, or quartz-sericite alteration characterize the advanced stages of the alteration. The K-silicate alteration is commonly associated with copper mineralization in the Washington Cascades, and appears to be directly related to late-stage magmatic fractional crystallization processes (Grant, 1969).

A schematic diagram of a Cascade linear porphyry copper intrusion is shown in Figure 6. Structural control results in linear shatter

TYPE	DEPTH OF PLUTON EMPLACEMENT	EXAMPLE	REMARKS
Deep	>5 km	Glacier Peak (Snohomish Co.) North Cascades	Only lower portions of system still remain.
Intermediate	2-3 km	Middle Fork (King Co.) Central Cas- cades	Deroofing of intrusion has occurred relatively recently.
High	<2 km commonly breaks to surface	Silver Star (Skamania Co.) South Cas- cades	Intrusive breccias common. Believed to overlie inter- mediate level systems.

Figure 5. Classification of Cascade porphyry systems (after Grant, 1982).

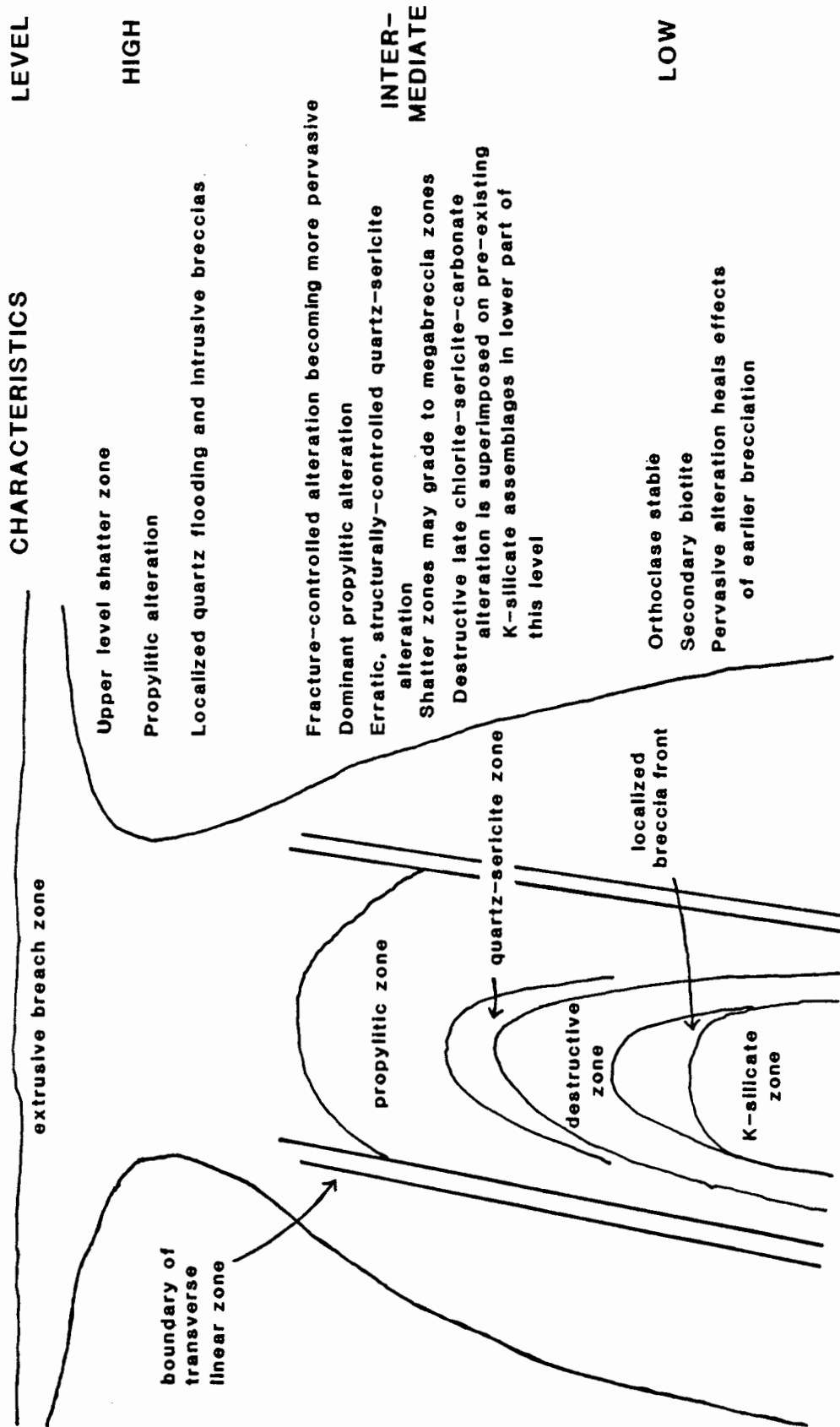


Figure 6. Schematic diagram of a Cascade linear porphyry copper intrusion (from Grant, 1982).

zones bounded by relatively massive rocks. Vertical shattering may extend for thousands of feet. Later hydrothermal activity is concentrated mainly in the vertical dimension while lateral zoning is narrow or nonexistent. Wallrock alteration was produced by deuteritic and hydrothermal processes, the intensity of which depends primarily on the amount of fracturing of the country rock prior to introduction of secondary material (Grant, 1982).

#### ECONOMIC GEOLOGY—ST. HELENS AND WASHOUGAL MINING DISTRICTS

Most of the metallic mineral occurrences of southwestern Washington are located within the St. Helens and Washougal mining districts (Fig. 7). These are the southernmost mining districts in Washington and are located on the western slopes of the Cascade Range. They are also the closest mining districts to the Wind River prospect. In the Washougal district, mineralization occurs mainly along the eastern edge of the Silver Star stock, while in the St. Helens district, mineralization occurs along the southeastern part of the Mt. Margaret stock and along the south-central section of the Goat Mountain stock. Location of metal deposits in the southern Washington Cascades is shown in Figure 7. Host rock stratigraphy in these districts is shown in Figure 2.

Stocks in both districts are composed mainly of granodiorite, but also contain quartz diorite, quartz monzonite, and minor dacite. K-Ar dates of the Mt. Margaret and Goat Mountain stocks of the St. Helens district, and of the nearby Camp Creek stock range from 16.2 to 24.0 Ma (Engels and others, 1976; Armstrong and others, 1976), suggesting the plutons of the St. Helens district and associated sulfide mineralization

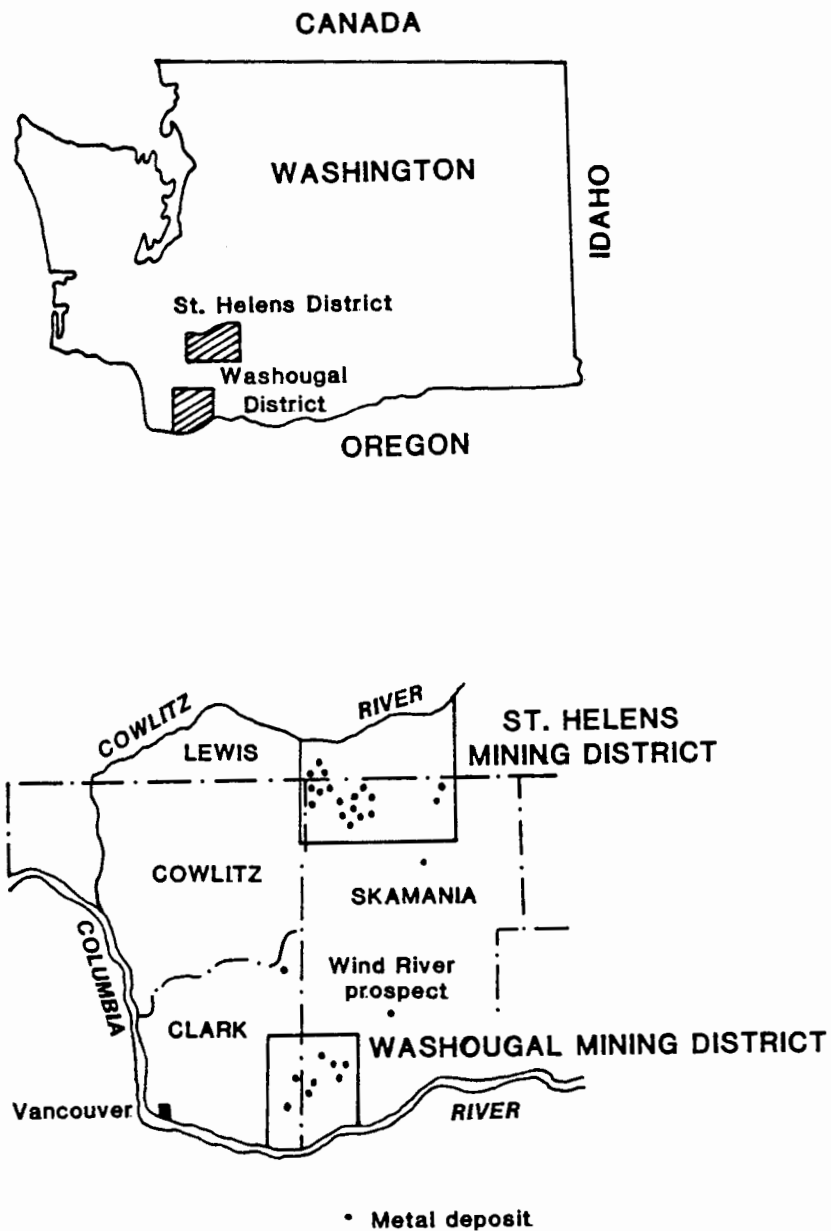


Figure 7. Location of the St. Helens and Washougal mining districts and distribution of metal deposits in these districts (modified from Moen, 1977).

are related to the Snoqualmie intrusive episode (Moen, 1977). The Silver Star stock of the Washougal district has been inferred to have been emplaced between middle Oligocene and early Miocene times (Shepard, 1979; Moen, 1977).

Mineral deposits in the St. Helens and Washougal districts consist of mineralized stockworks, breccia zones, and narrow fissure veins containing moderate amounts of copper and small amounts of lead, zinc, molybdenum, gold, and silver. Veins occur in the granodiorite intrusions and in the volcanic host rocks near the intrusive contacts. Gangue material consists of quartz, calcite, and wall rock fragments. Pyrite, chalcopyrite, bornite, sphalerite, and galena are the main sulfide minerals. At some occurrences, the sulfide minerals are accompanied by free gold, especially in the oxidized portions of veins (Moen, 1977). Distribution of high-grade ore in the veins is spotty. Zoning of wallrock alteration outward from the veins consists of silicification, quartz-sericite, argillization, and propylitic zones. Mineralization is believed to be of middle to late Miocene age (Moen, 1977).

Outside the boundaries of the St. Helens and Washougal districts, several copper-gold deposits occur in the Camp Creek area of McCoy Creek in north-central Skamania County, while the gold-producing area with the largest production in southwestern Washington has been the Wind River prospect.

The St. Helens and Washougal districts have produced only small amounts of metal. Although numerous claims were staked in these districts beginning as early as 1892 (Moen, 1977), none of the

properties ever developed into a mine with large production. Forest fires during the early part of this century destroyed the buildings at many mines and operations were never re-opened at many properties.



## WIND RIVER PROSPECT AREA

### INTRODUCTION

The Wind River prospect is located on a minor tributary of the Wind River in section 9, T5N, R7E (Plate 1) of the Wind River 15' quadrangle. The prospect does not lie within an organized mining district, but is located approximately 16 km northeast of the Washougal district, and to the south of the St. Helens district. The area is 32 km north of the town of Carson, Washington, near the headwaters of the Wind River.

### STRATIGRAPHY

Wise (1961, 1970) mapped the area surrounding the Wind River gold prospect as a sequence of massive andesite flows within the Ohanapecosh Formation. Mapping done in the course of this study has revealed the presence of other lithologic units in the area. The geology is given in Plate 1 and the generalized stratigraphy of the area is summarized in Figure 8.

Aside from alluvial deposits in the major stream valleys, the youngest deposits in the area are two Quaternary basalt units erupted from vents outside the study area. The younger of the two units is informally designated the Basalt of Falls Creek in this study. This

UNIT	NAME	DESCRIPTION
Quaternary		
Qfc	Basalt of Falls Creek	Dark gray vesicular basalt. 10-15% plagioclase phenocrysts to 1 mm, aphanitic groundmass.
Qjc	Basalt of Juice Creek	Light gray, platy olivine basalt. 5% olivine phenocrysts to .5 mm, aphanitic groundmass.
Tertiary		
Tsr	Stevens Ridge Formation	Friable, light colored ash flow tuffs. Primary quartz phenocrysts present in some exposures. Silicified wood fragments also found in some exposures.
To	Ohanapecosh Formation	Interstratified andesitic pyroclastic rocks, andesitic lava flows, and lahars (see Figs. 9 and 10 for descriptions of subunits).
Ti	Intrusions	Hornblende diorite. Intrusive into Ohanapecosh Fm., ages unknown.

Figure 8. Generalized stratigraphy of the study area.

dark gray, vesicular basalt is exposed to the east of North Butte and Middle Butte, and as intracanyon flows along Falls Creek and the southern part of Wind River valley in the study area. This basalt has not been age-dated, but shows evidence of glaciation during the last glacial epoch (Hammond, 1984, pers. comm.). The older basalt, here informally named the Basalt of Juice Creek, is a light gray, platy olivine basalt that has been dated at  $1.40 \pm 0.06$  Ma by the K-Ar method (Hammond, 1984, pers. comm.). This basalt is exposed to the east and northeast of Lava Butte.

Tertiary units in the area consist of the Stevens Ridge Formation, the Ohanapecosh Formation, and intrusions. The Stevens Ridge Formation is middle Oligocene to early Miocene in age. It consists of light colored, in some places nearly white, fine-grained, friable tuffs exposed in the north part of the study area. The contact with the underlying Ohanapecosh Formation is uncertain. Intrusions of hornblende diorite are exposed in the far northwest part of the study area. These intrusions have not been age-dated. They are intrusive into the Ohanapecosh Formation, but their time relations with the younger Stevens Ridge Formation are not known.

The Ohanapecosh Formation comprises most of the bedrock geology of the study area, and has been divided into eight subunits, the essential characteristics of which are summarized in Figures 9 and 10. The most important of these subdivisions in this study are the P<sub>1</sub> and P<sub>2</sub> pyroclastic rocks and the A<sub>1</sub> and A<sub>2</sub> lava flow groups. Descriptions of these units are given in Figure 9. The stratigraphically lowest of these subunits consists of a sequence of pyroclastic rocks that is

NAME	DEPOSIT TYPE	DESCRIPTION
P <sub>2</sub> Western pyroclastic sequence	Andesitic pyroclastic rocks	20-30% olive green to tan fine-grained vitric-crystal tuffs and airfall units with accretionary lapilli, 70-80% crystal-rich lithic lapilli tuffs, minor andesite lava flows.
A <sub>2</sub> Upper lava flows	Andesitic lava flows, flow breccias, minor intercalated pyroclastic rocks	Porphyritic andesite flows with partly glassy groundmass, 20-25% plagioclase phenocrysts 1-2 mm long, occurring mainly as single crystals. 5-10% amphibole and pyroxene phenocrysts .5-1 mm.
A <sub>1</sub> Lower lava flows	Andesitic lava flows, flow breccias, minor intercalated pyroclastic rocks	Porphyritic to glomeroporphyritic lava flows with well-developed platy fracturing in outcrop, 20% plagioclase phenocrysts 2-3 mm in length, the majority of which occur in irregularly shaped glomerocrysts 5-6 mm in diameter, 5-10% amphibole and pyroxene phenocrysts .5-1 mm.
P <sub>1</sub> Lower pyroclastic sequence	Andesitic pyroclastic rocks	Crystal-rich lithic lapilli tuffs and lithic lapilli tuffs, minor andesite lava flows (see Figs. 11 and 12 for tuff stratigraphy and lithologic descriptions in the vicinity of the prospect).

Figure 9. Laterally extensive subdivisions of the Ohanapecosh Formation in the study area.

NAME	DEPOSIT TYPE	DESCRIPTION
P <sub>4</sub> Northern pyroclastic sequence	Undifferentiated pyroclastic rocks	Poorly exposed pyroclastic rocks containing buff colored, friable tuffs which may have originally contained pumice.
P <sub>3</sub> Pumice lapilli tuffs	Pyroclastic rocks	Light colored, buff to olive green crystal-rich pumice lapilli tuffs. 20-25% plagioclase crystal clasts, 20-30% subround pumice lapilli to 5 cm diameter. Local, dark blue-green celadonite alteration.
L <sub>2</sub> Western laharic unit	Lahar(s)	Poorly exposed unit containing 30-40% sub-angular to subround, unsorted lithic clasts to at least 15 cm in diameter.
L <sub>1</sub> Northern laharic unit	Lahars	Sequence of lahars, each containing 40% sub-angular to subround, unsorted lithic clasts to boulder size. Locally contains carbonized wood fragments 30 cm or more in length. Local, darker blue-green celadonite alteration. Volcanic sedimentary interbeds 15-30 cm thick consisting of silt to fine sand size material. Uppermost exposed lahar shows considerable rust-red discoloration suggesting the lahar was hot when deposited.

Figure 10. Other subdivisions of the Ohanapecosh Formation.

collectively referred to as  $P_1$ .  $P_1$  rocks are crystal-bearing lithic lapilli tuffs and lithic lapilli tuffs with minor intercalated andesite lava flows.

The  $P_1$  pyroclastic sequence is overlain by lava flows which have been divided into two groups on the basis of primary textures. The sequences of lava flows are thickest in the North Butte-Middle Butte area, where they are up to 415 m thick. Individual flows in both groups are separated by flow breccias and subordinate quantities of intercalated pyroclastic rocks.

Flows of the lower flow group,  $A_1$ , are porphyritic to glomeroporphyritic andesites wherein the majority of the plagioclase phenocrysts occur in glomerocrysts. The upper group of flows,  $A_2$ , have finer-grained, more abundant phenocrysts than those of  $A_1$ , and fewer glomerocrysts. The groundmass of the  $A_2$  flows is a very dark blue-gray color and contains a high glass content.

Towards the west, the number of flows in the  $A_1$  and  $A_2$  flow units decreases and the proportion of intercalated pyroclastic rocks increases. The flow units interfinger with the  $P_2$  pyroclastic sequence, and the section becomes dominated by pyroclastic rocks in the western part of the study area.

Pyroclastic rocks of the  $P_2$  (western) pyroclastic sequence contain a higher proportion of fine-grained vitric-crystal tuffs and airfall units with accretionary lapilli than the pyroclastic rocks of  $P_1$ .

The other four subdivisions of the Ohanapecosh Formation,  $P_4$ ,  $P_3$ ,  $L_1$ , and  $L_2$  consist of pyroclastic rocks and laharic units of more restricted areal extent. Descriptions of these units are given in

Figure 10. In most cases, the exact stratigraphic relationships of these units to the other Ohanapecosh Formation subunits is unclear.

The P<sub>4</sub> pyroclastic unit appears to interfinger with the A<sub>1</sub> and A<sub>2</sub> flow units in the north and northeast parts of the study area, and is overlain by the Stevens Ridge Formation.

In the vicinity of the prospect (sec. 4 and 9, Plate 1), the P<sub>1</sub> pyroclastic sequence has been subdivided into four subunits on the basis of field relations and textural criteria, including proportion and type of crystal clasts and lithic clasts. These subunits, T<sub>1</sub> to T<sub>4</sub>, are shown on the geologic map of the area immediately surrounding the prospect (Fig. 11) and lithologies are described in Figure 12. Widespread alteration has affected the pyroclastic rocks to a greater degree than the associated lava flows. The tuff units T<sub>1</sub> to T<sub>4</sub> are difficult to trace laterally for more than short distances due to poor exposures and the general lithologic similarity of the units.

#### INTRUSIONS

Three groups of intrusions, D<sub>1</sub>, D<sub>2</sub>, and D<sub>3</sub>, have been recognized within the area near the Wind River prospect. Locations of dikes exposed along the exploratory roadcut are shown in Plate 2. These intrusions are divided into two groups on the basis of degree of alteration and apparent relations to the most intensely altered pyroclastic rocks which they cut. A third group was distinguished on the basis of geochemical differences. Away from the zones of most intense alteration, it would be difficult to distinguish different groups of dikes.

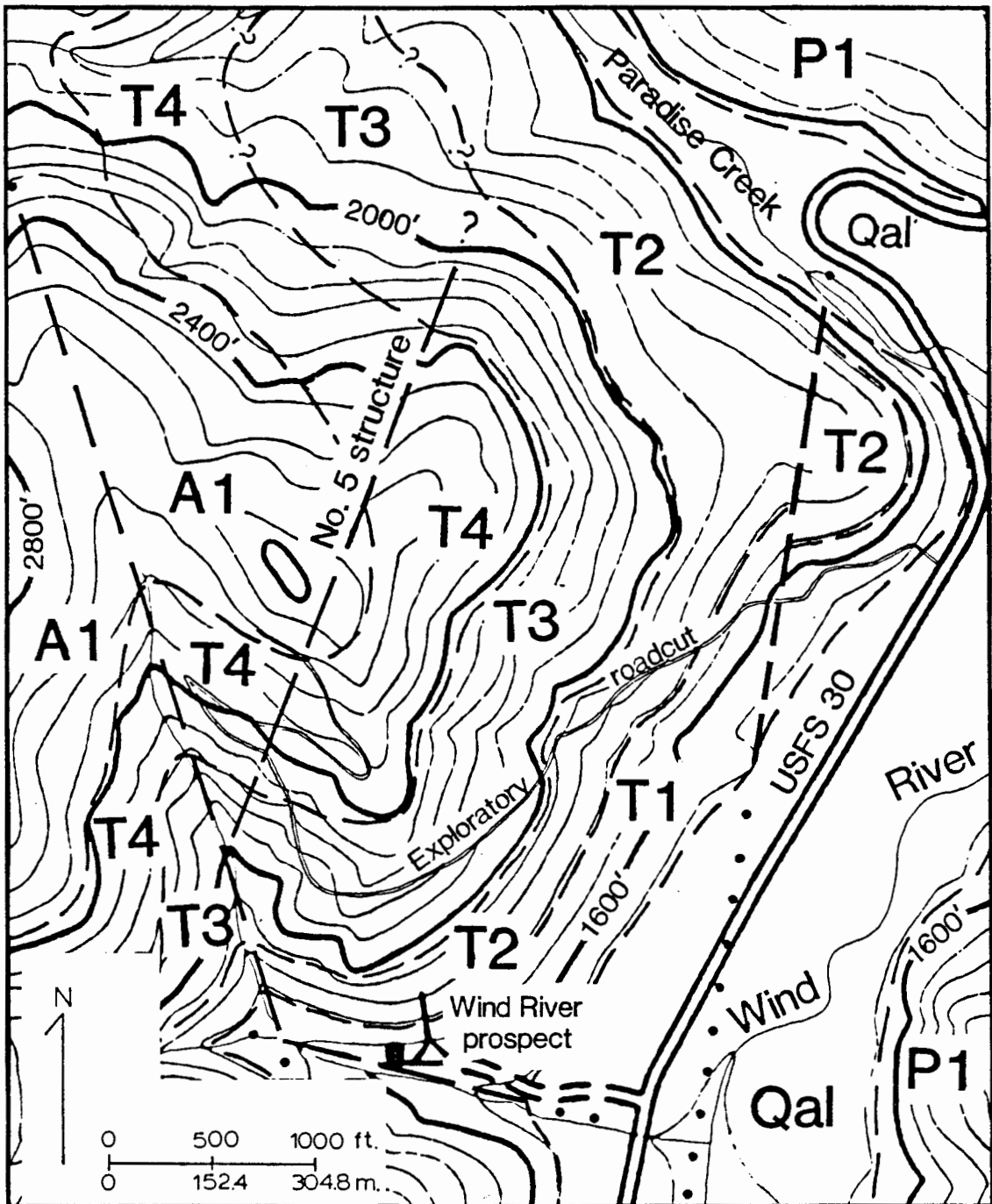



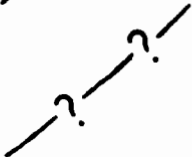




Figure 11. Distribution of tuff units  $T_1$  to  $T_4$  in the vicinity of the Wind River prospect. Map symbols are described on the following page. Lithologies are described in Figure 12.



	Faults or fractures, known and inferred, dotted where projected under cover
	Fault or fracture, projection uncertain
	Contact, located approximately
	Contact, location uncertain
	Adit
	Building

Map symbols for Figure 11

UNIT	COLOR	CRYSTAL CLASTS	LITHIC CLASTS	MATRIX	TEXTURE/ STRUCTURE	DEPOSIT TYPE	REMARKS
T <sub>4</sub>	olive green	15% plagioclase 5% amphibole	25-30% andesitic lithic clasts	vitric ash		crystal-bearing lithic lapilli tuff	Forms resistant outcrops in stream channels. Difficult to distinguish from T <sub>3</sub> where gray ash layer not present.
gray ash	dark gray			fine vitric ash		air fall	Discontinuous layer
T <sub>3</sub>	olive green	20-25% plagioclase 3% amphibole	5-10% andesitic lithic clasts	vitric ash	welded	crystal-rich lithic lapilli tuff	Weathering of lithic clasts produces pitted appearance on weathered fracture surfaces. Forms resistant outcrops in stream channels. % lithic clasts varies; locally resembles an altered lava flow.
T <sub>2</sub>	olive green	15% plagioclase 5% amphibole	20% andesitic lithic clasts	vitric ash		crystal-bearing lithic lapilli tuff	Poorly exposed
T <sub>1</sub>	olive green to tan	10% plagioclase 5% amphibole	15-20% flat-tened black glassy lenticles	vitric ash	weak to moderate eutaxitic layering	vitric-crystal tuff	Poorly exposed

Figure 12. Description of tuff units T<sub>1</sub> to T<sub>4</sub>.

D<sub>3</sub> dikes are dark blue-green to blue-gray in color, fine-grained, porphyritic dikes containing both pyroxene and amphibole as mafic phases, and 1 to 3% fine-grained sulfide blebs occurring in the groundmass. The dikes are narrow, approximately 1 to 6 m wide, and appear to be emplaced along fractures aligned with regional structural trends. They can be found intruding highly altered pyroclastic rocks, and contacts with the altered pyroclastic rocks are sharp. The dikes show greater fracturing than the pyroclastic rocks into which they are intrusive. Aside from coatings of Fe-oxides on the fracture surfaces, alteration along fractures in the dikes is minimal to nonexistent. In thin sections, the primary textures of the groundmass of the dikes are preserved. Some of the D<sub>3</sub> dikes are crosscut by quartz veins, or have quartz veins emplaced between the margin of the dike and the pyroclastic rocks into which it is intrusive.

D<sub>1</sub> dikes may also be found intruding the more altered zones. They have somewhat coarser phenocrysts and a higher proportion of glomerocrysts than do D<sub>3</sub> dikes. These dikes show differing degrees of alteration. Where weakly altered, they show the dark blue-green color of the D<sub>3</sub> dikes. Groundmass textures are still preserved in thin section and pyroxenes show partial alteration to chlorite. Amphiboles, however, are completely altered to chlorite and calcite. These dikes may be traced into more strongly altered areas.

With increasing intensity of alteration, the dikes become lighter in color and may show 6 to 8 cm wide bleached haloes along fractures. Moderately altered D<sub>1</sub> dikes show greater alteration of phenocrysts than weakly altered D<sub>1</sub> dikes, and primary textures are not preserved within

the groundmass. Contacts with the altered pyroclastic rocks which they cut are sharp, and fracturing of the dike rock is equal to or greater than that of the host rocks. Fracture surfaces of some outcrops may be coated by thin layers of quartz and K-feldspar. Sulfide blebs may be found in the groundmass, associated with phenocrysts, or along microfractures.

Where most intensely altered, D<sub>1</sub> dikes are very light in color, pale buff to almost white. They are somewhat more resistant in outcrop than the surrounding altered pyroclastic rocks, but the two rock types are otherwise very similar in appearance and alteration mineralogy, and mutual contacts are difficult to determine. Strongly altered D<sub>1</sub> dikes often contain sulfide veinlets that have been partly to completely oxidized. These veinlets fill fractures in the dikes. Quartz-sulfide veinlets are also found.

One D<sub>2</sub> dike was distinguished on the basis of geochemical differences. This dike is cut by the No. 2A quartz vein. Field and petrographic studies were not able to distinguish this dike from a weakly altered D<sub>1</sub> dike.

## STRUCTURES

The flow units cap the ridges and are folded by a southeast-plunging anticlinal warp over the length of Paradise Ridge (Plate 1). This structure plunges to the southeast at an angle of approximately 30°. Location of the axis of the anticline was inferred from strikes and dips of bedding and flow foliation. Dips on units on the limbs of this fold are gentle to moderate, with measured values ranging from 10° to 30°.

Topography and stream drainage are controlled by three major high-

angle fracture and fault sets. The most prominent set of fractures is oriented N40<sup>o</sup> to N50<sup>o</sup> W, and controls the trend of Paradise Creek, the north fork of the creek near the adit, and numerous other tributaries to Wind River. The second set, oriented north-south to approximately N20<sup>o</sup> E, controls Wind River within the study area, the south fork of the creek near the adit, and parts or all of several tributaries to Paradise Creek and Wind River. The third set is oriented approximately east-west and controls Falls Creek, the lower portion of the creek near the adit, and other small drainages.

Displacement of up to approximately 70 m may have occurred across the Wind River valley, but on the whole, displacement along faults in the area is difficult to determine due to poor exposures and the lithologic similarities among the units.

Fracture trends along the exploratory roadcut are most commonly oriented northwest and north-northeast (Plate 2). East-west-trending fractures are present but less common. The veins exposed along this roadcut also follow these trends, with the north-northeast orientation predominant. Areas of quartz-cemented brecciation have been identified along Paradise Creek and tributaries associated with both north-northeast- and northwest-trending fractures.

In the area near the adit in sections 4 and 9, numerous small sags occur along lineaments which parallel or are aligned with the Wind River valley. The sense of displacement suggested by these features is down to the east.

## HYDROTHERMAL ALTERATION

### INTRODUCTION

Three associations of hydrothermal alteration and rock brecciation have been recognized in the study area. Distribution of these types is shown in Plate 1.

Type 1 alteration occurs at the periphery of the hydrothermal system. These zones of least intense alteration or 'rootless' zones lack readily apparent structural controls. They are located peripheral to the main system at similar elevations. Breccias found in these zones are cemented by a thin layer of massive white quartz, with coarsely crystalline euhedral quartz grown into the interstices. Calcite is found grown into open spaces in the euhedral quartz in some locations. Some of the massive quartz contains bladed cavities that are thinly coated by Fe and/or Mn oxides. Clasts in these breccias are weakly altered and contain smectites, illite, and some chlorite. Sulfide minerals have not been observed in these zones.

Type 2 alteration zones are located peripheral to the main system at higher elevations. This type is found on Paradise Ridge to the west and northwest of the prospect. It occurs in larger, more continuous areas than Type 1, but also lacks obvious structural controls. The

rocks include strongly altered lavas and tuffs which are bleached and/or silicified. Alteration of tuff layers in general is more intense and appears to be more extensive laterally than alteration of lavas.

Silicification occurs more frequently in the tuffs. Kaolinite, illite, and poorly crystalline or amorphous clays are common alteration products in all rock types. No quartz veins have been found, but rare quartz-cemented breccias have been noted. The quartz matrix is very fine-grained and may exhibit 'frothy' textures. Breccia clasts are strongly altered to kaolinite, illite, and quartz. Sulfide minerals have not been observed in these zones.

Celadonite alteration has been noted peripheral to both Type 1 and Type 2 alteration zones. Where it occurs, celadonite alteration is more pervasive in tuffs, lahars, and flow breccias than in lava flows. It has been found in A<sub>1</sub> lava flows on the northeast side of Lava Butte, in some exposures of the P<sub>3</sub> tuffs to the east of North and Middle Buttes, and in part of the L<sub>1</sub> laharic unit. These areas are located near or between observed 'rootless zones'. Celadonite alteration also affects the groundmass of A<sub>2</sub> flows and matrix and clasts of A<sub>2</sub> flow breccias on Paradise Ridge in sections 16 and 17 to the south of areas of Type 2 alteration on Paradise Ridge.

Type 3 alteration is associated with structures and is found at the Wind River prospect. Although numerous alteration zones have been found along fault and fracture zones near the prospect, none of these is as extensive as that found at the prospect. Zoned alteration at the prospect is distributed relative to the No. 5 structure (Plate 2), and grades from weak to intense. Large banded quartz veins cut the

alteration zones. Calcite is intergrown with quartz in the veins at lower elevations in the system, but at higher elevations, the large veins show bladed cavities lined with drusy quartz.

Breccias at the prospect occur marginal to the large quartz veins. These breccias are quartz-cemented and contain clasts altered to smectite, chlorite, illite, and quartz. Several poorly exposed quartz-cemented breccias not associated with quartz veins were noted along the exploratory roadcut. These breccias have strongly altered clasts, but neither they nor the vein margin breccias contain appreciable amounts of sulfide minerals.

Sulfide-rich breccias are associated with fault and fracture zones along Paradise Creek and its tributaries at moderate distances from the prospect. These breccias do not appear to be vein-margin breccias, but may have small quartz or quartz-calcite veins crosscutting them. The breccias show evidence of multiple episodes of brecciation and cementation. Cement is fine-grained, sulfide-rich quartz, and may contain drusy cavities. Clasts are strongly altered to kaolinite, illite, and quartz.

#### HYDROTHERMAL ALTERATION AT THE WIND RIVER PROSPECT

The alteration zones at the Wind River prospect are best exposed within the adit which is developed along the No. 2 quartz vein (Plate 3), and along the exploratory roadcut which runs from USFS road 30 to the top of the lobe of Paradise Ridge located in sections 4 and 9 (Plate 2). This road was constructed to expose the alteration and provide access for drilling the alteration zones.

The alteration is developed in the P<sub>1</sub> pyroclastic sequence which



underlies Paradise Ridge and the D<sub>1</sub>, D<sub>2</sub>, and D<sub>3</sub> dikes which are intrusive into the pyroclastic rocks. In an attempt to characterize the alteration in the area, each of the four tuff units described earlier (T<sub>1</sub> to T<sub>4</sub>) were traced into the zone of alteration from areas of low alteration. The same was done for the intrusive units. The systematic changes in alteration mineralogy, textural patterns, and veining in the rocks are given in Figure 13. The most extensive data has been obtained from the T<sub>3</sub> and T<sub>4</sub> tuffs and the D<sub>1</sub>, D<sub>2</sub>, and D<sub>3</sub> dikes, owing to more extensive exposures of these rocks along the exploratory roadcut. Alteration is distributed relative to the northeast-trending No. 5 structure, which contains discontinuous quartz stringers in a clay matrix but lacks the prominent banded quartz veins found elsewhere in the area surrounding the prospect.

The most intense alteration is found in a narrow zone that is 16 to 31 m wide and centered on the No. 5 structure. In this zone, alteration mineralogy consists of illite, kaolinite, and quartz. This zone grades outward to a carbonate-clay-quartz zone containing calcite, Fe-carbonate, illite, kaolinite, and quartz. Calcite content in rocks of this zone ranges up to about 20%. K-feldspar and albite are also present as secondary minerals. The presence of both feldspars was confirmed by x-ray diffraction. This zone is 155 to 185 m wide on the footwall side of the No. 5 structure, and may be wider on the hanging wall.

In the next zone outward, a yellow-brown clay that appears on the basis of optical studies to be a smectite clay, is the dominant clay. Illite and some chlorite are also present. Quartz, albite, and calcite

Unit D <sub>1</sub> , intrusion	
Textural feature	
Phenocrysts	<p><b>Fresh rock</b> Plagioclase</p> <p><b>Weakly altered</b> Plagioclase + minor chlorite</p> <p><b>Moderately altered</b> albite, calcite, chlorite illite</p> <p><b>Strongly altered</b> calcite + albite &amp;/or k-spar illite + albite &amp;/or k-spar + calcite albite &amp;/or k-spar + illite illite + albite &amp;/or k-spar + calcite + clay illite + albite &amp;/or k-spar + clay all assemblages contain tr. Fe-carbonate</p> <p><b>Extreme alteration</b> albite &amp;/or k-spar + calcite + clay albite &amp;/or k-spar + clay clay + albite &amp;/or k-spar + illite calcite, illite, clay Fe-oxide</p>
	<p><b>Pyroxene</b> pyroxene + chlorite</p> <p><b>Amphibole (inferred)</b> chlorite + calcite</p> <p><b>Groundmass</b> smectite clay, chlorite, quartz</p>
	<p><b>Plagioclase</b> plagioclase</p> <p><b>Pyroxene</b> chlorite</p> <p><b>Amphibole</b> chlorite</p> <p><b>Opagues</b> opagues</p> <p><b>Open-space</b> quartz</p> <p><b>Filled</b> chlorite, quartz calcite, quartz (mosaic textured)</p>
	<p><b>Replacement of chlorite &amp; smectite in groundmass by illite, carbonate, quartz</b> quartz, illite, calcite, Fe-carbonate (distributed in patches), albite, k-spar</p> <p><b>Oxidation of Fe-carbonate</b> quartz, illite, calcite, Fe-oxides (patchy distribution), albite, k-spar</p>
	<p><b>Destruction of primary groundmass textures</b> chlorite, smectite, quartz</p> <p><b>opagues, visible sulfide</b> opagues, visible sulfide</p> <p><b>quartz, sulfide, Fe-oxide</b> quartz, sulfide, Fe-oxide</p> <p><b>sulfide, quartz, (some with plumose textures)</b> sulfide, quartz, (some with plumose textures) calcite + quartz (mosaic)</p>

Figure 13. Alteration mineralogies and textures noted in lithologic units at differing intensity of alteration. Correspondence of intensity of alteration with alteration zones described in text is as follows: weakly altered=chlorite-smectite zone, moderately altered=smectite-chlorite zone, strongly altered=carbonate-clay-quartz zone, extreme alteration=clay-quartz zone. 'Clay' in extreme alteration is a mixture of illite+kaolinite. 7 Å clay is kaolinite.

Unit D<sub>2</sub>, intrusion

Textural feature	Fresh rock	Weakly altered	Moderately altered	Strongly altered	Extreme alteration
Phenocrysts	Plagioclase		plagioclase (albite) + calcite + chlorite albite + calcite + clay	These intrusions have not been found in these zones	
	Amphibole (hornblende inferred)		blue-green amphibole + calcite &/or chlorite		
	Pyroxene (inferred)		chlorite or chlorite + calcite		
	Opaque		opaques Near-total replacement of some plagioclase phenocrysts by calcite. Mafic phases all show complete replacement by alteration products.		
Groundmass	Glass Plagioclase Mafics ] Inferred		Groundmass is completely recrystallized to aggregates of clay, possible illite, and patches of chlorite		
Veining	Open Filled		quartz + k-spar quartz + chlorite + sulfides		

Unit D<sub>3</sub>, intrusion

Phenocrysts	Plagioclase	pyroxene + trace chlorite chlorite (rims) + quartz (core) (amphibole cross-sections and prismatic grains show same alteration pattern)	opaques	plagioclase	trace pyroxene + chlorite chlorite yellow-brown clay opaques - 1-3% visible sulfides	Fe-oxides on fracture surfaces mosaic quartz + chlorite + opaques chalcedonic quartz mosaic quartz
Groundmass	Pyroxene Amphibole (inferred)	Plagioclase	Pyroxene Amphibole (inferred)	Plagioclase	Pyroxene Amphibole	Glass (inferred)
Veining	Open Filled					

These intrusions have not been found in these alteration zones

Unit T<sub>1</sub>, tuff

Textural feature	Fresh rock	Weakly altered	Moderately altered	Strongly altered
Clasts	Pumice inferred - development of weak eutaxitic layering by flattened black lenticles		Boundaries of black glassy lenticles with matrix are sharp in hand sample but not as sharp in thin section  quartz, more coarsely grained to center of lenticles, + traces of smectite	
Crystal clasts	Plagioclase (inferred)  Mafics (inferred)		albite + illite + zeolite + smectite  smectite + quartz	
Matrix	Glass (inferred)		smectite + quartz + illite + chlorite Matrix shows incipient to partial recrystallization of quartz to coarser grains. Matrix textures partly destroyed	
Veining	Filled		quartz	

Unit T<sub>2</sub>, tuff

Lithic clasts				
Groundmass	Glass inferred		chlorite, smectite, illite, quartz (lighter colored clasts have a higher % of illite than darker colored clasts)	
Phenocrysts	Plagioclase Mafic	Inferred	quartz, trace smectite or chlorite, albite smectite, chlorite, quartz	
Crystal clasts	Plagioclase		illite + smectite + quartz Boundaries of crystal clasts are blurred in thin sections	
Matrix	Mafic Glass Plagioclase Mafics	Inferred	chlorite + smectite + quartz  Matrix textures are not preserved  smectite, chlorite, quartz	
Veining	Open	laumontite		

Figure 13. (continued)

Unit T <sub>3</sub> , Tuff	Fresh rock	Weakly altered	Moderately altered	Strongly altered	Extreme alteration
Textural feature					
Lithic clasts					
Groundmass	Glass Plagioclase Mafics Opauques	Inferred	Loss of easily distinguished mafic phenocryst grain boundaries		illite + 7Å clay + quartz
Phenocrysts	Plagioclase Mafic Opauques	Inferred	smectite, chlorite, quartz opalque calcite + albite chlorite + smectite		opalque mosaic quartz + illite + 7Å clay mosaic quartz
Crystal clasts	Plagioclase Mafic Opauques	Inferred	opalque albite, calcite, smectite chlorite smectite, chlorite, calcite quartz (mafic grain boundaries indistinct) opalque		illite + quartz + 7Å clay (clay dominant) mosaic quartz + illite (quartz dominant)
Matrix	Glass Plagioclase Mafics Opauques	Inferred	smectite, chlorite, quartz (partial recrystallization of patches of matrix quartz to grains up to 1 mm), albite		illite + 7Å clay + quartz
Veining	Open Filled		opalque quartz (with euhedral forms) quartz + k-spar mosaic quartz		opalques are rare quartz

Figure 13. (continued)

Unit 14, tuff

Textural feature

Lithic clasts

Groundmass

Glass  
Plagioclase } Inferred  
Mafics }

Opauques  
Plagioclase } Inferred  
Mafic }

Phenocrysts

Crystal clasts

Plagioclase } Inferred  
Mafic }

Groundmass

Glass  
Plagioclase  
Mafics  
Opauques

Veining

Filled

Weakly altered

Moderately altered

Strongly altered

Extreme alteration

Groundmass textures of clasts are partly to completely destroyed  
smectite, chlorite, calcite

opauques

mostly calcite + albite, trace illite  
smectite, chlorite, quartz

calcite + albite

smectite, chlorite, calcite, quartz

Groundmass textures are partly to completely destroyed  
smectite, chlorite, quartz, carbonate albite

opauques

quartz  
quartz + calcite  
quartz shows undulatory or plumose extinction

Patchy distribution of Fe-oxides in groundmass  
illite + Fe-oxides + micro crystalline quartz

Fe-oxides ?

albite &/or k-spar, illite, Fe-oxide, clay - possible kaolinite

albite &/or k-spar, illite, clay - kaolinite  
Fe-oxides

microcrystalline quartz, illite

Fe-oxides ?

Figure 13. (continued)

are the other important alteration minerals. This zone lacks the heavily carbonate-dominated signature of the previous zone, and is about 245 m wide. Beyond this zone, alteration assemblages contain a higher proportion of chlorite. Yellow-brown smectite clays, quartz, albite, and zeolites are present and the alteration merges with the regional alteration.

## VEINS

Veins of several compositions occur within the study area including laumontite, quartz-laumontite-heulandite, quartz-laumontite, quartz-K-feldspar, quartz-calcite, and quartz.

Laumontite veins are not found along the exploratory roadcut, but they are present in the tuffs exposed along the Wind River highway, USFS road 30. The laumontite occurs as a white, powdery material lining fractures.

Quartz-laumontite veins occur in several locations along the Wind River highway. The quartz is chalcedonic, but may form drusy linings in open spaces. The presence of laumontite in these veins was identified by x-ray diffraction. These veins are found cutting lava flows and flow breccias. Heulandite was found in the drusy quartz-lined cavities of a sample containing similar veins that was found in float along the lower part of the exploratory road cut. The source of this material has not been located.

Quartz-K-feldspar veins are common fracture coatings in tuffs and dikes of the smectite-chlorite zone on the lower part of the roadcut near the Wind River highway.

Quartz-calcite veins do not occur along the roadcut, but have been identified in areas associated with quartz-cemented breccias along Paradise Creek and its tributaries. Calcite occurs in the veining within the adit developed along the No. 2 vein filling open spaces lined with euhedrally terminated quartz. Calcite also occurs intergrown with massive white quartz within bands in the veins.

The prospect contains at least four mineralized quartz veins which cut andesitic pyroclastic rocks. The veins range from 15 cm to about 2 m in width, strike generally to the north, with dips ranging from steeply to the west to nearly vertical. Veins range from milky white quartz to chalcedonic, and are commonly banded to vuggy. Pyrite, although sparse, is the main visible sulfide mineral of the veins. Traces of malachite indicate the presence of altered copper sulfides, primarily chalcopyrite, in the No. 2 vein at the adit level.

A map of the prospect adit is given in Plate 3. The adit was driven along the No. 2 vein. At the adit level, this vein consists of thick, banded, milky white quartz which is often vuggy. Calcite is intergrown with the quartz in bands, but carbonate is not evenly distributed over the length of the vein. Zones where the vein is narrow contain less carbonate than wider parts of the veins. Vuggy bands in the vein are common, but bladed cavities are developed only locally.

The No. 2 vein pinches and swells several times along its length. Parts of the No. 2 vein show quartz-cemented breccia 'pods' rather than a definite vein. Quartz-cemented breccias are present along both hanging wall and footwall margins of much of the vein. These breccias grade outward to quartz-stockworked andesite or to sheared andesite



zones. Marginal breccias and/or andesite wallrock may show considerable brownish discoloration in parts of the adit. Wallrocks are altered to quartz, chlorite, and calcite to the extent that primary textures can rarely be distinguished.

At the level of the exploratory roadcut, the large quartz veins show development of bladed cavities lined with drusy quartz. Smaller veins consisting of chalcedonic quartz with open space textures also crop out on the roadcut. The quartz and quartz-calcite veins are associated with known mineralization.

#### FLUID INCLUSIONS

Fluid inclusion data for primary inclusions in the No. 2 vein at the level of the adit is shown in Figure 14. Inclusions gave homogenization ranges of 220<sup>o</sup> to 259<sup>o</sup> C and freezing ranges of -0.6<sup>o</sup> to -1.0<sup>o</sup> C. Daughter minerals were not observed in the inclusions. Plotting the homogenization temperatures on a depth vs. boiling temperature curve (Fig. 15) gives minimum depths of 300 to 600 m for formation of the system. The freezing ranges indicate fluids of very low salinities of less than 1% NaCl equivalent.

Although two-phase inclusions were observed to have vapor bubbles of varying size relative to the size of the inclusions, the range of bubble sizes was not large enough to be taken as conclusive evidence for boiling of the fluids (Roedder, 1984).

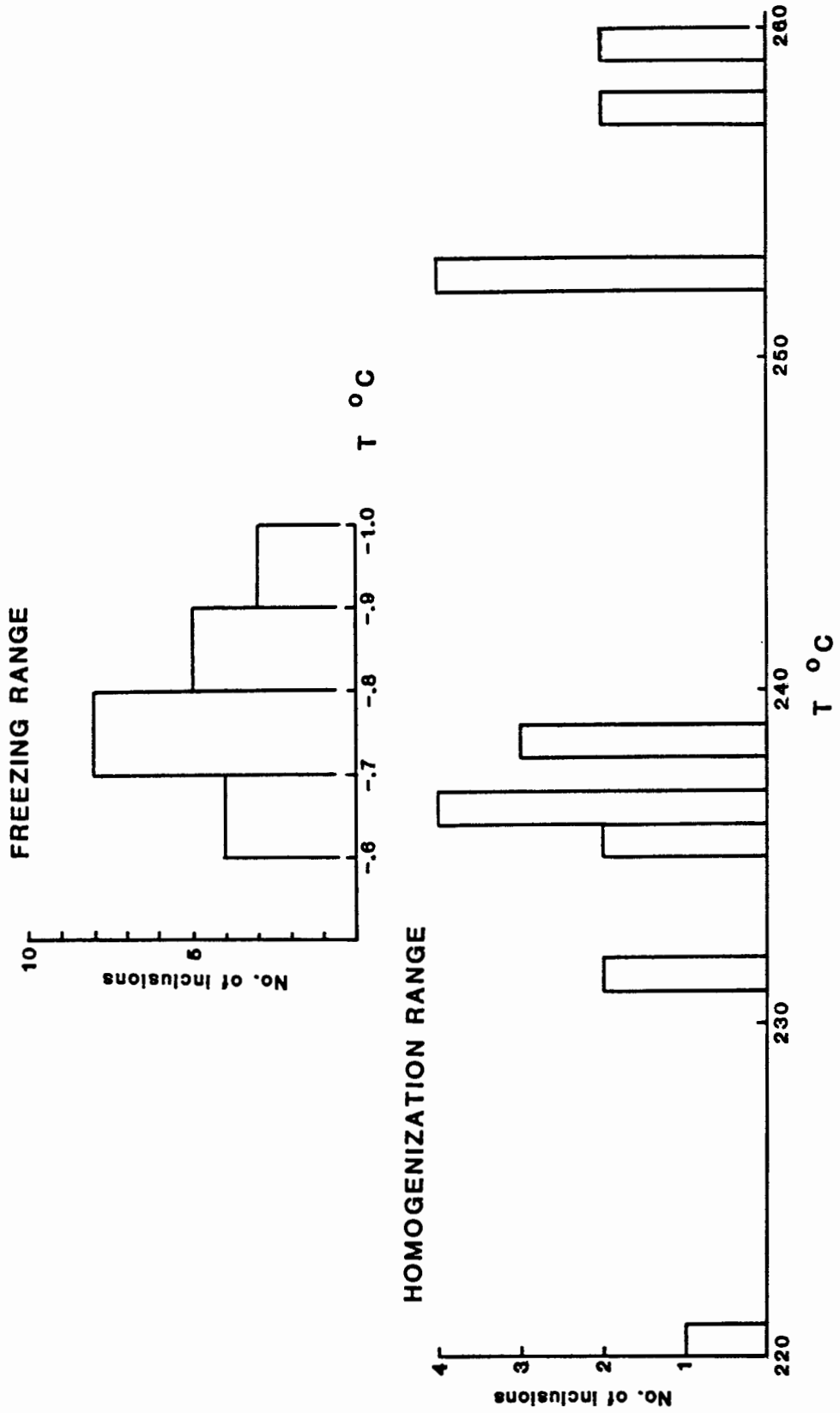


Figure 14. Fluid inclusion data.

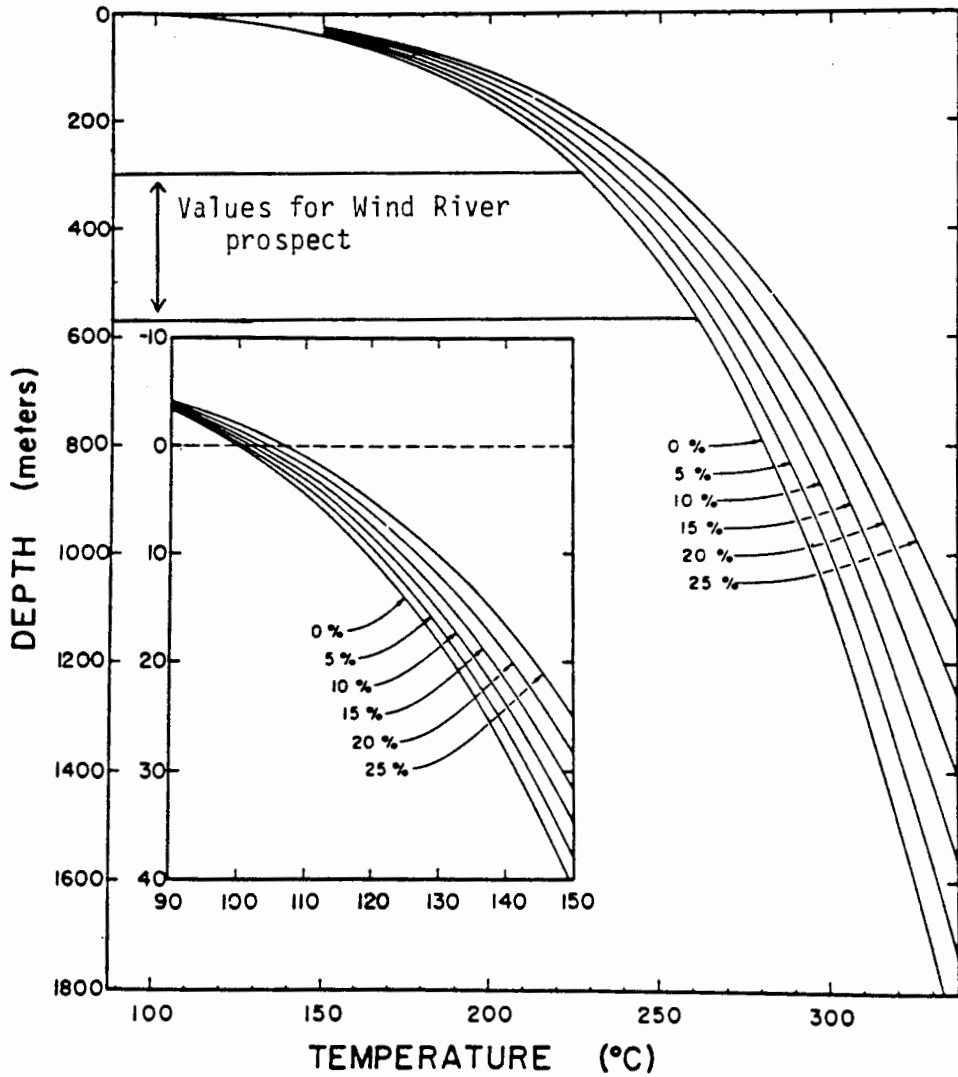


Figure 15. Depth vs. boiling curves. Percentages indicate wt percent NaCl for brines of constant composition (from Haas, 1971).

## GEOCHEMISTRY

### INTRODUCTION

Trace element geochemistry for a total of 122 samples from the Wind River area was determined by instrumental neutron activation analysis (INAA). Data for these samples and sample preparation methods are given in Appendix A. Rare earth element (REE) values used for normalization in chondrite-normalized REE plots were taken from the data of Ekambaram and others (1984). These values are also given in Appendix A.

### ANDESITES

Eleven samples of andesite flows were collected from different parts of the study area and at different stratigraphic levels within the A<sub>1</sub> and A<sub>2</sub> flow groups. Alteration of the lavas is weak. These samples were analyzed geochemically to determine the variation in trace element chemistry of the Ohanapecosh lava flows. Trace element chemistry for A<sub>1</sub> and A<sub>2</sub> flows is summarized in Table I.

Figure 16 is a plot of the incompatible elements Th vs. Hf and shows that the andesites of A<sub>1</sub> and A<sub>2</sub> are not distinguished from each other on this basis. Figure 17 shows plots of Co vs. Hf and Co vs. Ta, respectively. While all the A<sub>2</sub> lavas plot in one group in these

TABLE I

TRACE ELEMENT VALUES FOR A AND A ANDESITES

SAMPLE	A <sub>1</sub>					A <sub>2</sub>				
	201-1	203-1	FC152a-3	NB-3	PCNT2-5	WRH-1A1	101-2	127-1	PT124-3	6401-5B
La/Sm *	2.47	2.55	2.48	2.26	2.80	2.49	2.45	2.41	2.40	2.68
La/Yb *	3.89	4.68	4.60	3.98	5.34	4.49	4.35	3.93	3.94	4.61
Tb/Yb *	1.09	1.32	1.17	1.16	1.28	1.22	.93	.98	.89	1.25
% Fe 0 2 3	8.58	6.56	7.00	7.94	6.15	8.27	6.85	8.00	8.17	7.51
Sc ppm	20.25	13.95	17.46	19.51	13.71	19.86	18.40	22.11	19.99	20.68
Co ppm	20.90	9.80	12.70	17.30	11.40	18.70	18.10	19.70	20.45	17.30
Hf ppm	6.60	7.40	6.40	6.70	6.70	5.70	3.90	5.00	5.40	5.50
Ta ppm	1.30	1.17	1.13	1.56	1.02	1.28	.77	.91	1.10	1.20
Th ppm	6.75	7.60	6.80	7.20	9.20	5.00	3.45	5.60	5.75	6.90
As ppm	-	2.30	-	-	-	-	10.65	-	10.15	-
Sb ppm (2)	-	.98	-	-	-	-	-	-	-	.62
As/Sb	-	2.35	-	-	-	-	-	-	-	-

\* Chondrite-normalized REE values

(2) Weighted average of 57% <sup>122</sup>Sb, 43% <sup>124</sup>Sb

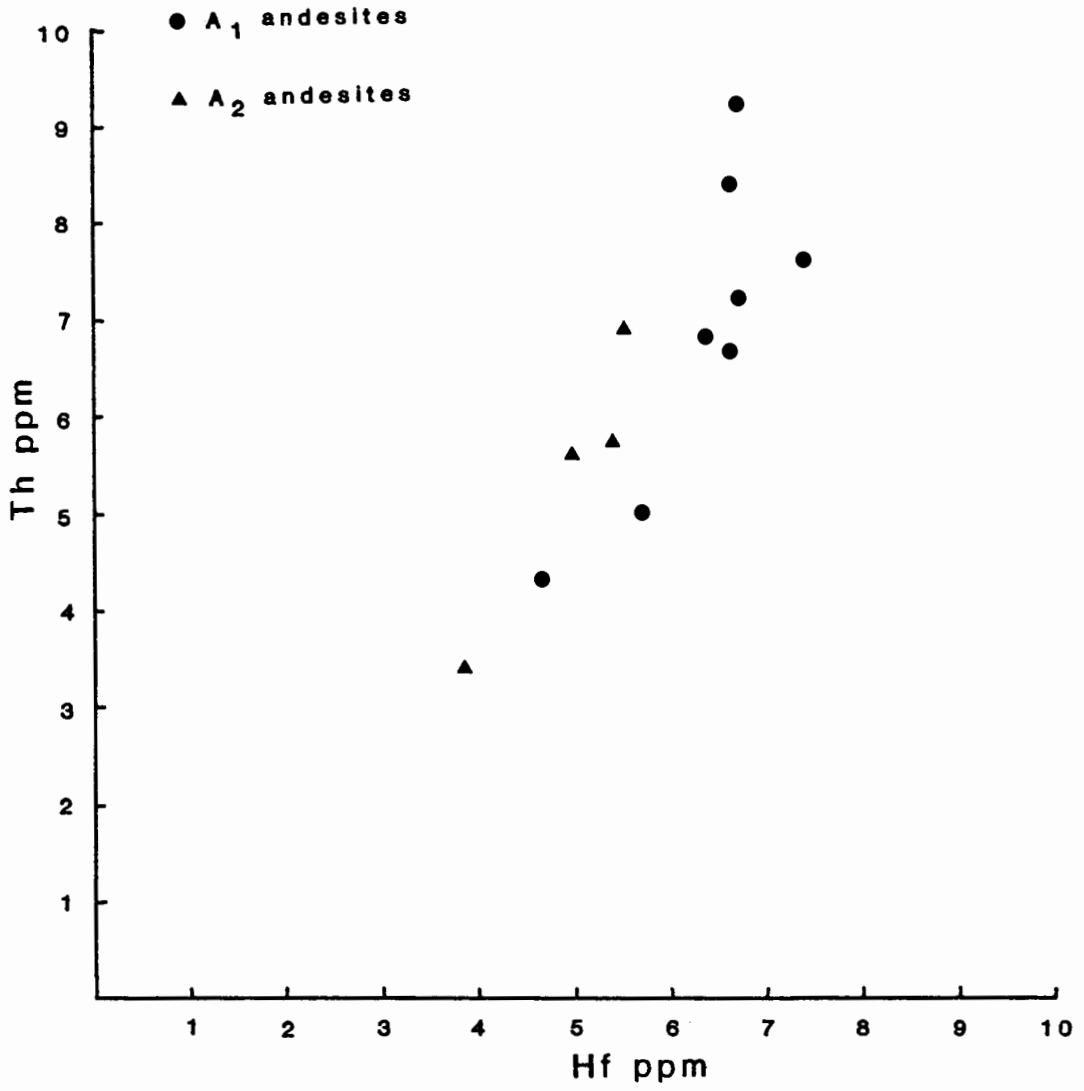


Figure 16. Th vs. Hf for A<sub>1</sub> and A<sub>2</sub> andesites.

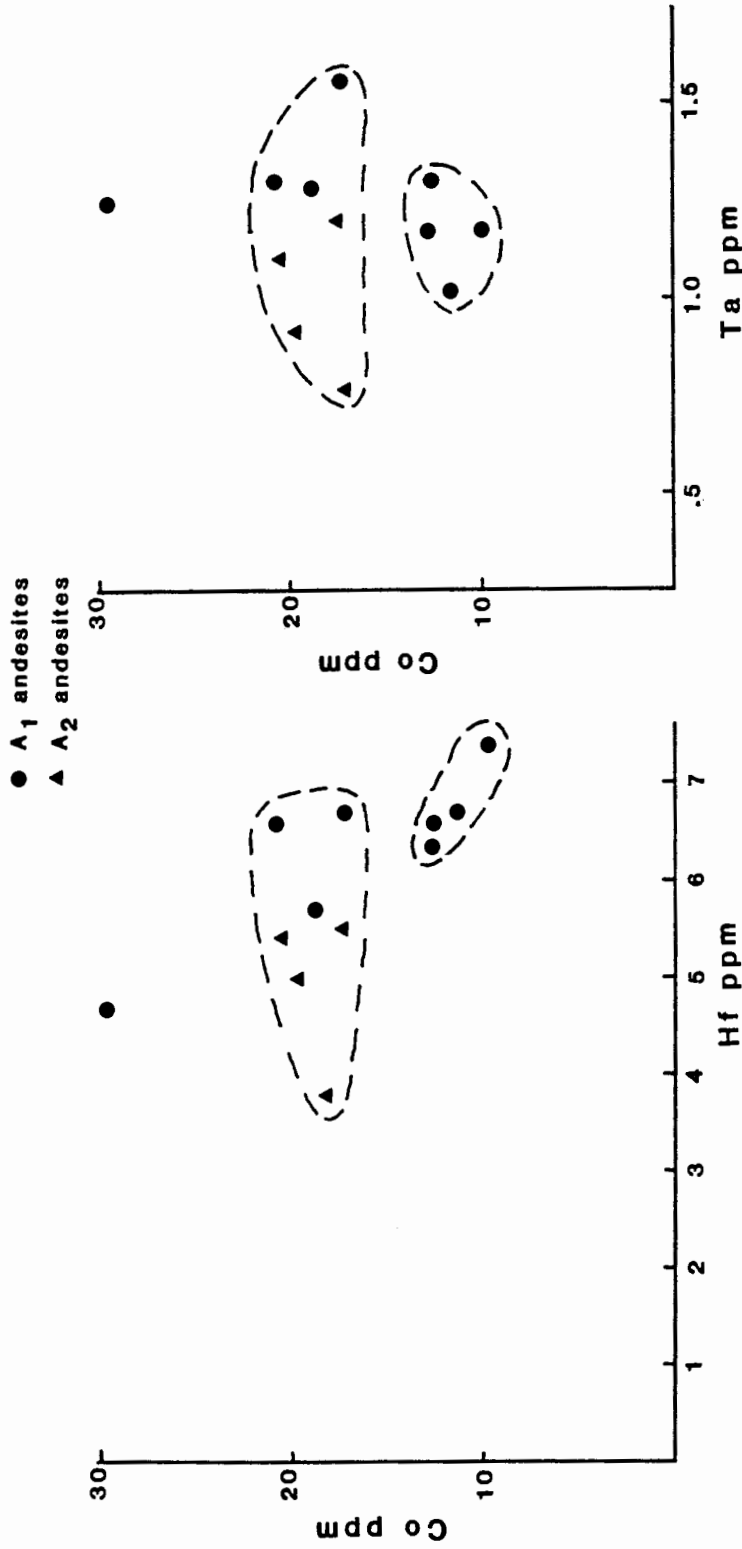


Figure 17. Co vs. Hf and Co vs. Ta for A<sub>1</sub> and A<sub>2</sub> andesites.

diagrams, the A<sub>1</sub> lavas are distributed between groups.

Rare earth element plots for the lavas are shown in Figure 18.

The lavas show some difference in their REE patterns. A<sub>1</sub> lavas have a more pronounced negative Eu anomaly and higher total REE abundances than do A<sub>2</sub> lavas. Ratios of La/Sm, La/Yb, and Tb/Yb are all generally lower for the A<sub>2</sub> flows. Absolute amounts of REE are somewhat lower for the A<sub>2</sub> lavas. A<sub>2</sub> lavas have a flatter slope in the heavy REE range. Although the A<sub>1</sub> and A<sub>2</sub> lavas may be distinguished on the basis of field criteria, geochemically they do not separate well into two distinct groups.

## DIKES

On the basis of field and petrographic studies, two groups of dikes were distinguished along the exploratory roadcut. These dikes were studied geochemically to determine whether or not the groups of dikes could be distinguished by their trace element chemistry. Also, the dikes can be traced into the zone of most intense alteration, and changes in trace element content with increasing degree of alteration can be observed. Study of alteration in the dikes is advantageous in that the dikes have fewer bulk compositional variables affecting them than do the surrounding pyroclastic rocks. A third dike, D<sub>2</sub>, represented by three samples, was distinguished geochemically. Trace element data for these dikes is summarized in Tables II and III.

Figure 19 shows plots of the incompatible elements Th vs. Hf and Th vs. Ta for D<sub>1</sub>, D<sub>2</sub>, and D<sub>3</sub> dikes. These graphs show three groups of dikes. The D<sub>2</sub> dike was found to be chemically distinct from D<sub>3</sub> and D<sub>1</sub> dikes in that it is higher in Th and lower in Hf.



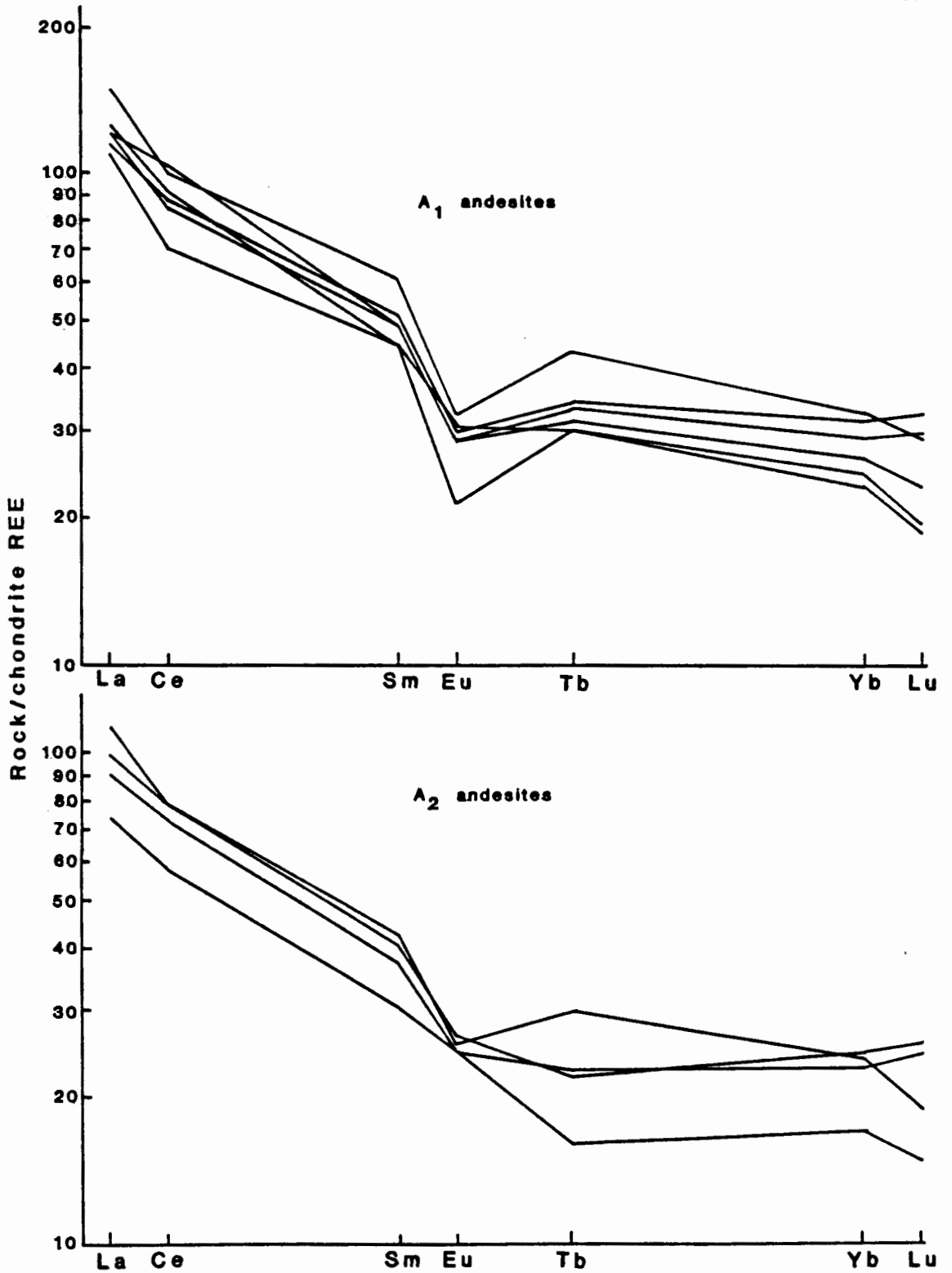


Figure 18. Chondrite-normalized REE plots for A<sub>1</sub> and A<sub>2</sub> andesites.

TABLE II  
TRACE ELEMENT VALUES FOR D<sub>2</sub> AND D<sub>3</sub> DIKES

SAMPLE	D <sub>3</sub>			D <sub>2</sub>			WRR-57		
	WRR-1C	WRR-5	WRR-6	WRR-8	MF24-40	WRR-52		WRR-53	WRR-58
La/Sm *	2.19	2.25	2.33	2.28	2.30	3.04	2.95	2.96	2.66
La/Yb *	3.25	4.25	3.40	3.70	5.75	5.36	4.88	5.39	5.75
Tb/Yb *	.99	1.22	.78	1.02	1.58	1.44	.96	1.33	1.50
% Fe O <sub>2,3</sub>	9.91	8.88	8.91	8.94	8.85	5.68	6.26	4.06	1.86
Sc ppm	27.01	24.92	24.82	25.41	21.09	15.00	15.96	13.52	4.39
Co ppm	31.30	24.90	25.10	25.40	30.70	14.30	14.60	11.60	3.44
Hf ppm	3.70	4.90	4.70	5.20	4.60	3.00	3.00	3.00	1.70
Ta ppm	.70	.94	.80	.94	1.17	1.05	.93	1.08	.29
Th ppm	3.40	4.80	4.50	4.80	4.10	10.60	10.10	10.40	2.71
As ppm	-	-	1.50	12.40	16.10	22.60	15.96	25.70	47.90
Sb ppm (2)	2.70	2.31	2.03	1.83	3.30	2.19	2.14	1.93	14.65
As/Sb	-	-	.74	6.78	4.88	10.32	7.43	13.32	3.27

\* Chondrite-normalized REE values  
122 124  
(2) Weighted average of 57% Sb, 43% Sb

TABLE III  
TRACE ELEMENT VALUES FOR D DIKES

SAMPLE	weakly altered		moderately altered				strongly altered					
	WRR-2B	R-023	MF9+20	MF15-20	WRR-TH2	MF17-55	MF22-20	MF21-20	R-019	R-025	R-036	84-CC1
La/Sm *	2.57	2.91	2.96	2.82	2.85	2.92	2.54	2.84	2.75	2.86	2.70	2.70
La/Yb *	4.70	4.88	4.57	4.68	5.73	6.09	4.00	4.80	5.01	5.01	6.02	4.38
Tb/Yb *	1.23	1.19	1.13	1.10	1.32	1.41	1.09	1.06	1.31	1.17	1.55	1.01
Zr ppm	7.25	6.34	5.83	6.55	5.65	5.26	6.11	7.25	5.27	4.75	5.27	5.42
Sc ppm	16.63	18.79	17.75	18.75	14.68	16.48	15.46	13.11	12.93	15.44	17.33	13.81
Co ppm	15.90	14.50	15.50	14.10	10.80	12.70	10.90	9.60	9.10	11.10	14.70	8.50
Hf ppm	6.30	5.30	4.80	5.90	6.50	5.60	6.70	6.40	7.50	7.90	7.50	7.10
Ta ppm	1.14	-.8	.74	1.05	1.14	.82	1.08	.96	.97	1.05	1.12	.97
Th ppm	7.50	6.90	7.00	7.60	8.10	6.60	8.20	8.40	7.50	7.90	7.50	7.10
As ppm	1.70	3.20	6.30	3.30	1.70	20.10	6.30	33.40	13.20	6.50	587.00	10.40
Sb ppm (2)	1.51	-	.90	.56	.80	1.26	1.67	1.44	1.16	1.32	2.40	.52
As/Sb	1.13	-	7.00	5.89	2.13	15.95	3.77	23.19	11.38	4.92	244.58	20.00

\* Chondrite-normalized REE values

(2) Weighted average of 57% <sup>122</sup>Sb, 43% <sup>124</sup>Sb

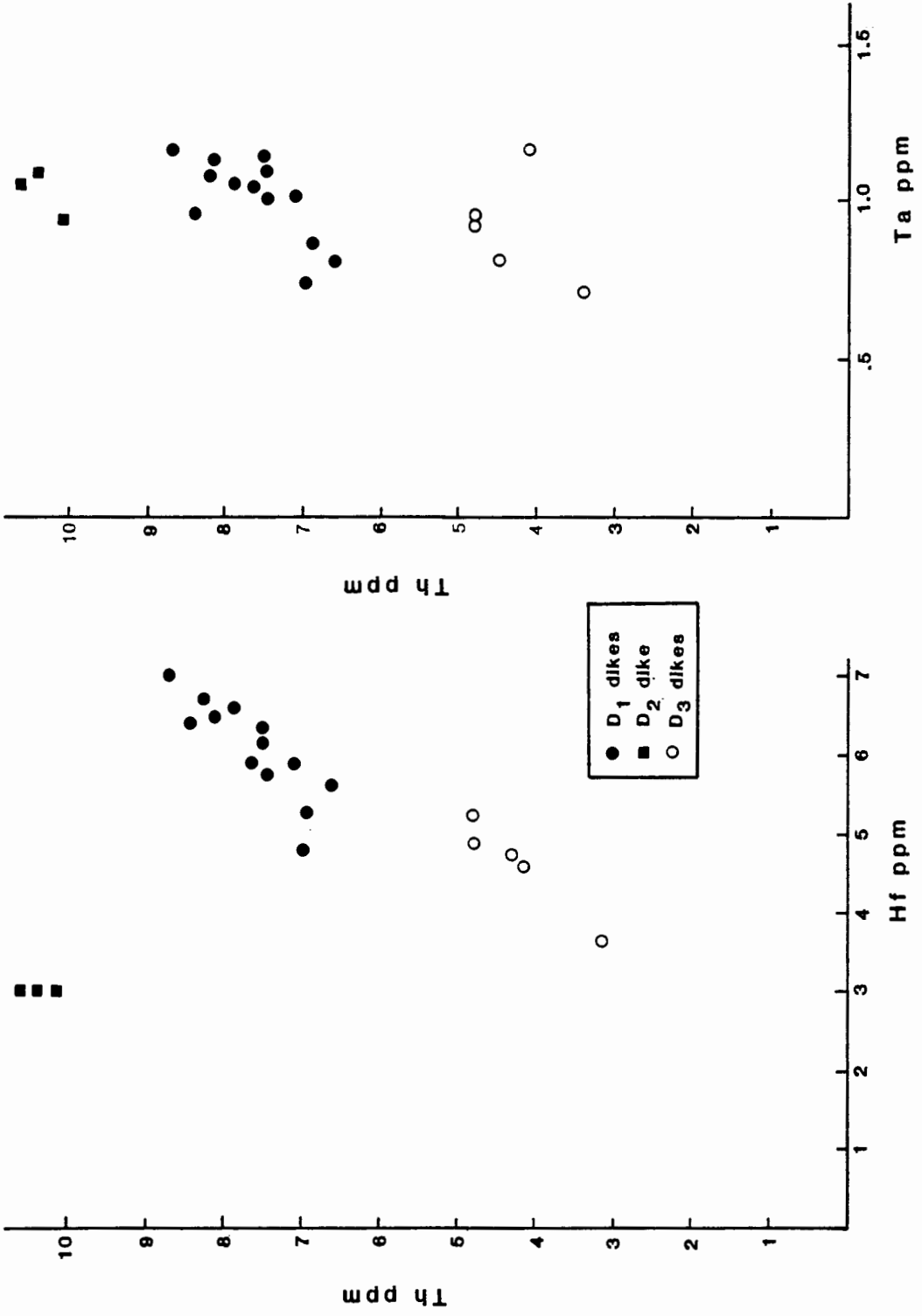


Figure 19. Th vs. Hf and Th vs. Ta for D<sub>1</sub>, D<sub>2</sub>, and D<sub>3</sub> dikes.

D<sub>3</sub> dikes are all weakly altered, but D<sub>1</sub> dikes do not all show the same degree of alteration. Changes in mineralogy and texture with increasing degree of alteration for these dikes are summarized in Figure 13. Plots of Co vs. Th and Co vs. Hf (Fig. 20) indicate a possible separation of the D<sub>1</sub> dikes into two subgroups. While Th and Hf are geochemically incompatible elements, Co is a compatible element, and along with Sc, Cr, Fe, is preferentially fractionated into mafic phases. Co and Sc are plotted vs. Fe<sub>2</sub>O<sub>3</sub> in Figure 21 for weakly, moderately, and strongly altered D<sub>1</sub> dikes. This plot shows a general decrease in Sc and Co with decreasing Fe<sub>2</sub>O<sub>3</sub> content of the dikes.

Rare earth element geochemistry for the D<sub>1</sub>, D<sub>2</sub>, and D<sub>3</sub> dikes is presented in Figures 22 to 24. Compared to the other dikes, D<sub>3</sub> dikes (Fig. 22) show only a slight negative Eu anomaly and greater variation in heavy REE values. Absolute concentrations of REE are somewhat lower than for the other dikes.

The D<sub>2</sub> dike samples (Fig. 22) are all from the same dike and were collected at different distances from the No. 2A quartz vein. The strongly altered sample represents bleached and sheared material collected from the margin of the quartz vein. No primary textures remain in this material. It plots parallel to and below the curves for the less altered samples. Ce and Eu both show depletions relative to less altered samples.

REE plots for D<sub>1</sub> dikes (Figs. 23 and 24) were grouped according to degree of alteration of the dikes. Range of REE values for all the dikes regardless of degree of alteration is given by the shaded area in Figure 24. REE patterns for weakly, moderately, and strongly altered

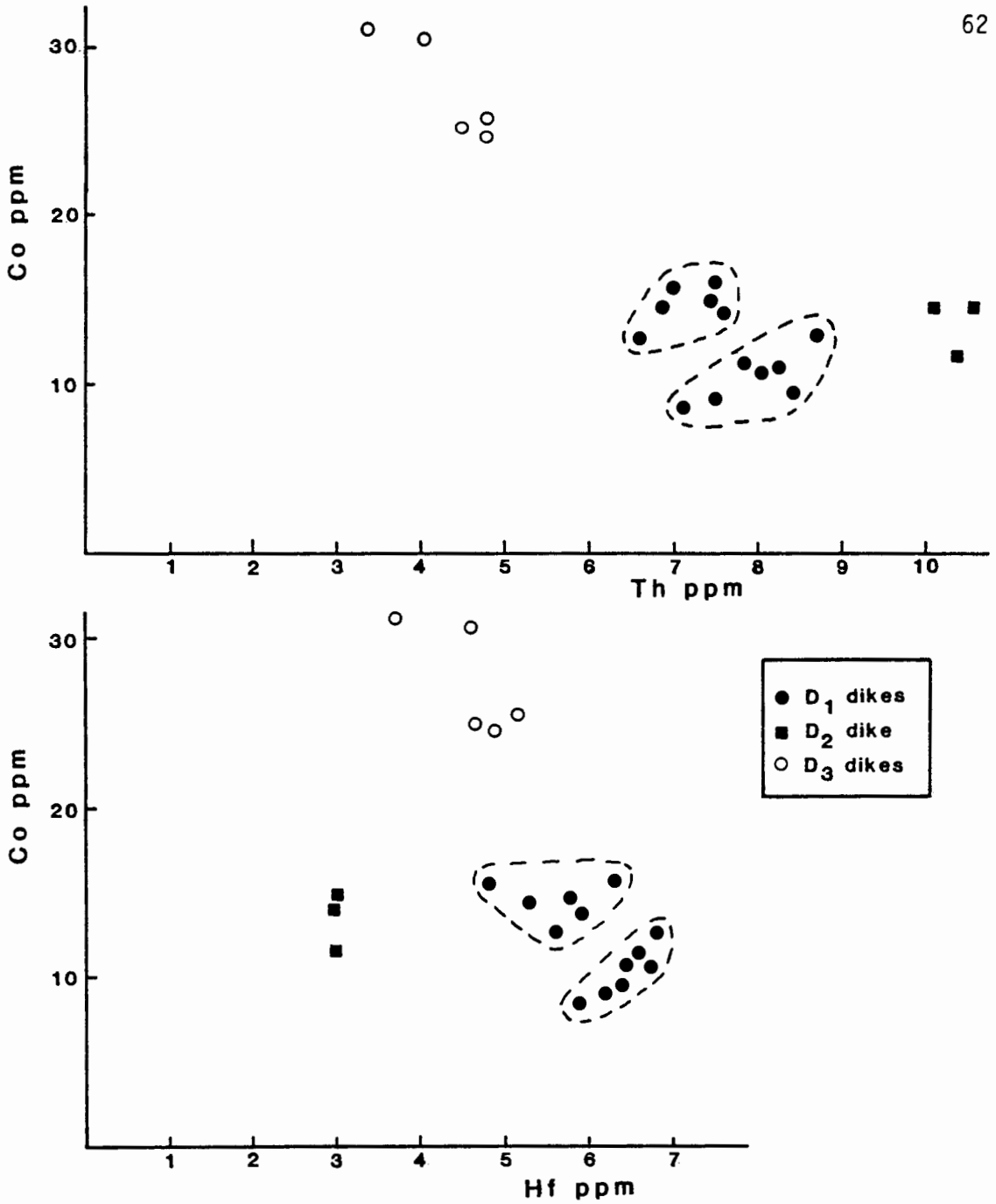


Figure 20. Co vs. Th and Co vs. Hf for D<sub>1</sub>, D<sub>2</sub>, and D<sub>3</sub> dikes.

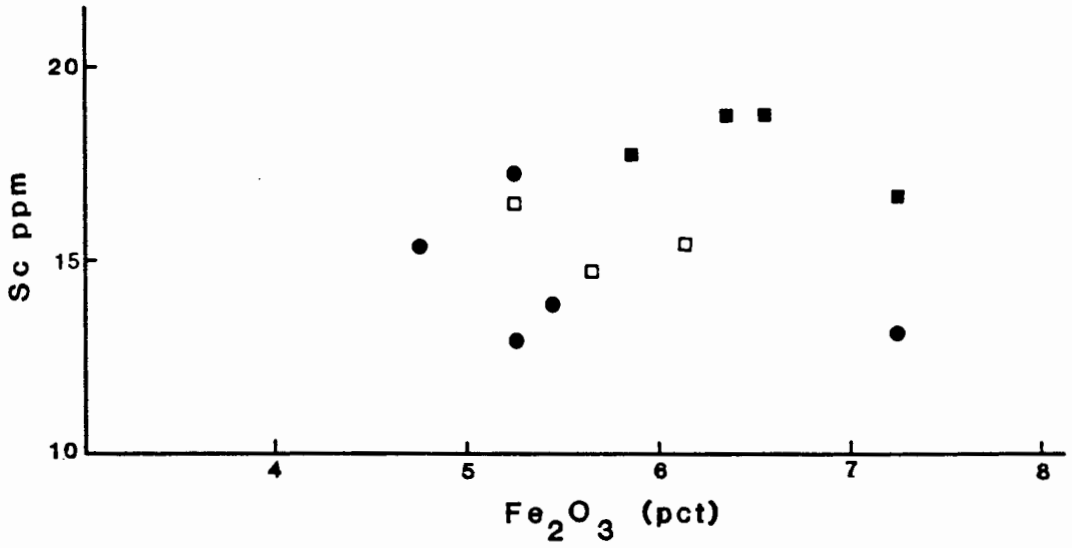
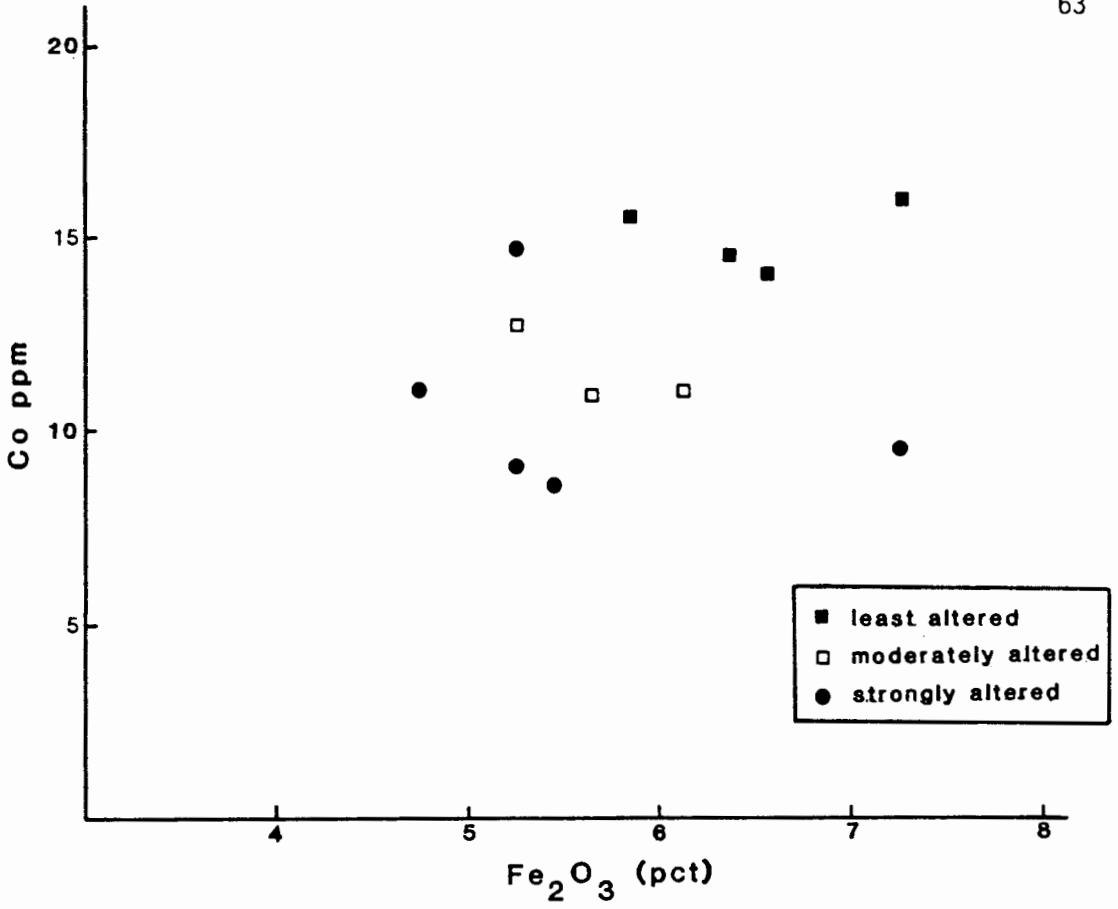


Figure 21. Co vs. Fe<sub>2</sub>O<sub>3</sub> and Sc vs. Fe<sub>2</sub>O<sub>3</sub> for D<sub>1</sub> dikes.

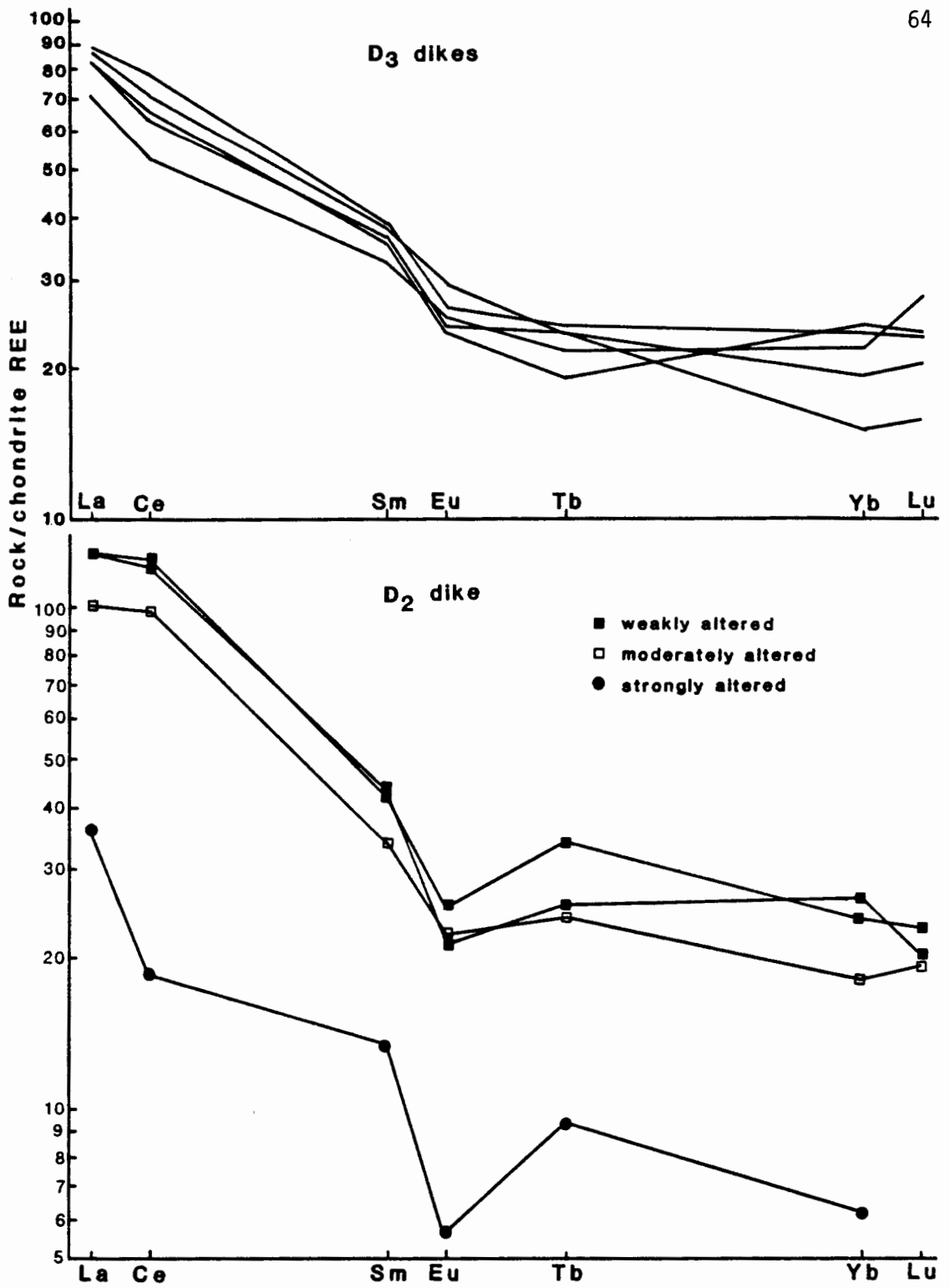


Figure 22. Chondrite-normalized REE plot for D<sub>3</sub> dikes and for weakly, moderately, and strongly altered D<sub>2</sub> dike samples.



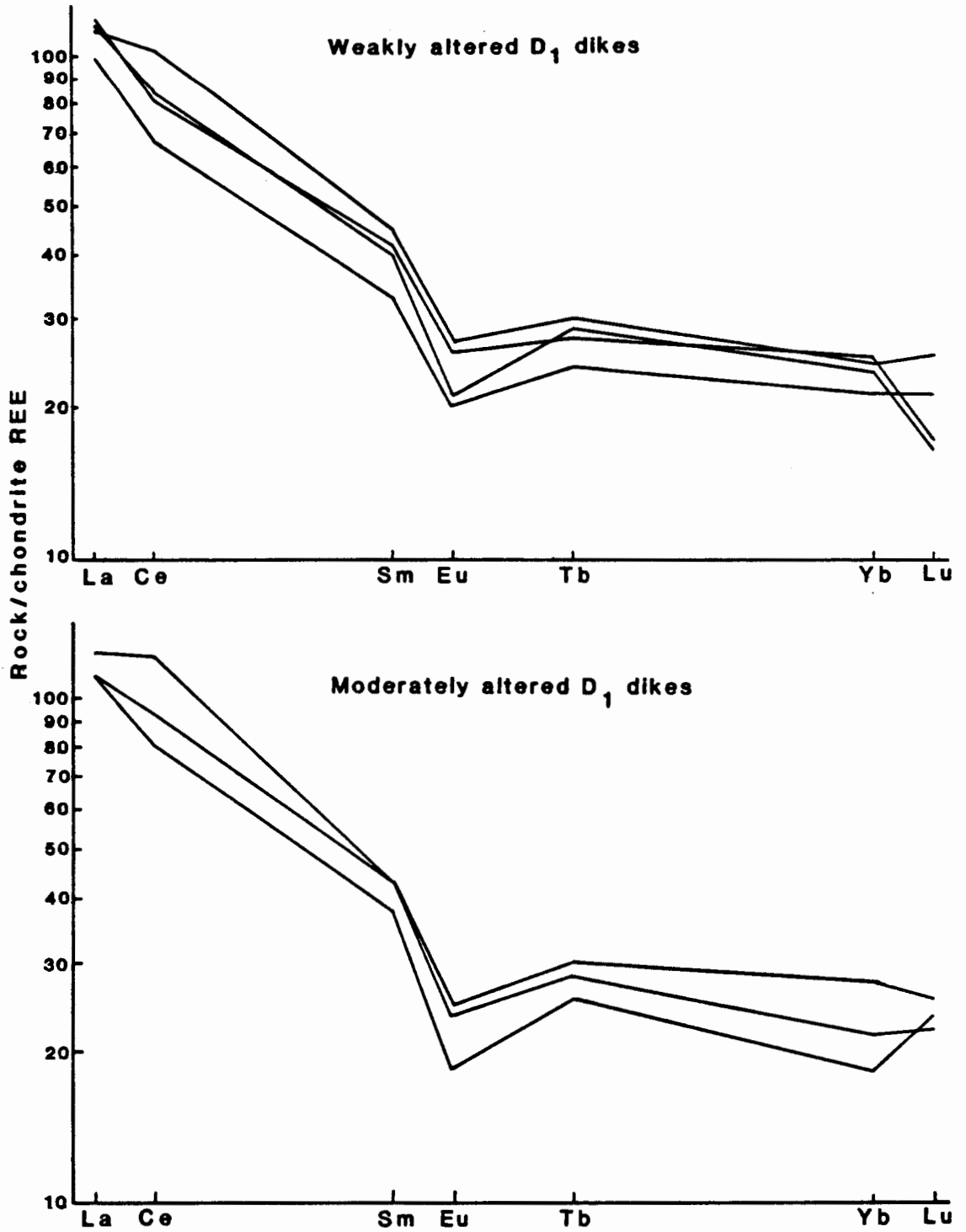


Figure 23. Chondrite-normalized REE plot for weakly and moderately altered D<sub>1</sub> dikes.

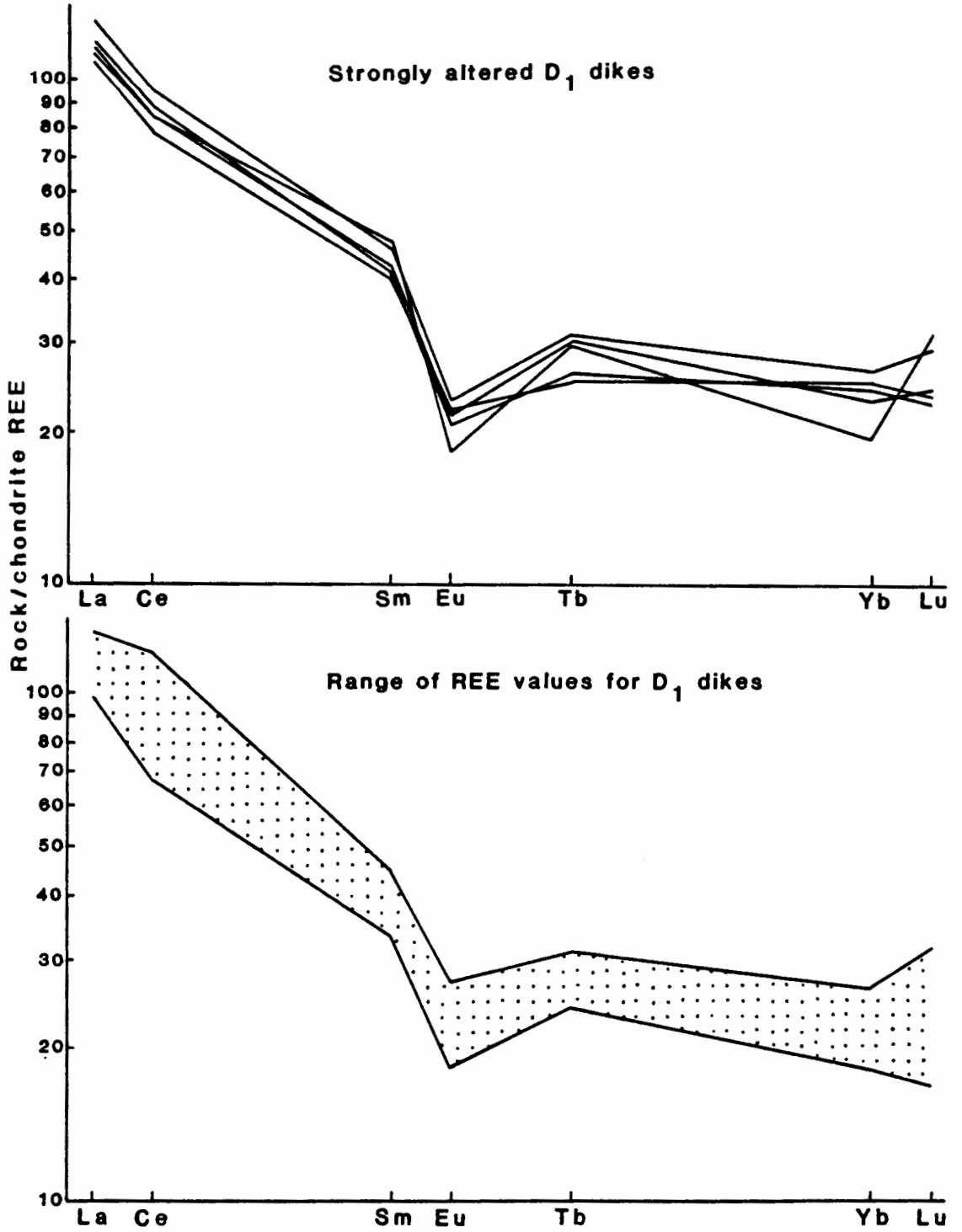


Figure 24. Chondrite-normalized REE plot for strongly altered D<sub>1</sub> dikes and range of REE values for D<sub>1</sub> dikes regardless of alteration.

dikes are very similar in shape of the curve and in total REE abundance.

#### LAVAS AND DIKES

A plot of La/Sm vs. Th for A<sub>1</sub> and A<sub>2</sub> andesites and D<sub>1</sub>, D<sub>2</sub>, and D<sub>3</sub> dikes is shown in Figure 25. In general, the D<sub>3</sub> dikes and A<sub>2</sub> lavas form one group, while D<sub>1</sub> dikes and A<sub>1</sub> lavas form another group.

#### TYPES 1 AND 2 ALTERATION

Samples from Types 1 and 2 alteration are identified in Appendix A. Geochemical anomalies of Sb were detected in breccia quartz and clasts from Type 1 alteration. Anomalies of As and Sb were detected in rocks from Type 2 alteration zones.

#### TUFFS

REE plots for two sets of tuffs are shown in Figure 26. Tuffs within each group show different degrees of alteration. The REE patterns for the tuffs are observed to shift to lower values with increasing degree of alteration. In Figure 26, the T<sub>4</sub> tuffs show a slight spread in the light REE and larger Eu depletions relative to the least altered sample than do the T<sub>3</sub> tuffs.

Figure 27 shows REE plots for a set of strongly altered tuffs from the top switchback of the exploratory roadcut, at higher elevations than the tuffs in Figure 26. These tuffs are strongly altered and contain varying proportions of clay minerals and quartz. The most clay-rich and the most quartz-rich samples are indicated in the graph. The other tuffs represent intermediates between these two extremes. The tuffs are seen to show a fanning in the light REE range and a tight clustering in the middle and heavy REE range. A less altered tuff is shown for

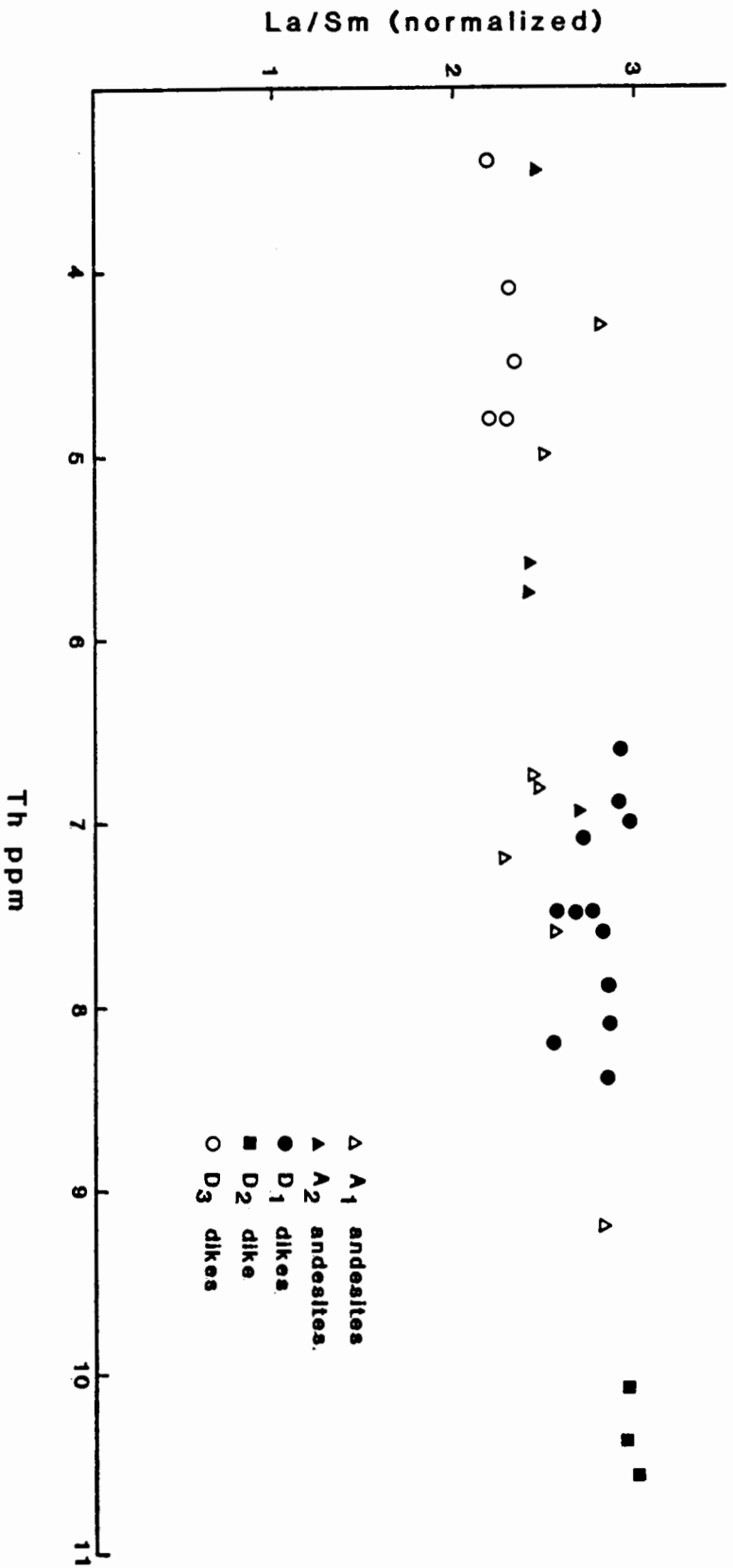


Figure 25. La/Sm vs. Th for A<sub>1</sub> and A<sub>2</sub> lavas and D<sub>1</sub>, D<sub>2</sub>, and D<sub>3</sub> dikes.

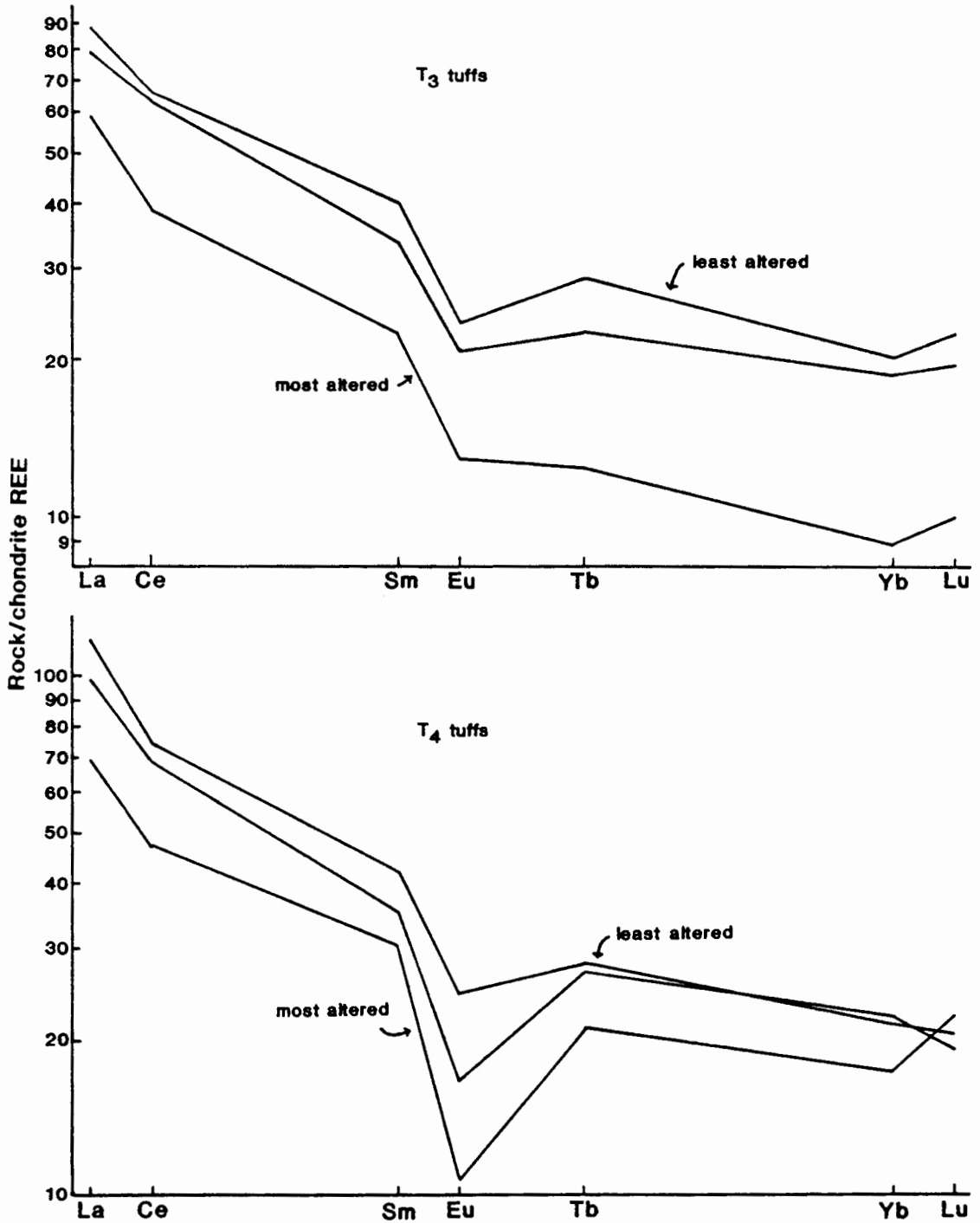


Figure 26. Chondrite-normalized REE plot for altered T<sub>3</sub> and T<sub>4</sub> tuffs.

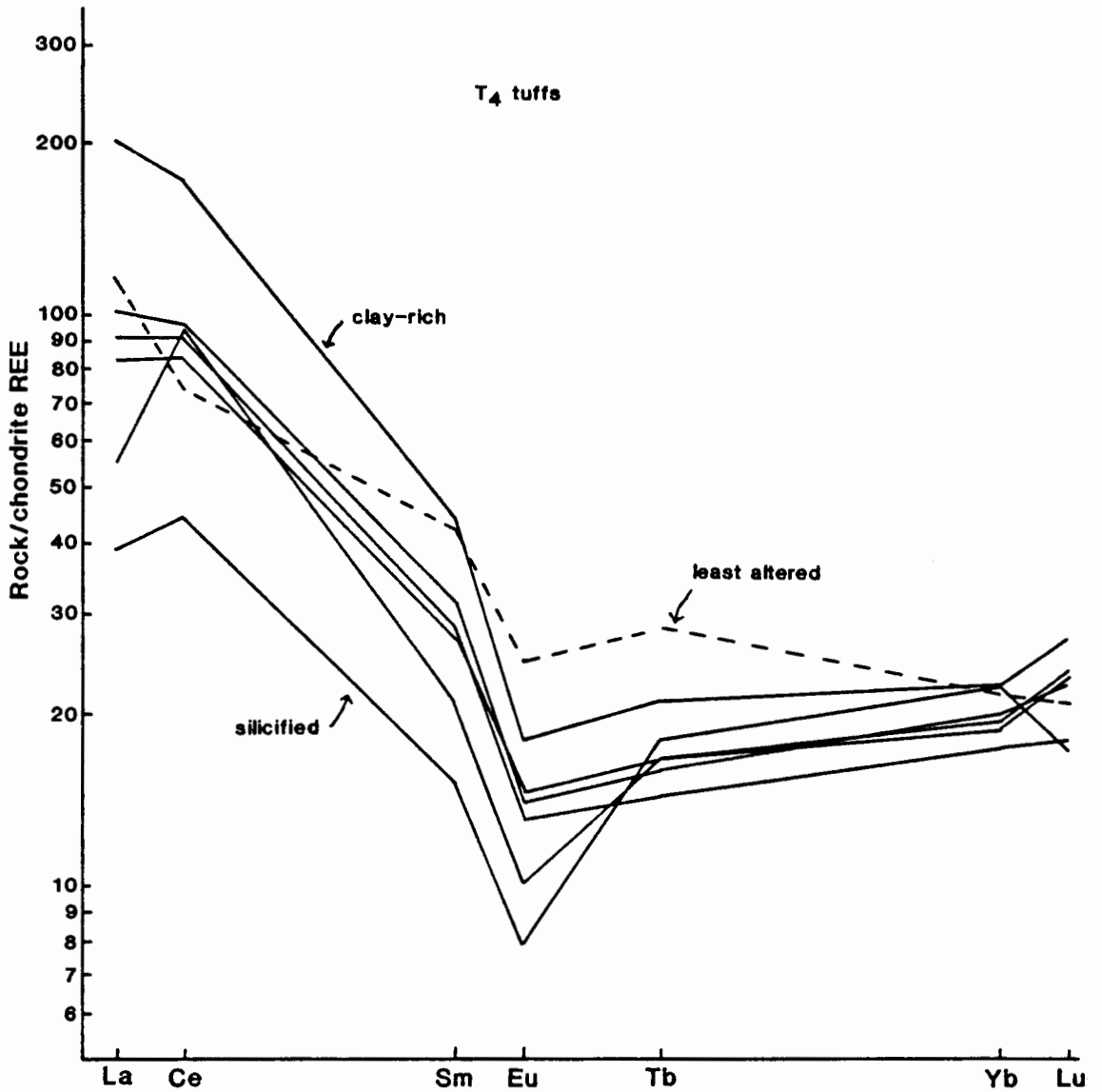


Figure 27. Chondrite-normalized REE plot for altered  $T_4$  tuffs from the top switchback of the exploratory roadcut.

comparison. The middle and heavy REE part of the curve is seen to have changed direction of slope relative to the less altered tuff.

#### NO. 5 STRUCTURE

Samples from the No. 5 structure are identified in Appendix A. Geochemical anomalies of Au, Ag, As, Sb, Hg, and W were detected in rocks from this structure.

Figure 28 shows REE patterns for rocks from the No. 5 structure. Samples were collected from the lower and middle switchbacks of the exploratory roadcut (Plate 2). The samples show some variation of REE abundances within the group, but form a continuous spectrum over the range of REE values represented. The curves show strong parallelism with one another.

#### NO. 2 VEIN

Detailed sample traverses were made across the No. 2 vein in the adit at several locations (see Plate 3 for locations of traverses). The traverse at station C includes channel samples as well as grab samples. The traverse in the small stope past station G includes only grab samples. Trace element data for samples from these traverses is summarized in Table IV.

A sketch of the vein and surrounding wallrock zones in the adit at station C is shown in Figure 29. REE data for hanging wall and footwall vein margin samples at station C are shown in Figures 30 and 31. Footwall green andesite samples are observed to show two patterns, one of which has only a slight negative Eu anomaly and a flat pattern in the heavy REE range. Samples from the footwall andesite breccia zone plot

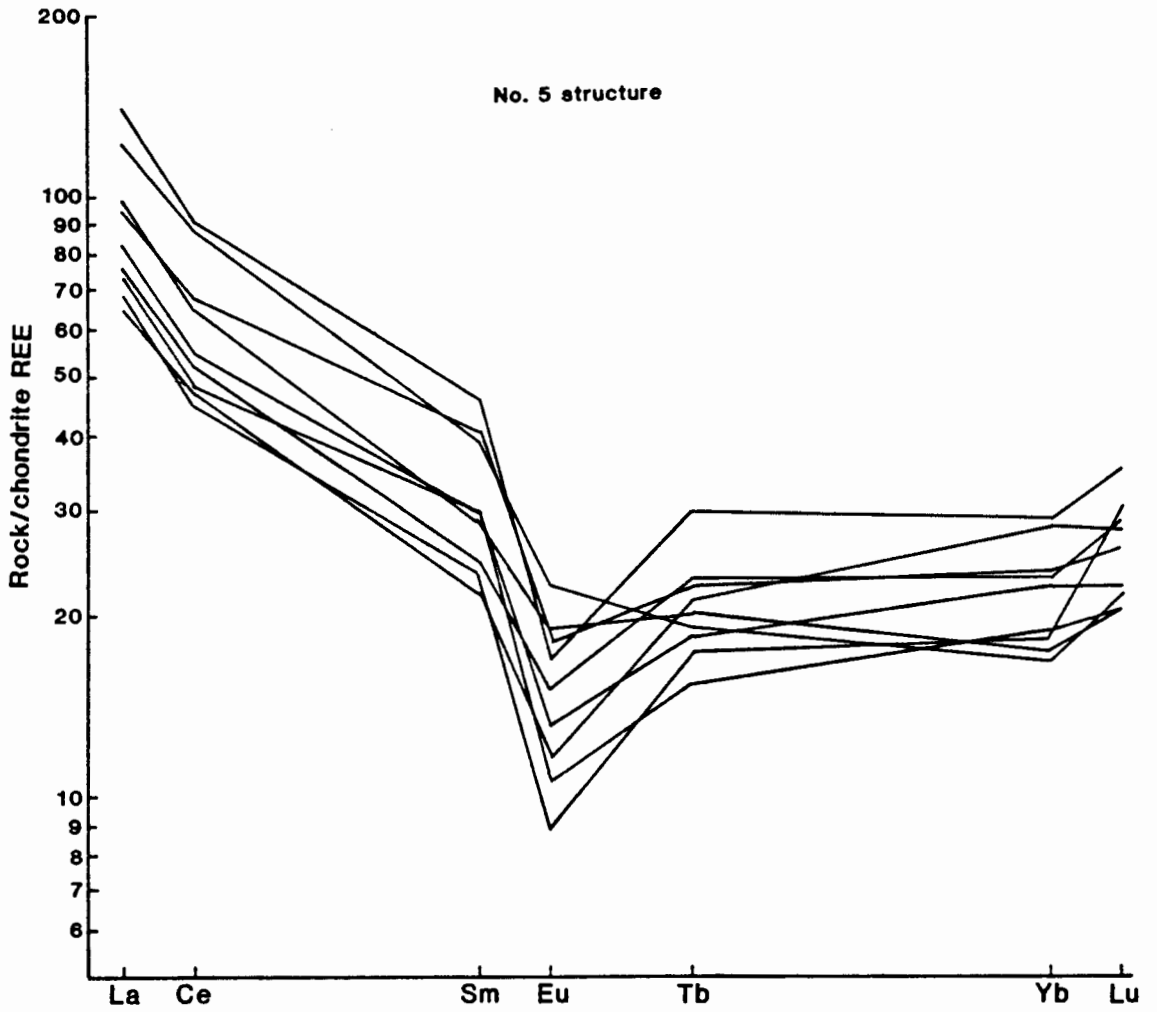


Figure 28. Chondrite-normalized REE plot for samples from the No. 5 structure.



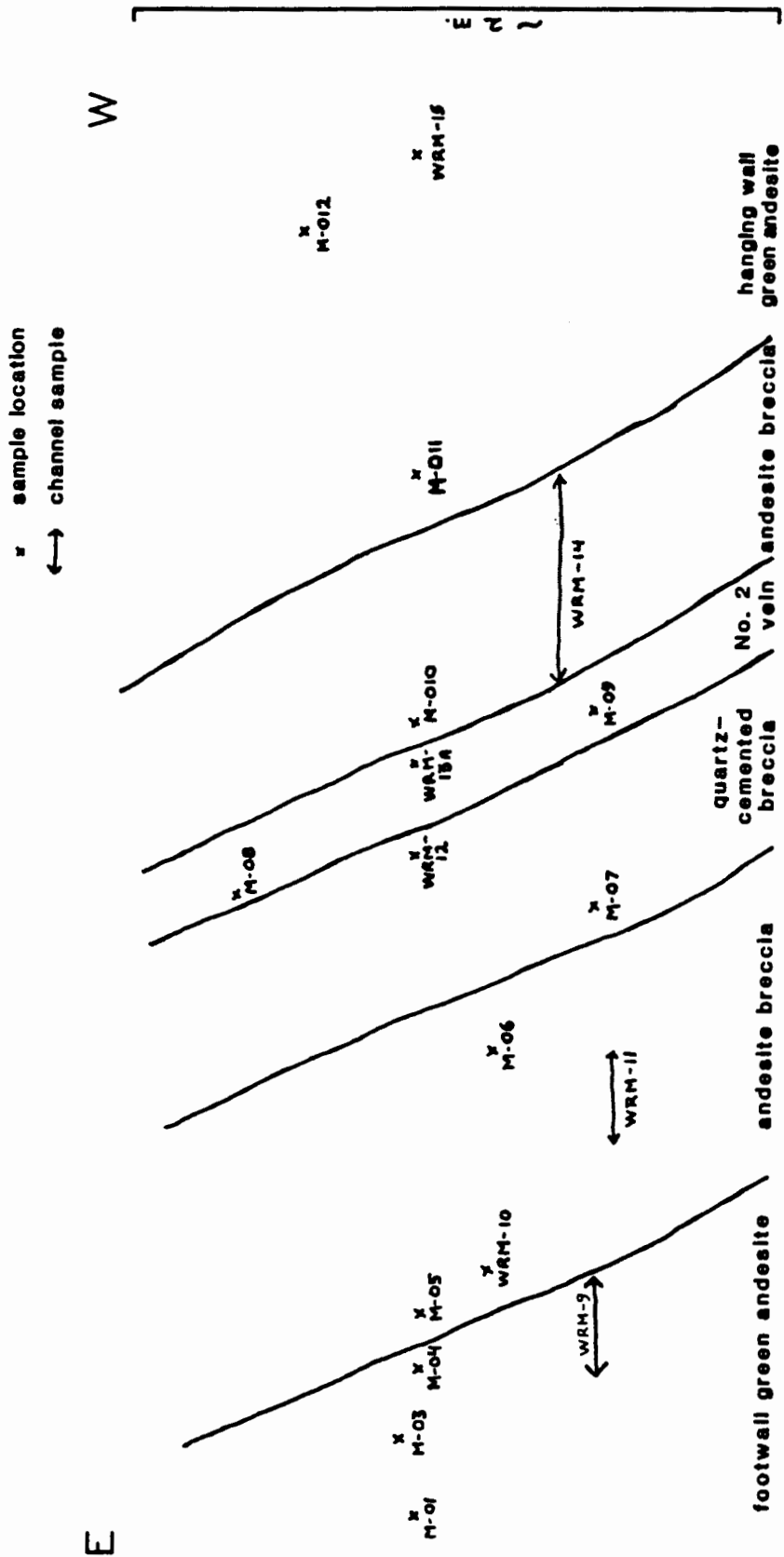


Figure 29. Sketch of the No. 2 vein and wallrock zones in the adit at station C.

TABLE IV  
STATION C

TRACE ELEMENT VALUES FOR SAMPLES FROM THE ADIT

SAMPLE	footwall green andesite			footwall andesite breccia			footwall quartz-cemented breccia				
	M-01	M-03	M-04	WRM-1	WRM-9 (ch)	M-05	M-06	WRM-10	WRM-11 (ch)	M-07	WRM-12
La/Sm *	2.17	2.48	2.46	2.70	2.19	2.50	2.59	2.77	2.49	2.23	2.29
La/Yb *	3.49	4.01	4.65	4.90	4.15	5.46	-	7.10	6.54	4.46	3.77
Tb/Yb *	1.11	1.18	1.41	1.19	.91	1.20	-	1.40	1.80	1.01	1.28
Au ppm	-	-	-	-	-	.14	.49	.38	.22	.01	.02
As ppm	9.30	9.80	16.40	17.90	12.60	89.80	77.40	129.70	91.80	37.30	44.50
Sb ppm (2)	.78	.67	1.15	1.19	1.46	4.52	6.58	4.26	5.51	5.32	6.70
As/Sb	11.92	14.63	14.26	15.04	8.63	19.87	11.76	30.45	16.66	7.01	6.64
Ag (3)	-	-	-	-	-	-	-	-	-	-	-
Hg (3)	-	-	-	-	-	-	-	-	-	-	-

(ch) Channel sample

\* Chondrite-normalized REE values

122 124

(2) Weighted average of 57% Sb, 43% Sb

(3) This element was detected in samples designated 'yes', but concentrations in ppm are not available.

TABLE IV (continued)

SAMPLE	vein		hanging wall andesite breccia		hanging wall green andesite	
	M-08	M-09	M-010	WRM-14 (ch)	M-011	M-012 WRM-15
La/Sm *	-	-	2.61	2.89	2.74	2.14 2.63
La/Yb *	-	-	5.94	5.82	3.27	4.08 6.06
Tb/Yb *	-	-	1.57	1.03	.88	1.39 1.32
Au ppm	16.65	.07	-	.03	-	- -
As ppm	2.25	.49	21.50	99.90	43.60	46.30 7.10
Sb ppm (2)	24.75	12.22	3.50	3.60	1.11	1.50 -
As/Sb	.09	.04	6.14	27.73	39.28	30.87 -
Ag (3)	yes	yes	-	-	-	- -
Hg (3)	yes	yes	-	-	-	- -

TABLE IV (continued)  
STOPE PAST STATION G

SAMPLE	footwall green andesite	footwall breccia	vein	hanging wall andesite breccia	hanging wall green andesite
	M-042	M-043	M-045	M-046	M-048
La/Sm *	2.56	2.89	1.98	1.95	2.09
La/Yb *	3.80	4.89	-	-	3.30
Tb/Yb *	1.13	1.35	-	-	1.12
Au ppm	-	-	26.00	.88	-
As ppm	5.80	11.80	.66	4.04	13.70
Sb (2)	.66	.93	10.46	7.20	1.32
As/Sb	8.79	12.69	.06	.56	10.38
Ag (3)	-	-	yes	yes	-
Hg (3)	-	-	-	-	-

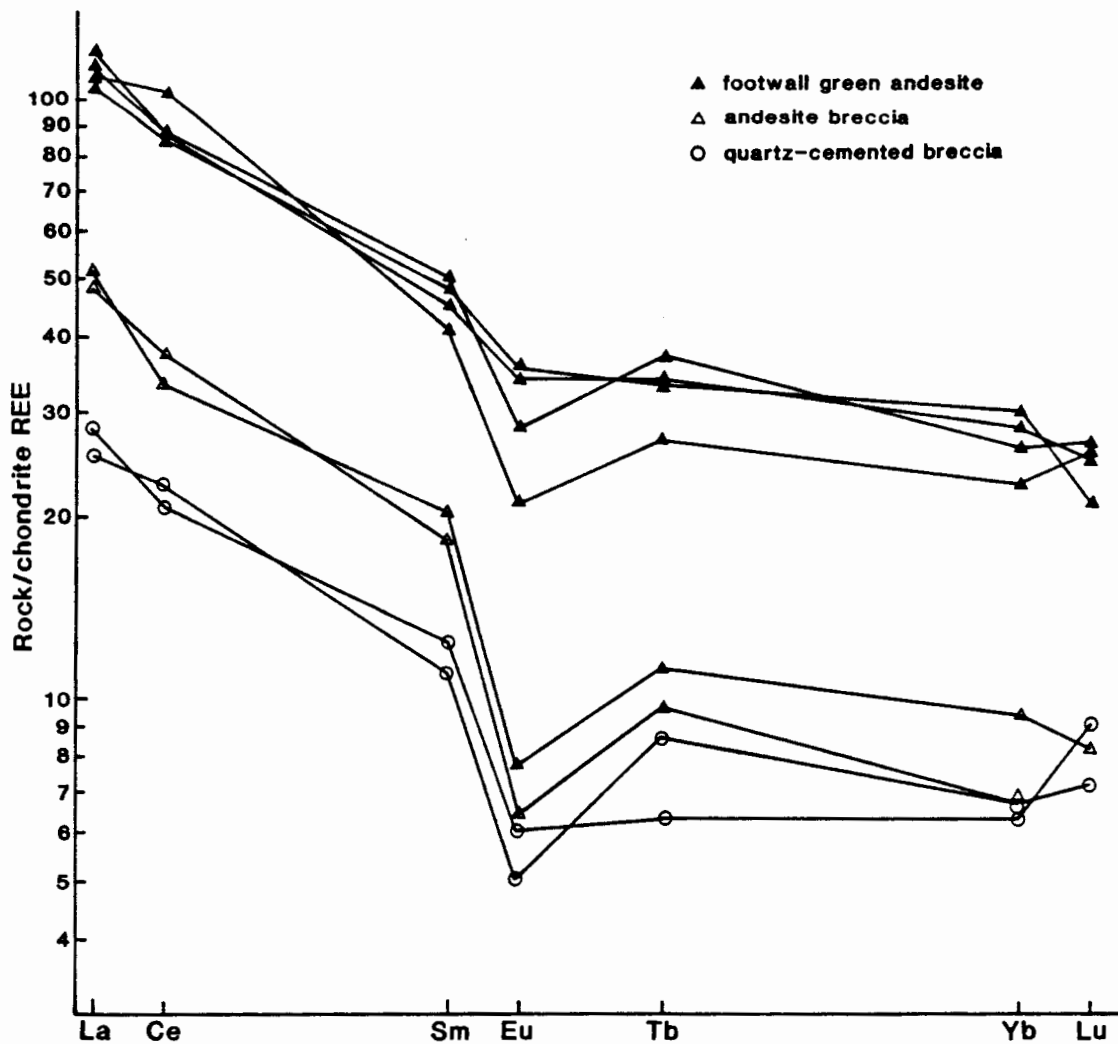


Figure 30. Chondrite-normalized REE plot for samples from the footwall of the No. 2 vein in the adit at station C.

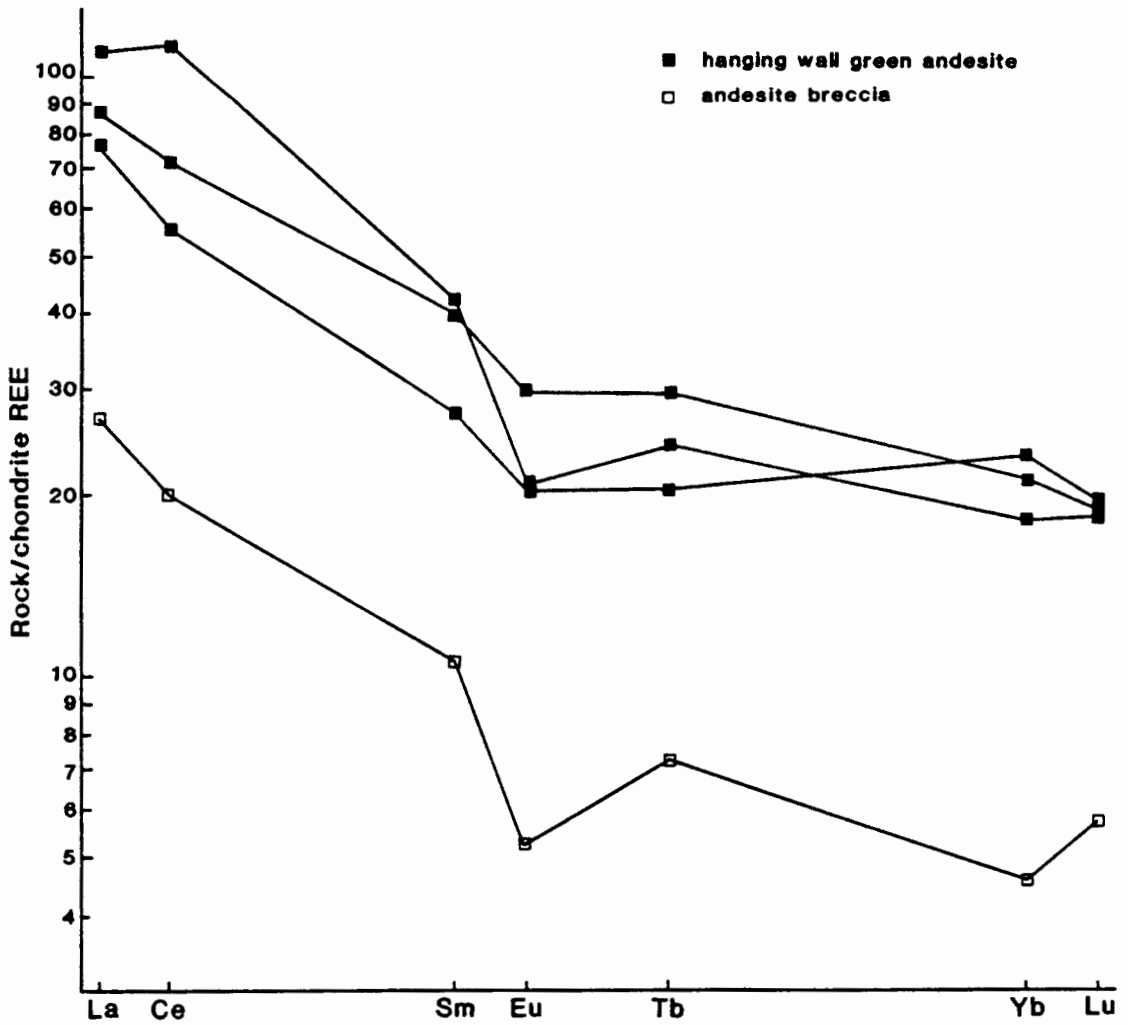


Figure 31. Chondrite-normalized REE plot for samples from the hanging wall of the No. 2 vein in the adit at station C.

well below those of the green andesite zone, and the curves are generally parallel. Eu shows greater depletion in the andesite breccia relative to the green andesite. Quartz-cemented breccias plot below the other two footwall zones and generally parallel to them, although one sample shows a very flat heavy REE pattern.

Hanging wall samples shown in Figure 31 show a similar progression toward the vein, although the hanging wall green andesites show somewhat more spread than do the footwall green andesites.

Sampling in the stope past station G was not as extensive as that for station C. A sketch of the vein and wallrock zones at this location is shown in Figure 32. REE patterns for these samples are shown in Figures 33 and 34. The footwall breccia is observed to plot below and parallel to the footwall andesites. Ce and Eu show depletions relative to the least altered samples. Patterns for the hanging wall samples show the rusty shear zone shown in Figure 34 to plot higher than the andesite located at greater distance from the vein.

A sketch of the Nos. 2 and 2A veins and wallrock zones on the exploratory roadcut is shown in Figure 35. Data for alteration metal concentrations (Figs. 29, 32, 35, Table IV, and Appendix A) show the following patterns:

- 1). The highest Au concentrations are found in the quartz veins. Of three vein samples taken at station C in the adit, the highest Au concentrations are in samples coming from the margins of the vein. Vein samples from the stope past station G show the highest Au concentrations in the vuggy quartz zone of the vein. The highest Au concentration on the roadcut was in the No. 2A

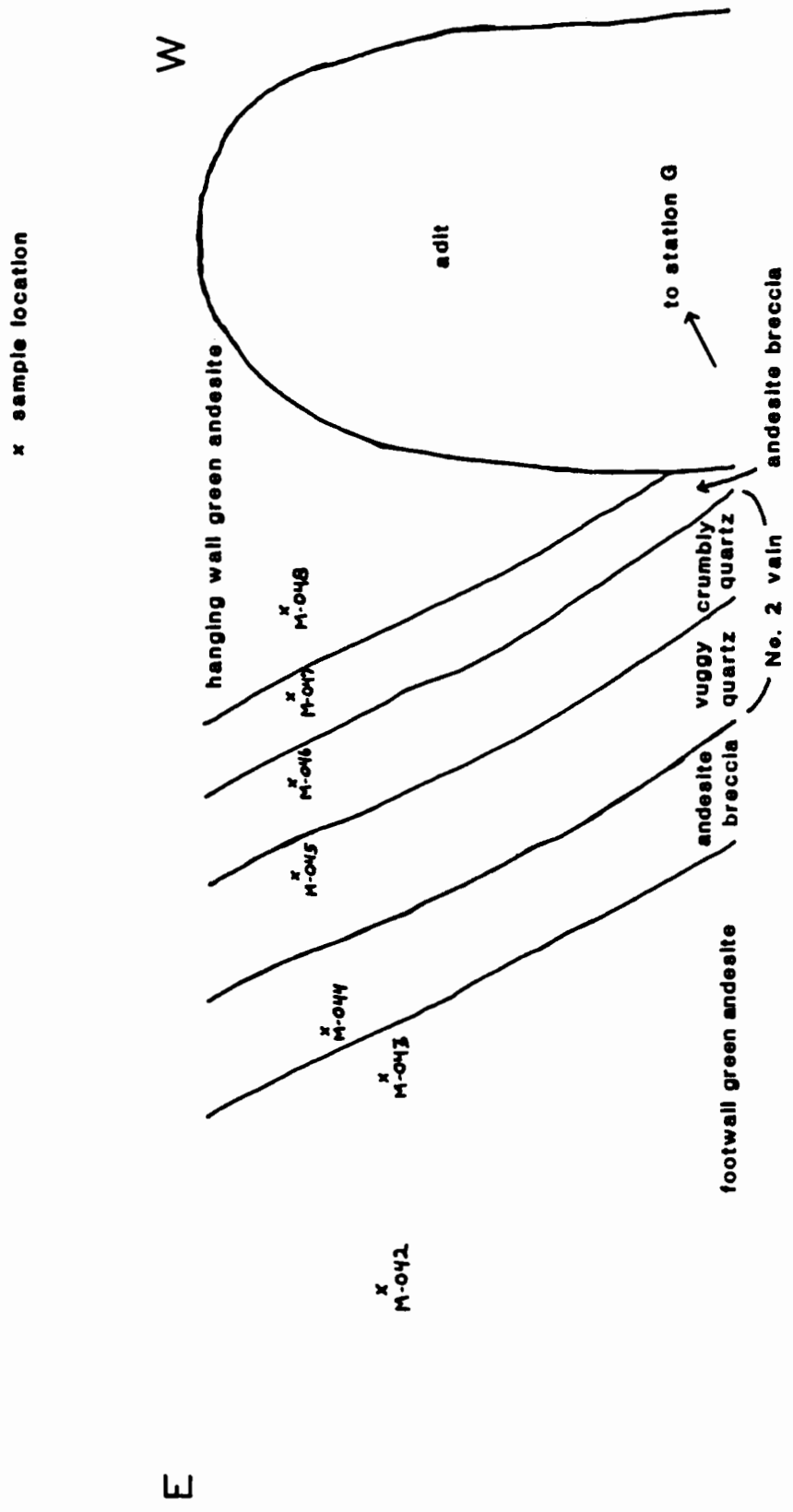


Figure 32. Sketch of the No. 2 vein and wallrock zones in the adit past station G.



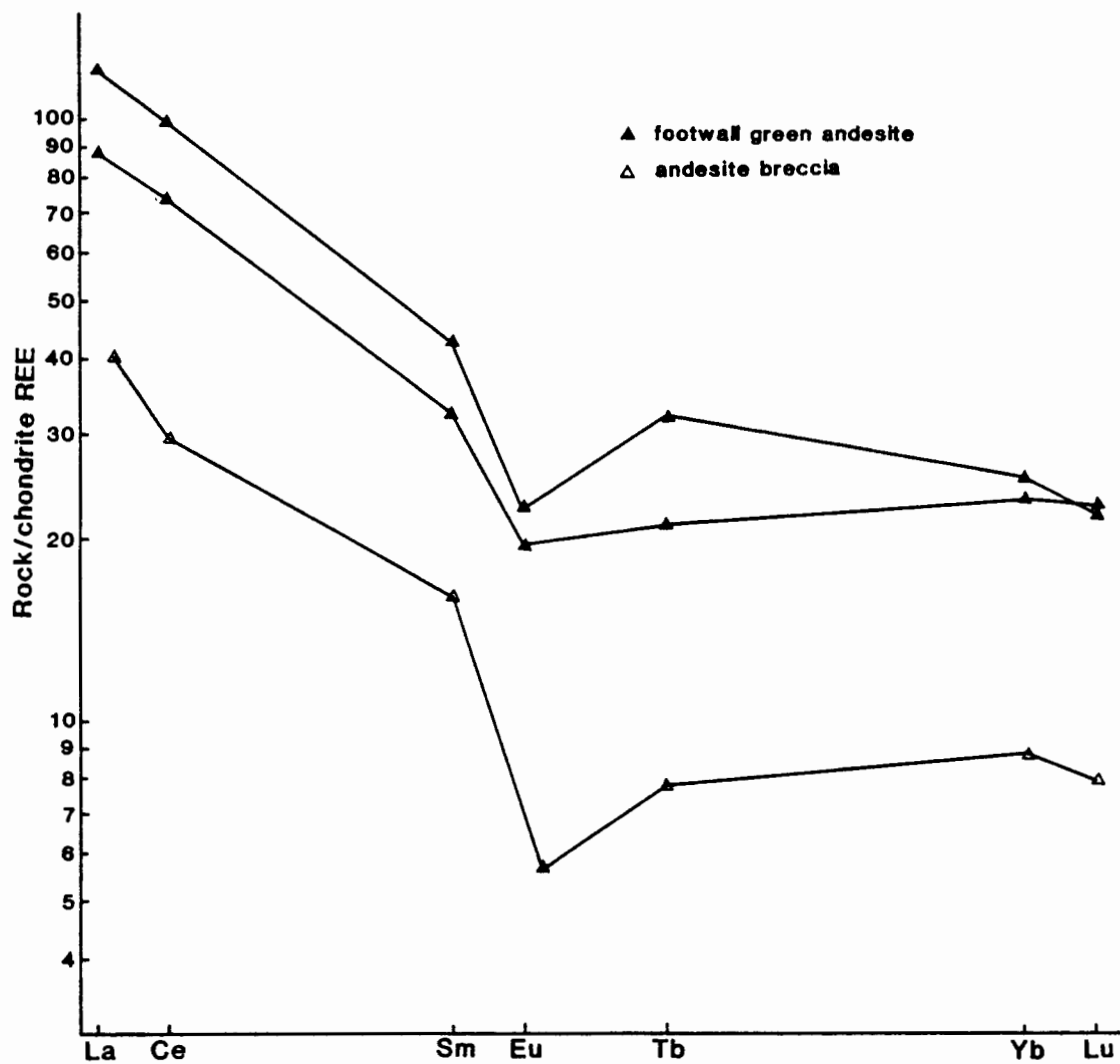


Figure 33. Chondrite-normalized REE plot for samples from the footwall of the No. 2 vein in the adit past station G.

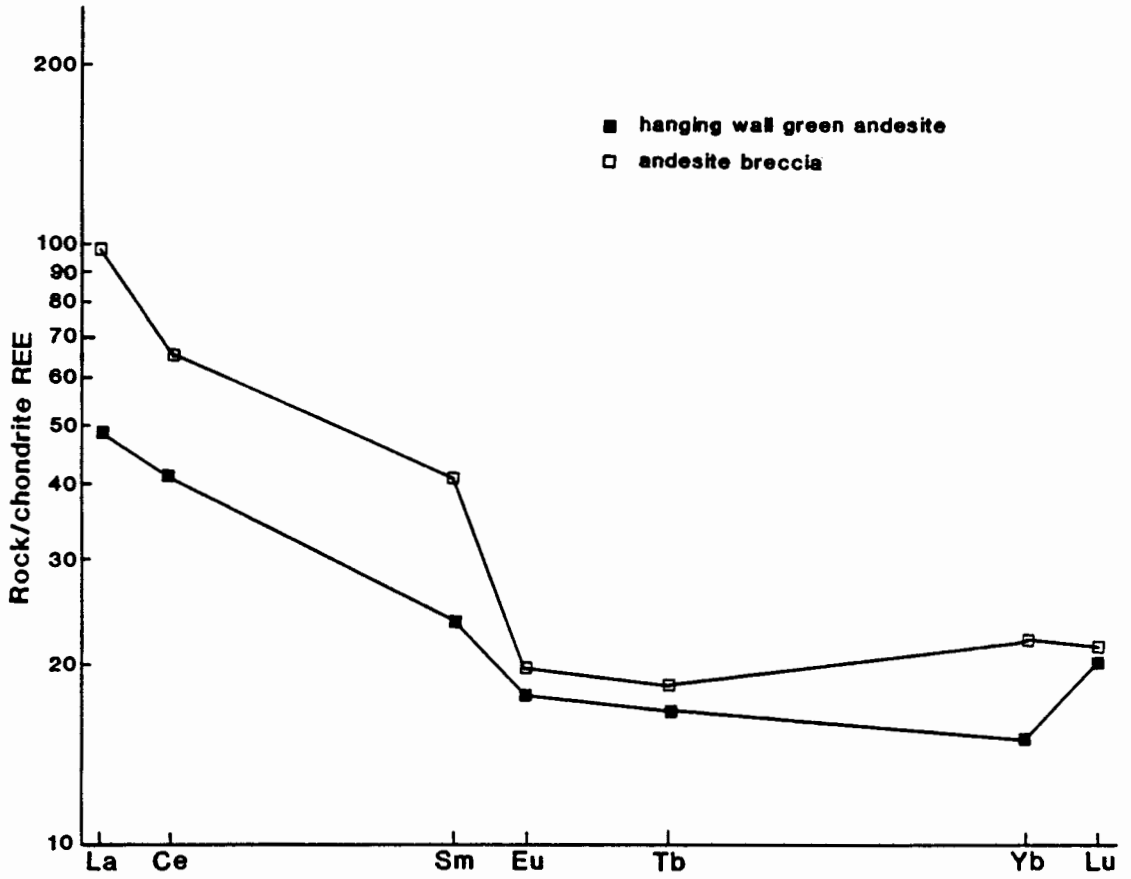


Figure 34. Chondrite-normalized REE plot for samples from the hanging wall of the No. 2 vein in the adit past station G.

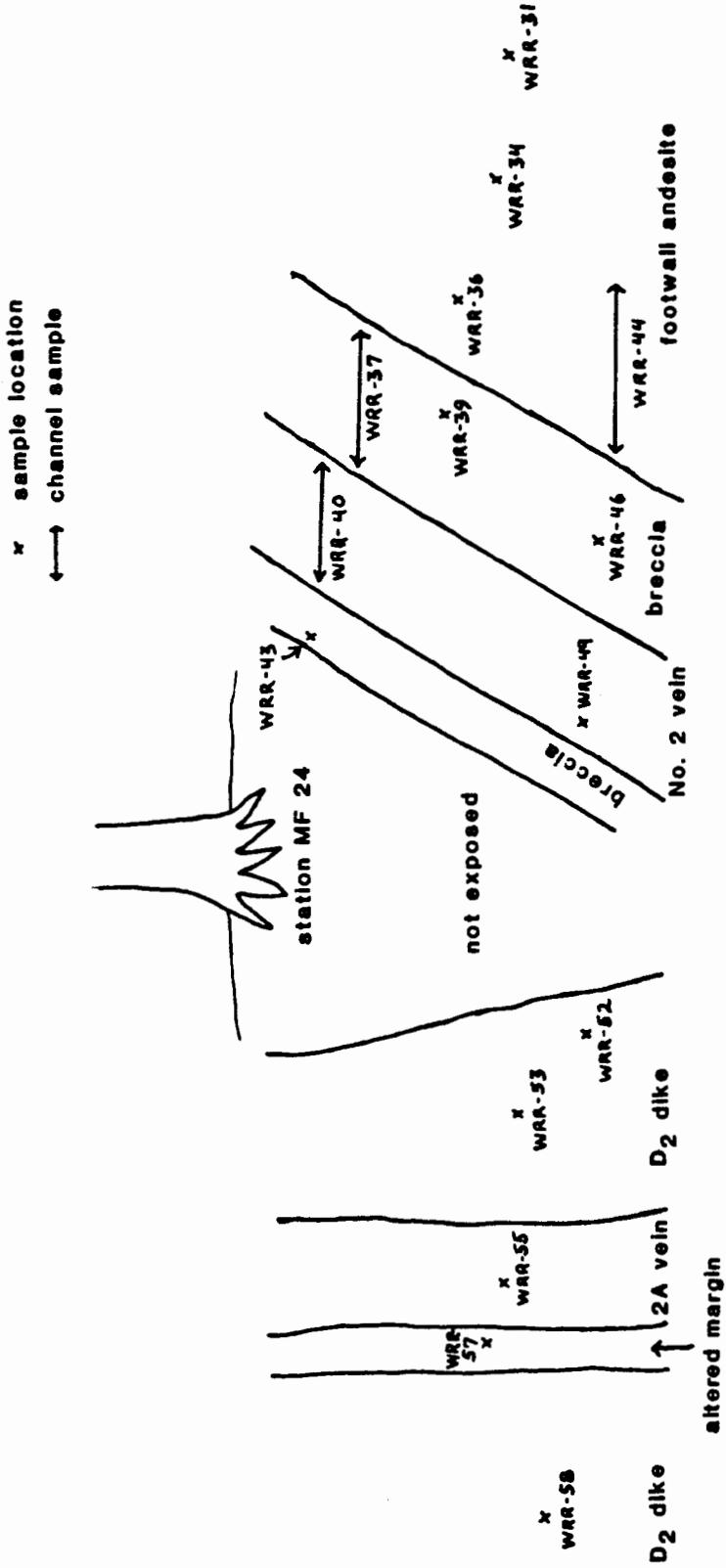


Figure 35. Sketch of the Nos. 2 and 2A veins and wallrock zones on the exploratory roadcut.

- vein rather than the No. 2 vein.
- 2). Ag is found only in quartz veins. Since a standard containing Ag and Hg was not included in the INAA runs, values for these elements in ppm. are not available, although they were detected in some samples. Highest Ag concentration appear to occur in those samples also having the most Au. Hg occurs mainly in the veins, but has been detected in several other samples as well, including samples from the No. 5 structure and the Paradise Creek breccias.
  - 3). Arsenic increases toward the veins, but concentrations are lowest within the veins. Quartz-cemented breccias contain less As than breccias or shears which contain little quartz. At station C in the adit, the As halo has penetrated farther into the footwall than the hanging wall.
  - 4). Sb concentrations increase toward the veins and are highest in the veins. Sb haloes also appear to have penetrated farther into the footwall of the vein in the adit than into the hanging wall.
  - 5). As/Sb ratios are lowest in the veins and increase away from the veins. Quartz-cemented breccias have lower As/Sb than breccias or shears containing less quartz.

## DISCUSSION AND CONCLUSIONS

Cenozoic epithermal precious metal deposits are primarily hosted by Tertiary volcanic rocks. Ore metals commonly exhibit a base- to precious metal zoning with decreasing depth (Buchanan, 1981; White, 1981; Berger and Eimon, 1982) that is genetically related to the ore forming process. Deposits in Tertiary andesitic terrains appear to be closely associated with extensive propylitization linked with high K mobility, resulting in K-metasomatism of the propylitized rocks and of the wallrock alteration zones of the gold-bearing veins (Boyle, 1979).

These deposits are believed to be fossil equivalents of high temperature geothermal systems such as Steamboat Springs, Nevada and Broadlands, New Zealand, which are currently depositing ore-grade precipitates (Ewers and Keays, 1977; Schoen and others, 1974; Schoen and White, 1965; White, 1974, 1981). These systems show depth-related zoning of metals, with Au, As, Sb, Tl, and some Ag concentrated near the surface and base metals and Ag precipitated at greater depth and higher temperatures.

Zoning of alteration and mineralization in epithermal systems is genetically related to the ore-forming process, with location of metal deposition a function of the level of boiling of the ascending fluids

(Buchanan, 1981). Base metals deposit below and precious metals above the boiling horizon, which may fluctuate due to episodic buildup and release of pressure. Thallium is deposited in response to decreasing temperature, while the other metals are deposited as a result of the combined effects of decreasing temperature and boiling of the hydrothermal solutions in permeable horizons (Ewers and Keays, 1977).

At the level of boiling,  $\text{CO}_2$  and  $\text{H}_2\text{S}$  are released and selectively partitioned into the vapor phase. Mixing of the vapors with cooler groundwater and oxidation of  $\text{H}_2\text{S}$  to  $\text{H}_2\text{SO}_4$  produces acid solutions which percolate downward, forming a low pH advanced argillic assemblage of silica, alunite, and kaolinite. Beneath this horizon, illite, celadonite, and adularia may be formed by near-surface degassing. This assemblage passes with depth and toward the ore shoots to more well-ordered white micas. Montmorillonite or kaolinite may form an inner alteration halo on the fracture walls of ore shoots. The bleached zone forms an upward widening halo around individual ore shoots and is virtually absent below the precious metal horizon.

The Wind River prospect shows a complex interplay between volcanic, hydrothermal, and structural activity. Relations among the  $A_1$  and  $A_2$  lava flows, the  $D_1$ ,  $D_2$ , and  $D_3$  dikes, and regional structural controls form the setting for the hydrothermal system developed at the prospect.

Structural trends in the study area that parallel regional trends and which appear to be the most important in terms of providing foci for the flow of hydrothermal fluids are the north-northeast trend and, to a lesser extent, the northwest trend. Northwest-trending faults and folds

in the study area parallel the northwest trends developed regionally in the Washington Cascades. This northwest trend also parallels an older regional structural grain of the pre-Cenozoic terrain of the north Cascades (Hammond, 1979).

North-south structures in the study area appear to have been the main focus for movement of hydrothermal fluids in the study area. These north-south structures parallel the trend of the Straight Creek fault, but any extension of the Straight Creek fault south of the juncture with the Olympic-Wallowa lineament is apparently covered by middle to late Tertiary volcanic rocks. Tabor and others (1984) believe that structures developed during Tertiary times aligned with the north-south trend of the Straight Creek fault do not extend to the south. Davis (1977) and Schreiber (1981) suggest that the Straight Creek fault may have extended further south during pre-Tertiary times. Reconstruction of dextral slip along the trend of the Straight Creek fault would place Mesozoic basement rocks as far south as the town of Stevenson, Washington (R. Miller, 1984, pers. comm.).

The work of Tabor and others (1984) in central Washington indicates a Tertiary history of dominantly vertical movement along the Straight Creek fault and its southeasterly splays that merge with the Olympic-Wallowa lineament. These authors believe vertical movement tapered off during the Oligocene and ceased by Miocene times, when the fault was intruded by the 25 Ma Snoqualmie Batholith.

Much of the Quaternary volcanic activity in southern Washington is believed to have occurred on north-south trending fissure zones, indicating that north-south structures have been active until quite

recently. The Wind River area is located between the St. Helens and Indian Heaven fissure zones. Whether the north-south structures in the study area are related to reactivation of buried southern portions of the Straight Creek fault, or to other causes acting to produce similar trends is a matter of conjecture. The possible presence of older basement rocks beneath the Wind River area might be an important factor in the development of a precious metal hydrothermal system in the area as a source for the gold.

Although the A<sub>1</sub> and A<sub>2</sub> lavas may be distinguished on the basis of field and textural criteria, they do not separate well into two geochemically distinct groups. While a detailed study of the petrogenesis of these lavas is beyond the scope of this study, the observed geochemical differences in the lavas may be due to fractionation of the parent magma with time, or to tapping different layers of a fractionated magma chamber through time.

Plots of geochemically incompatible elements (see Fig. 19) indicate there are three groups of dikes intruding the altered pyroclastic rocks at the Wind River prospect. D<sub>1</sub> and D<sub>3</sub> dikes may also be distinguished on the basis of field and petrographic studies, but the D<sub>2</sub> dike is distinguished only by geochemical means. Otherwise, this dike resembles a weakly altered D<sub>1</sub> dike. D<sub>3</sub> dikes are chemically distinct from D<sub>1</sub> dikes. They show differences in both compatible and incompatible trace elements. REE patterns for the two groups of dikes are also different. D<sub>3</sub> dikes show only a slight negative Eu anomaly and a relatively flat curve in the heavy REE range.

D<sub>1</sub> dikes contain higher overall REE concentrations than do D<sub>3</sub>



dikes and show a more pronounced negative Eu anomaly. REE patterns for the groups of D<sub>1</sub> dikes based on degree of alteration (Figs. 23 and 24) indicate there is little overall, systematic change in REE concentration or pattern related to degree of alteration of the dikes.

The chemical groupings of the D<sub>1</sub> dikes suggested by Figure 20 appears to be related to intensity of alteration of the dikes rather than to a magmatic fractionation trend. Figure 21 shows a good correlation of decrease in Sc and Co with decreasing FeO<sub>2-3</sub>. The strongly altered sample with higher FeO<sub>2-3</sub> contains more sulfide veinlets than do the other strongly altered samples, and its higher Fe content may be due to introduction of Fe that has been incorporated in sulfide minerals.

Some geochemical similarities exist between the A<sub>1</sub> andesites and the D<sub>1</sub> dikes, and between the A<sub>2</sub> andesites and the D<sub>3</sub> dikes. Figure 36 shows comparisons of the REE patterns for A<sub>1</sub> andesites and D<sub>1</sub> dikes, and for A<sub>2</sub> andesites and D<sub>3</sub> dikes. Shapes of the curves and concentrations of REE are similar.

Figure 25 shows that in general, the A<sub>2</sub> lavas group with the D<sub>3</sub> dikes, while the A<sub>1</sub> lavas group with the D<sub>1</sub> dikes. These geochemical similarities suggest that the A<sub>1</sub> flows were fed by the D<sub>1</sub> dikes and the overlying A<sub>2</sub> flows were fed by the D<sub>3</sub> dikes. The D<sub>3</sub> dikes would therefore be younger in age than the D<sub>1</sub> dikes.

Chemical differences in the D<sub>1</sub> dikes appears to be related to degree of alteration rather than to fractionation of the source magma. However, dikes of varying degrees of alteration are observed to cut intensely altered pyroclastic rocks at the prospect. The difference in

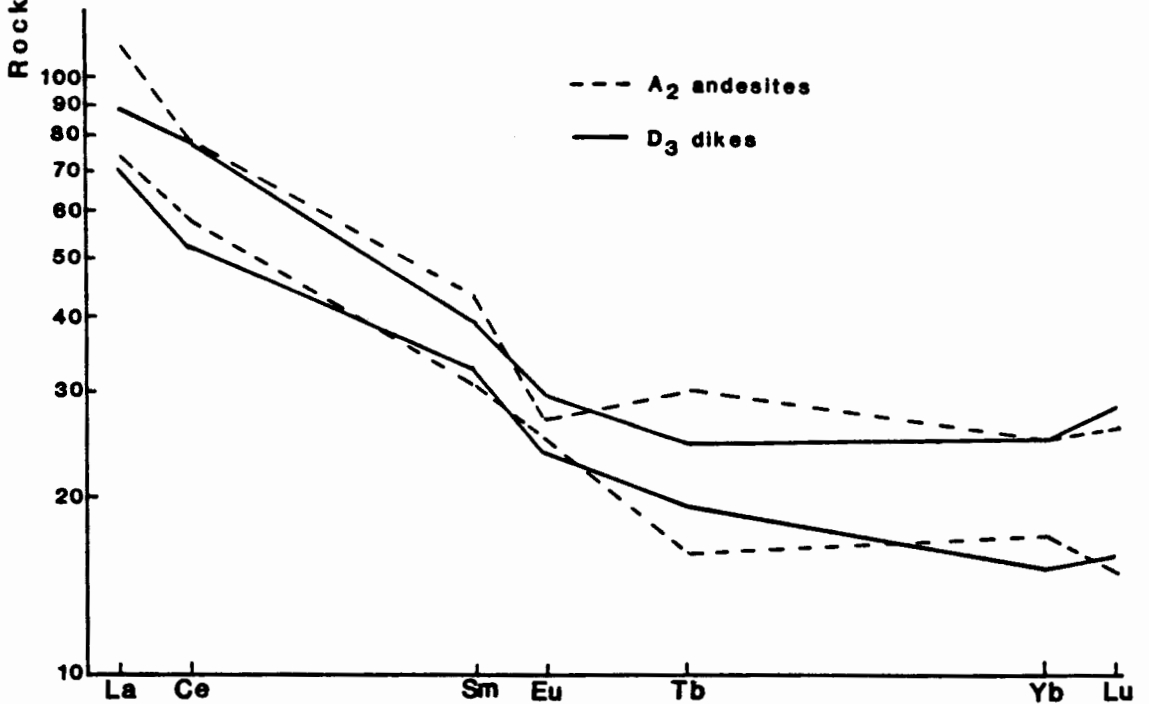
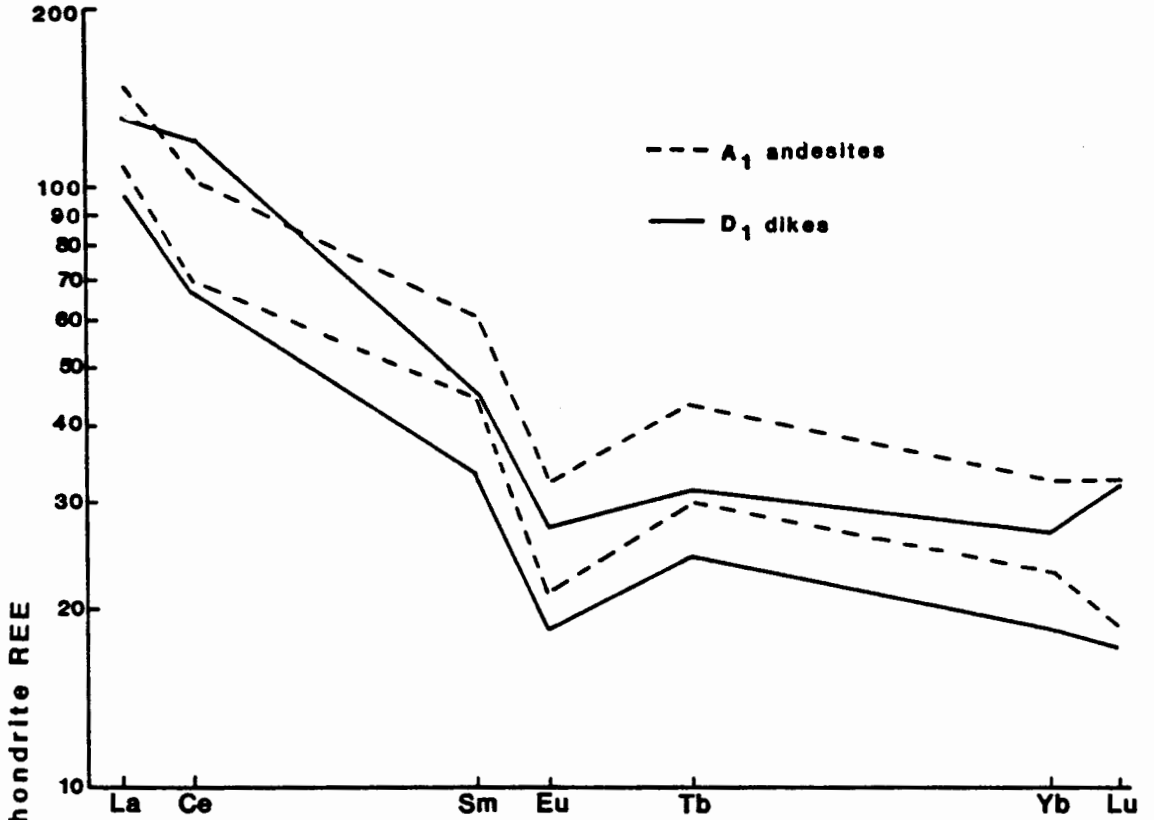


Figure 36. Comparison of REE patterns for A<sub>1</sub> andesites and D<sub>1</sub> dikes, and for A<sub>2</sub> andesites and D<sub>3</sub> dikes.

degree of alteration may be related to the timing of dike emplacement relative to activity of the hydrothermal system, with the strongly altered dikes emplaced the earliest. The range of time over which the D<sub>1</sub> dikes were emplaced was evidently not large enough for the parent magma to have undergone appreciable differentiation, so the dikes do not show appreciable geochemical differences other than those which may be attributed to alteration.

Rocks of the Ohanapecosh Formation in the type area of Mt. Rainier National Park exhibit varying degrees of alteration. The tuffaceous units are generally more altered than flows or intrusions, and the formation as a whole is usually more altered than the overlying formations (Fiske and others, 1963). Many rocks contain laumontite or wairakite and varying amounts of prehnite, epidote, chlorite, albite, quartz, and clay minerals. Zeolites and albite are usually found as alteration minerals after plagioclase. Rocks containing wairakite or prehnite are well-indurated, but those containing laumontite are soft and friable due to hydration of the laumontite (Fiske and others, 1963). The Ohanapecosh zeolite facies in the Mt. Rainier area probably formed by a combination of temperature and pressure rise related to burial and dispersion of heat from cooling intrusions.

Wise (1961) extensively studied the alteration mineralogy of the Ohanapecosh Formation in the Wind River area, but worked mainly in the pyroclastic and volcanoclastic sequences south of the present study area. He found zeolites, quartz, chlorite, a smectite tentatively identified as griffithite, calcite, and celadonite to be the most common alteration minerals. Unlike the type section at Mt. Rainier, conditions

apparently did not reach the stability of wairakite or epidote in the regional metamorphism. Since the base of the section is not exposed in the Wind River area, higher grade assemblages may be present at greater depth than is exposed. Also, thermal effects of plutons intrusive into the Ohanapecosh Formation in the Wind River area may not have been great enough to have raised the metamorphic grade.

The hydrothermal alteration found in the Types 1, 2, and 3 alteration zones in the study area has been superimposed on the regional zeolite-grade alteration. This alteration extends up through the A<sub>1</sub> and A<sub>2</sub> lava flow groups capping the ridges and widens upward. Areas of Type 1 alteration are found in rocks of the lava flow groups on Lava Butte and Middle Butte. Areas of Type 2 alteration are found in the lava flow groups on top of Paradise Ridge. Both types of alteration have geochemical anomalies of Sb and/or As associated with them, indicating transport of alteration metals into these areas.

Type 1 alteration is interpreted to represent areas where hydrothermal activity was not of sufficient duration or intensity to produce all the features associated with the main system at the prospect. Intergrowth of calcite plates with quartz in the Type 1 breccias and local development of bladed cavities in the quartz are textures similar to those found in the large quartz veins at the prospect, but the Type 1 breccias are of restricted extent. Hydrothermal activity in these zones has consisted of fracturing followed by cementation with chalcedony and then by deposition of quartz + calcite in the interstices. Evidence for repeated brecciation in these zones is lacking, and alteration of wallrock and clasts is only

moderate.

It may be concluded that individual 'rootless zones' were not subject to extended hydrothermal activity. These areas do provide information that is lacking in the main system. Overgrowth of chalcedonic quartz by euhedral quartz in the breccias may indicate thermal progradation of the hydrothermal system, since saturation of hydrothermal solutions with amorphous silica occurs at a lower temperature than does saturation with quartz.

The widespread Type 2 alteration found along the crest of Paradise Ridge is laterally extensive. Alteration mineralogies are similar to those found in intensely altered zones at the prospect, but lack carbonate. Although observed alteration mineralogies indicate intense degrees of alteration of these rocks, minerals such as alunite or jarosite were not detected, and these zones cannot positively be identified as belonging to an advanced argillic assemblage. Trace metal anomalies of As and Sb exist in rocks from Type 2 zones, including lavas that are not strongly altered. Similar lavas from the North Butte-Middle Butte area do not contain these metals in detectable concentrations.

The regional Types 1 and 2 alteration are probably structurally controlled, although field evidence for this control is not obvious due to poor exposures. Type 1 alteration zones were produced in response to restricted 'leaks' from the main hydrothermal system at the prospect. Host structures did not become major channels for fluid flow and did not develop into large veins. Fluid flow was not prolonged enough to produce more intense alteration of clasts and wallrock.

Type 2 alteration is more pervasive and more uniform in tuffs intercalated in the lava flow groups. Intercalated tuffs are more strongly altered than the lavas, and more frequently show evidence of silicification. The tuffs would probably react more readily than the lavas to hydrothermal solutions due to a higher proportion of less stable constituents and greater permeability. The less reactive lavas would be more readily altered in proximity to structures, where greater fracture permeability allowed more interaction of the hydrothermal solutions with the rocks.

Areas of celadonite alteration are found peripheral to Types 1 and 2 alteration and may have formed in response to near-surface degassing and K-metasomatism (Schoen and White, 1967; Buchanan, 1981). The amount of Ca present and the partial pressure of  $\text{CO}_2$  are important controls on the formation of this mineral. In rocks with a high CaO content, low  $P_{\text{CO}_2}$  favors zeolite formation.  $\text{Fe}^{+2}$  and Mg form chlorite or smectite, and K,  $\text{Fe}^{+3}$ ,  $\text{Fe}^{+2}$ , and Mg go into celadonite. High  $P_{\text{CO}_2}$  favors more aluminous clay minerals and calcite, and celadonite would not form.

Alteration and mineralization at the prospect show strong relations to structures. Zoned alteration at the prospect is mineralogically most intense at and immediately surrounding the No. 5 structure. In view of the zoning of alteration mineralogies relative to the No. 5 structure, that is, intensity of alteration decreasing with distance from the structure, it is concluded that the zoned alteration at the prospect is in fact controlled by the No. 5 structure.

Concentrations of alteration metals decrease outward from the No. 5 structure. This structure contains anomalous concentrations of As,

Sb, and Au. Gold values, however, are low. Ag and Hg are present in some samples, and W is found only in rocks from the No. 5 structure. The large quartz veins cutting the zoned alteration have produced haloes of As and Sb that are superimposed on the effects of the No. 5 structure.

The large quartz veins at the prospect are structurally controlled. Quartz veins along the roadcut are frequently observed to be emplaced between the margins of a dike and the pyroclastic rocks into which the dike is intrusive. The veins also cross-cut some dikes. These features suggest that both dikes and veins were emplaced along the same zones of weakness. Even the smaller veins often show marginal shear zones and/or quartz-cemented breccias, which also indicates structural control of the veins. The No. 2 vein in the adit shows shearing of wallrocks parallel to vein margins, pinch and swell along its length, and vein-margin breccias. These features suggest this vein fills a fault, and that movement has occurred along the fault during the course of vein deposition.

The fluids responsible for alteration and mineralization in the Wind River system were shown by fluid inclusion studies to be of low salinities and temperatures. The fluids were probably of near-neutral pH, and the Au transported by S complexes. Alteration mineralogies and geochemistry indicate fluids that were high in  $\text{CO}_2$  and reducing in nature, and which became oxidizing at higher levels in the system.

Some controversy exists as to the transport of Au in epithermal systems, with both S and Cl complexing proposed (Boyle, 1969; Buchanan, 1981; Henley, 1973; Helgeson and Garrels, 1968; Seward, 1973; Weissberg,

1970). Deposits that are high in Ag and base metals but contain some Au and complex sulfosalts probably formed at greater depths and higher temperatures and salinities (White, 1981; Berger and Eimon, 1982; Buchanan, 1981). Base metals and Ag are transported mainly as Cl complexes that become unstable higher in the system with decreasing temperatures and salinity and increased pH from boiling, CO<sub>2</sub> loss, and wallrock reactions. Cl complexes of Au, As, Sb, Hg, and Tl either are not significant, or the complexing agent (Cl<sup>-</sup> vs. HS<sup>-</sup>) changes upward, resulting in a barren zone between the high-level, Au-rich deposits and the deeper, Ag-base metal deposits (White, 1981; Berger and Eimon, 1982; Buchanan, 1981).

Deep geothermal waters in systems such as Broadlands, Steamboat Springs, and Yellowstone are neutral to slightly alkaline in pH and of low salinity (Berger and Eimon, 1982; Ewers and Keays, 1977; Weissberg, 1970; Boyle, 1969). Solubility of Au in such fluids is much greater as thio complexes (Seward, 1973; Weissberg, 1970). In view of the low temperatures and salinities of the Wind River fluids, transport of Au most likely occurred as S complexes. Given the high amounts of As and Sb also found in the system, As and Sb complexes cannot be ruled out as a transporting mechanism, but little is known about the behavior of such complexes (Boyle, 1979.)

Weissberg (1969) suggests that Sb sulfides may act as collecting agents for Au and Ag, causing these metals to be co-precipitated when the solubility of the Sb sulfides in solution are exceeded. The high concentrations of Sb in the veins with the Au suggests that this may be one mechanism by which the Au in the Wind River veins was precipitated



from solution. The low amounts of As in the veins compared to the wallrocks may be related to its much greater solubility and ability to form stable colloidal dispersions (Weissberg, 1969), and it was not precipitated in the veins but was carried out into the wallrocks where it precipitated.

Some constraints on the composition of the fluid arise from observed alteration mineralogies. Abundant calcite in veins at the adit level and in the carbonate-clay-quartz zone of alteration exposed along the roadcut indicates solutions high in  $\text{CO}_2$ . Epidote has not been observed in any of the alteration assemblages at the Wind River prospect. Epidote forms in geothermal systems at temperatures of  $240^\circ\text{C}$  or greater, but a high  $\text{CO}_2$  content in the fluid favors formation of calcite rather than epidote (Browne and Ellis, 1970). At lower temperatures, smectite clays are the stable Ca-Al silicate phase (Giggenbach, 1984). Phase relationships of Ca-Al silicate minerals in equilibrium with calcite and chalcedony are shown in Figure 37. Temperatures obtained from fluid inclusion studies are just within or below the minimum temperature range for formation of geothermal epidotes, and smectite clays are abundant in the alteration assemblages at the Wind River prospect, suggesting that temperatures achieved in the system were either too low for epidotes to form, or that high concentrations of  $\text{CO}_2$  stabilized other phases.

A calcite-enriched zone near major upflow channels is consistent with the model developed by Giggenbach (1981, 1984) for geothermal systems of the Broadlands type. This model is summarized diagrammatically in Figure 38. The system is divided into a lower,

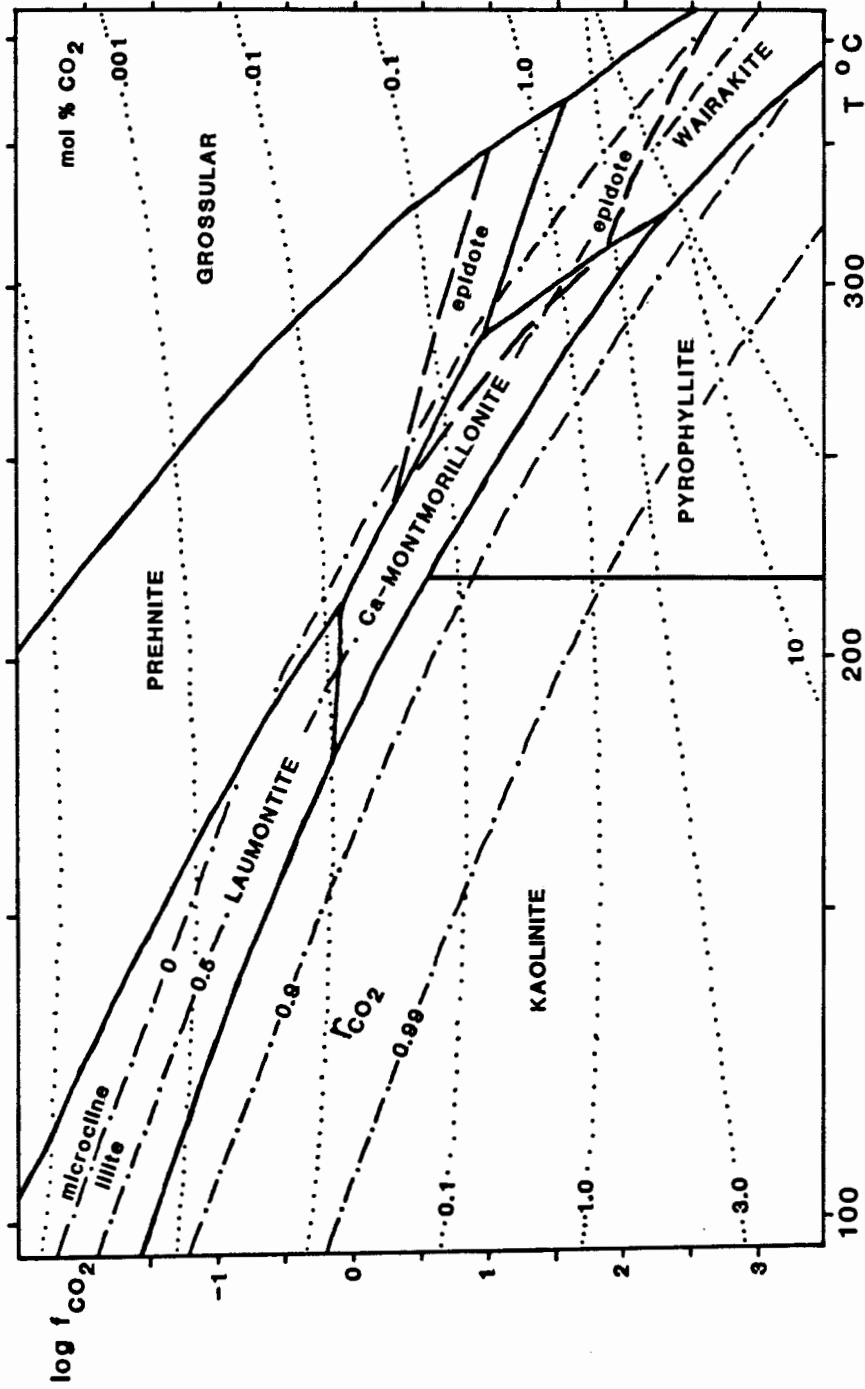


Figure 37. The stability of Ca-Al silicates in equilibrium with chalcedony and calcite as a function of  $\log f_{CO_2}$  and temperature. Heavy solid lines=stability fields, heavy dashed lines=stability field of epidote for  $X_{pistacite} = 0.22$ , dash-dot lines=reactivity  $r_{CO_2}$  with respect to full equilibrium as represented by the microcline-illite coexistence line, lines are liquid phase  $X_{CO_2}$  isopleths in mol % (from Giggenbach, 1984).

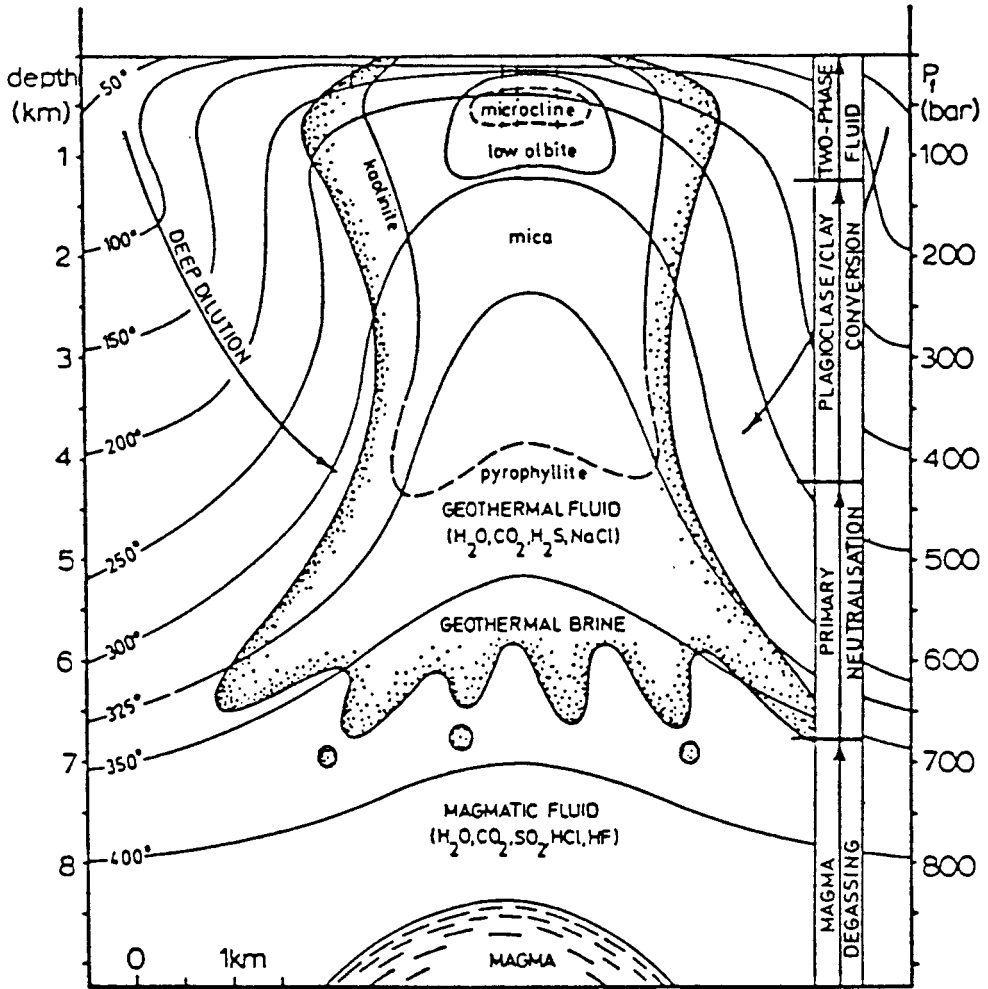


Figure 38. Schematic cross-section of a geothermal system of the Broadlands type (from Giggenbach, 1981).

magmatic-volcanic system in which  $\text{CO}_2$  is produced, and an upper, geothermal system in which  $\text{CO}_2$  is consumed. Major upflow zones where solutions ascend and cool such as the No. 5 structure, are characterized by silicification and K-metasomatism, resulting in alteration assemblages rich in K-clays, K-micas, or K-feldspar, plus quartz. At the Wind River prospect, illite is the most abundant K mineral in and near the No. 5 structure. K-feldspar is found in the carbonate-clay-quartz zone of alteration as a replacement mineral, and K-feldspar plus quartz forms fracture coatings in the smectite-chlorite zone. Since this K-feldspar is of hydrothermal origin, it is assumed to be adularia.

At increasing lateral distances from the major upflow zones, H-metasomatism is caused by attack of  $\text{CO}_2$  on Ca-Al silicates, leading to formation of Al-enriched alteration assemblages which may include clay minerals, micas, calcite, and quartz. Although micas are not found in the Wind River alteration assemblages, various clay minerals, calcite, and quartz are abundant. At increasing distances from the No. 5 structure, illite is replaced by smectite, then by chlorite + smectite. The scarcity of zeolites except at distances from the system may also be due to high  $\text{CO}_2$  favoring formation of calcite and clay minerals.

Several samples in the more altered zones adjacent to the No. 2 vein in the adit were observed to have lowered and flat patterns in the heavy REE. This behavior is not universally observed, and the significance of the pattern may be questionable, but Kerrich and Fryer (1979) have shown that in extremely  $\text{CO}_2$ -rich environments, heavy REE can be mobilized. Other evidence, such as deposition of calcite in the vein, and calcite in the wallrocks, point to  $\text{CO}_2$ -rich solutions. These

solutions may have contained enough  $\text{CO}_2$  to locally mobilize the heavy REE.  $\text{CO}_2$ -rich solutions are also favorable for Au transport.

Samples for successive wallrock zones going toward the vein in the adit show REE patterns that generally are seen to parallel the least-altered samples at successively lower REE abundances. Quartz-cemented breccias show the lowest REE abundances. This is believed to be due to the dilution effect produced by addition of REE-barren quartz (Ludden and others, 1984).

Several lines of evidence indicate the reducing nature of the hydrothermal solutions at the Wind River prospect. The observed decrease in Fe content with increasing intensity of alteration of D<sub>1</sub> dikes indicates the solutions were able to transport Fe<sup>+2</sup>. Since Fe<sup>+2</sup> is more soluble than Fe<sup>+3</sup>, the fluids were evidently reducing in nature. The reducing nature of the solutions is also indicated by behavior of the rare earth element Eu in vein margins. Samples in sheared zones or breccia zones often show depletions Eu relative to less altered wallrocks. Eu has a variable oxidation states and is more mobile in the reduced state. Interaction of the rock with reducing solutions would reduce some of the Eu and allow this elements to be moved out of the system. REE patterns for the strongly altered D<sub>2</sub> sample proximal to the 2A vein (Fig. 22) generally parallel those for the less altered samples, but also show depletions in Ce and Eu. Oxidation of the solution as it moves upward may have been responsible for the abundant sulfide veinlets filling fractures in the most intensely altered zones surrounding the No. 5 structure.

REE data from tuffs in the system (Fig. 26 to 27) shows a change

in behavior of the system with elevation. Alteration of the T<sup>3</sup> tuffs produces a parallel decrease in REE values. The first set of T<sup>4</sup> tuffs (Fig. 26) begins to show 'fanning' of the light REE lines, which becomes pronounced in the second set of T<sup>4</sup> tuffs (Fig. 27).

The light REE patterns indicate a fractionation of light REE in response to alteration. Light REE are most enriched in the sample with the greatest clay content and most depleted in a silicified sample. The patterns may reflect effects of different alteration conditions, with one acting to concentrate the light REE, and the other acting to deplete them. Change in slope of the heavy REE line from the least-altered pattern indicates that the heavy REE have also been moved, but that they do not show a variable response to conditions of alteration (Campbell and others, 1984).

This pattern overlaps the pattern for heavy REE in the No. 5 structure in similarity of shape and abundance of REE, suggesting that the conditions of alteration imposed by the No. 5 structure also affected the tuffs, and that subsequent modifications have involved light REE mobility only. In contrast to the tuffs, conditions of alteration have not affected REE in the dikes to any great extent.

Distribution of Au in the No. 2 vein suggests there may have been more than one episode of mineralization. An early pulse of weak mineralization in the structure hosting the No. 2 vein was followed by formation of quartz-cemented breccias along this structure by solutions that were barren of Au. The traces of Au in the quartz-cemented breccias can easily be accounted for if mineralized wallrock fragments from the previous episode of mineralization were included in the

breccias. Subsequently, the structure was active during the main episode of mineralization which produced the No. 2 vein.

Although the Cascades are metallogenically considered to be a copper province, with major deposits being of the porphyry copper type, the Wind River prospect does not fit well with this model. Work done on Cascade porphyry systems in Washington and Oregon (Field and Power, 1985; Grant, 1969, 1982) indicate a progression from south to north of increasing age, temperature, salinity of fluids, depth of emplacement of the intrusions, and a change of mineralization style from epithermal (Au-Ag) to mesothermal (Pb-Zn-Cu-Ag) to hypothermal (Cu-Mo). Field and Power (1985) consider epithermal Au-Ag deposits in the Oregon Cascades to be near-surface manifestations of porphyry systems at depth.

According to the model of Giggenbach (1981, 1984), porphyry systems would fit the magmatic-volcanic system classification, which grade with decreasing depth into geothermal systems which have similar alteration mineralogies to those observed at the Wind River prospect. If the thermal fluids were carrying Au and Ag, an epithermal precious metal deposit could be formed over such a porphyry system. Priest and others (1982) favor deep circulation as a source for geothermal fluids in currently active hot springs in the Cascades. With the data obtained in this study, there is at present no way to distinguish geothermal systems formed over porphyry systems at depth from those that might have been formed by other mechanisms. While it is possible that the heat source for hydrothermal activity at the Wind River prospect is a porphyry system at depth, this cannot be proven or disproven with the available data.

The Wind River prospect is spatially located between the Silver Star stock of the Washougal district and the Mt. Margaret, Goat Mountain, and Camp Creek stocks of the St. Helens district. These stocks are all intrusive into the Ohanapecosh Formation and represent typical examples of southern Washington porphyry systems at current levels of erosion.

Age dates on stocks of the St. Helens district range from 16.2 to 24.0 Ma (Engels and others, 1976; Armstrong and others, 1976). Published dates are not available for the Silver Star stock at this time but its age as estimated by Shepard (1979) would fall in this range. Porphyry mineralization of both districts probably occurred during the late stages of cooling of the intrusions. Moen (1977) estimated the mineralization of the St. Helens district to be of probable Miocene age.

Although Shepard (1979) did not do heating/freezing work on fluid inclusions in veins associated with the Silver Star stock, however, he reports that these inclusions commonly contain daughter crystals of halite. This would indicate greater salinities than inclusions from the Wind River prospect, which showed only slight freezing-point depressions and did not contain daughter minerals. Fluid inclusion data is not available for veins from the St. Helens district.

Deposits of the St. Helens and Washougal districts are reported to also contain Au, Ag, Pb, Zn, and Mo, but Cu is the major metal. Current levels of exposure of these systems fits with the mesothermal to possibly hypothermal environments of Field and Power (1985). Anomalous concentrations of As, Sb, and Hg have not been reported. As and Sb are found in rocks of the Wind River prospect, including those that do not



contain detectable Au. Hg is found in some parts of the system. These metals are all characteristic of epithermal deposits, and are also found in parts of the system above the precious metal horizon.

The Wind River prospect represents a shallower, cooler type of system than the south to north progression of Field and Power (1985) would allow for the part of the Cascades in which it occurs. Deposits of the St. Helens and Washougal districts represent what is typical of porphyry-related systems in the southern Washington Cascades. The geologic and geochemical differences of the Wind River prospect argue that the deposit is related to a different episode of mineralization than that responsible for the Cascade porphyry systems.

The hydrothermal system in the Wind River area appears to have had two main pulses of activity, the earliest being that associated with the No. 5 structure. Alteration associated with the No. 5 structure appears to have overlapped the intrusion of the D<sub>1</sub> dikes, and to have occurred somewhat earlier than emplacement of the quartz veins. Weakly, moderately, and strongly altered D<sub>1</sub> dikes intrude the zoned alteration about the No. 5 structure. The D<sub>1</sub> dikes are believed to have fed the A<sub>1</sub> flows. If degree of alteration of these dikes does reflect different timing of intrusion relative to hydrothermal activity on the No. 5 structure, then the weakly altered dikes must have been emplaced relatively late. Alteration associated with the No. 5 structure would have occurred concurrently with deposition of part of the A<sub>1</sub> flow sequence. Flows fed by the strongly altered D<sub>1</sub> dikes would have been in place when the hydrothermal system began. The activity on the No. 5 structure would have been waning by the time the weakly altered dikes

were intruded.

A second pulse of hydrothermal activity in the area may have been responsible for deposition of the large quartz veins. Quartz veins at the prospect are observed to crosscut D<sub>1</sub>, D<sub>2</sub>, and D<sub>3</sub> dikes. The D<sub>3</sub> dikes are believed to have fed the A<sub>2</sub> flows and therefore to be younger than the D<sub>1</sub> dikes. Since the D<sub>3</sub> dikes are cut by quartz veins, emplacement of at least some of the quartz veins must postdate the D<sub>3</sub> dikes and by inference, the A<sub>2</sub> flows.

Alteration associated with the No. 5 structure on the roadcut is quite extensive, while alteration associated with the quartz veins, other than geochemical anomalies, is not extensive at levels presently exposed. Since alteration associated with Tertiary epithermal vein deposits commonly widens upward (Buchanan, 1981), the No. 5 structure may actually represent the higher-level expression of a quartz vein at depth. Similarly, the large quartz veins exposed on the roadcut may once have had more extensive alteration envelopes developed at levels that have since been removed by erosion. The Type 2 alteration developed on Paradise Ridge may represent remnants of these alteration envelopes.

It is postulated that the locus of hydrothermal activity moved upward with time as the overlying volcanic pile thickened. Other changes in depth of alteration could be related to changes in boiling level of the hydrothermal fluids caused by episodic sealing and rupturing in the system (Buchanan, 1981; Berger and Eimon, 1982), and to changes in the level of the water table.

In view of the apparent timing of the alteration associated with

the No. 5 structure and the veins, the hydrothermal system appears to overlap and postdate deposition of the A<sub>1</sub> and A<sub>2</sub> flows. It is not possible to determine with currently available data how much time, if any, elapsed between the end of deposition of the A<sub>1</sub> and the beginning of deposition of A<sub>2</sub> flows, at what point during deposition of the A<sub>1</sub> flows the hydrothermal system began to develop, or how long the system postdated the A<sub>2</sub> flows.

The age of the andesite flows in the study area, if known, would constrain the age of the hydrothermal system. Correlation of stratigraphic units described in this study with stratigraphy outside the study was not a purpose of the study and is beyond the scope of this project. However, the thick and laterally extensive sequences of lava flows found in the study area is anomalous for the Ohanapecosh Formation as described elsewhere in Washington by other workers. The Ohanapecosh Formation in other areas and in the larger area studied by Wise (1961, 1970) consists mainly of volcanoclastic sediments and pyroclastic rocks with minor intercalated lava flows. Wise (1961, 1970) interpreted this concentration of lava flows as representing the core of an Ohanapecosh volcano. However, there is some belief by other workers in the southern Washington Cascades that the massive andesite flows in the study area are not part of the Ohanapecosh Formation, but are younger and of possible Miocene age (B. Phillips, 1985, pers. comm.). The flows may possibly be found to correlate with flows mapped in the lower Wind River valley by Berri and Korosec (1983).

Since the Wind River hydrothermal system postdates and may overlap deposition of the flows, it would then be Miocene or later in age, and

is different from the Cascade porphyry systems because it is related to a different volcanic-plutonic episode than that responsible for the porphyries.

Several models for epithermal precious metal deposits are presented by Berger and Eimon (1982). These models are summarized in Figure 39. Based on available lines of evidence, the Wind River prospect seems to best fit the stacked-cell convection model. Alteration and mineralization are structurally controlled. Veins are up to 2 m wide and have brecciated margins. The A<sub>1</sub> and A<sub>2</sub> flow groups have acted as a limited permeability barrier. Although flows have been largely eroded from above the P<sub>1</sub> pyroclastics at the prospect, in view of the occurrence of similar lava flows on Paradise Ridge to the west and the buttes to the east of the prospect, these flows were probably once continuous and covered the area of the prospect. P<sub>1</sub> pyroclastic rocks below the lava flows are altered, with the T<sub>4</sub> tuffs at and near the top of the hill in sections 4 and 9 being more altered than the underlying T<sub>3</sub> tuffs. The T<sub>3</sub> tuffs may have originally been welded tuffs, and less permeable than overlying nonwelded tuffs.

Alteration is laterally extensive in the higher levels of the system. Laterally extensive alteration in permeable horizons within and below the flow sequences would be facilitated by local structural disruption of the barrier, permitting venting of the hydrothermal fluids through the barrier. Individual flows in the sequence may have acted as smaller barriers, restricting much of the alteration to the more permeable and easily altered tuff layers. A cartoon of this model is shown in Figure 40. Operation of the model in the Wind River area is

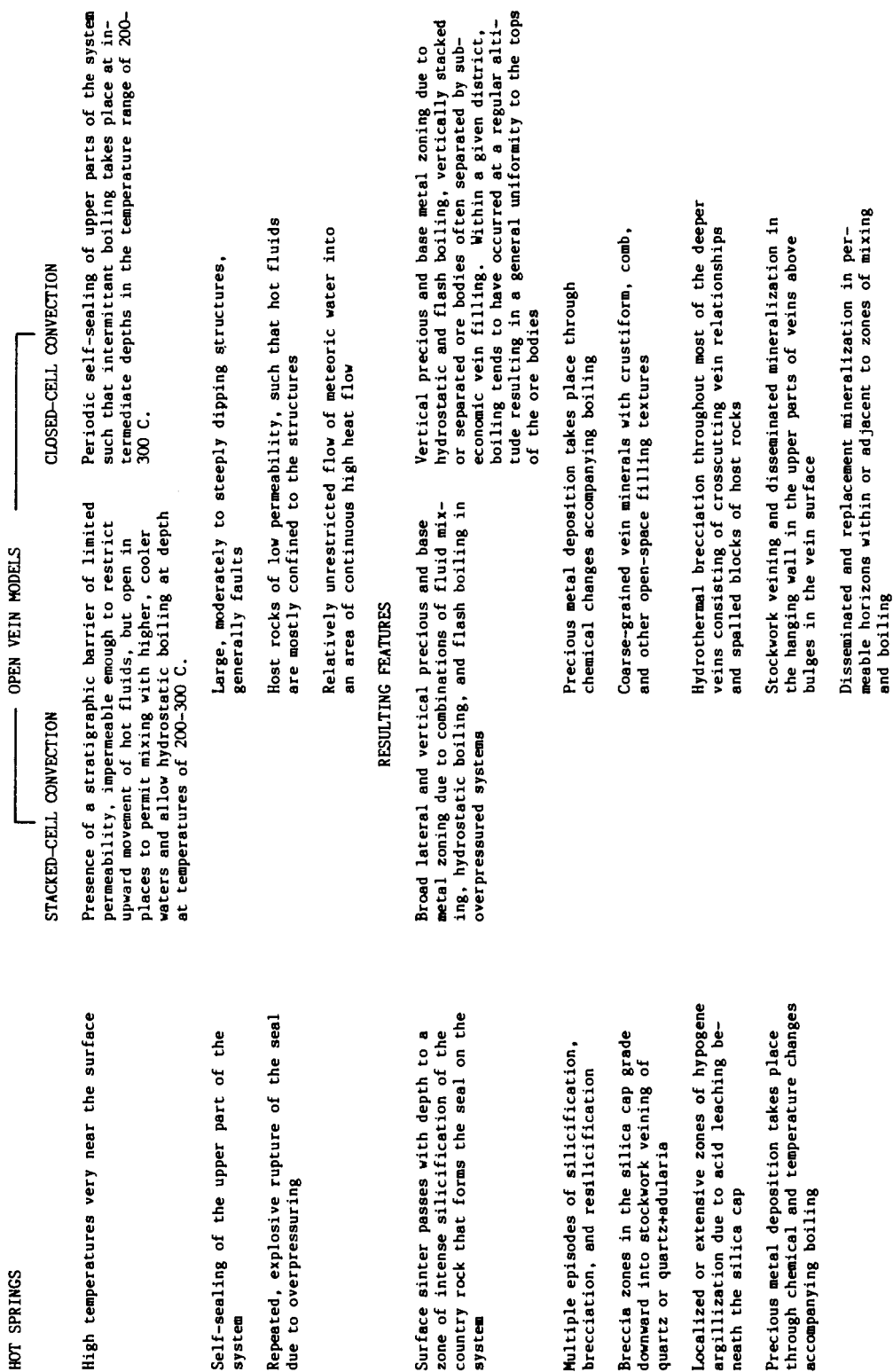


Figure 39. Summary of models for epithermal precious metal deposits (after Berger and Eimon, 1982)

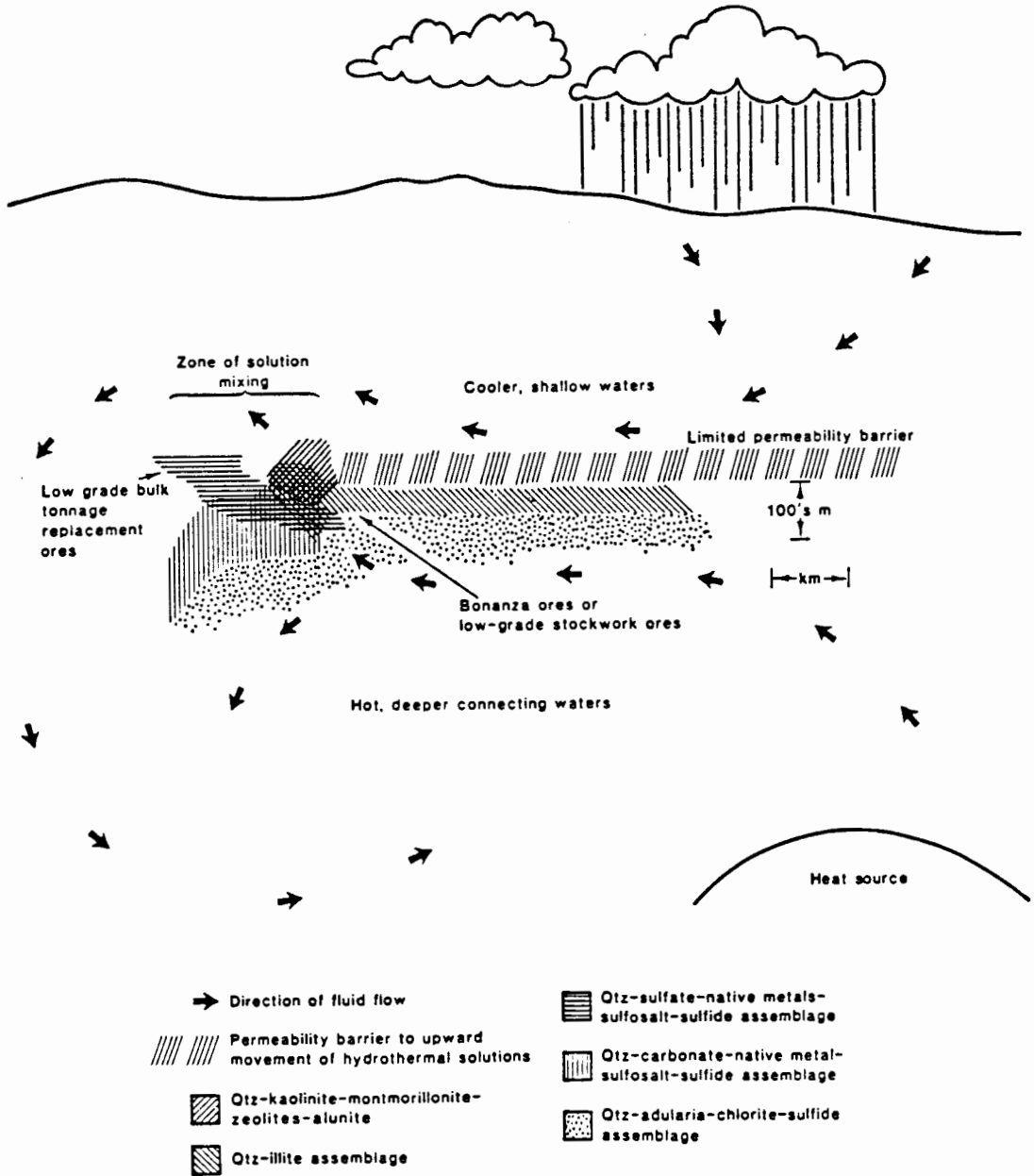


Figure 40. Cross-section of fluid flow patterns and lateral alteration zoning in the stacked-cell convection model of open-vein deposition (from Berger and Eimon, 1982).

envisioned as follows:

- 1). Thermal fluids rise along structures until they encounter the limited permeability barrier of the flow groups. Through-going faults or fractures vent fluids to the surface and allow mixing with fluids of cooler, overlying aquifers.
- 2). Intermittant boiling may have taken place along the barrier due to structural breaks or incomplete sealing of the system. Short-lived 'leakers' may be responsible for the 'rootless' zones on the margins of the system.
- 3). Major mixing or boiling activity takes place where structurally-produced breaks in the flow sequences allow contact between hot thermal fluids and cooler, shallower groundwater.
- 4). Violent boiling may have occurred in the upper, more fractured parts of the system. Flashing of waters to steam during periods of slow recharge to open fractures would increase the amount of acid-leach alteration occurring in this part of the system. This mechanism of acid leaching is most likely to occur in areas where the system was sealed and became overpressured.
- 5). Boiling levels in the system may fluctuate due to intermittant sealing and overpressuring of the system.

The development of the Wind River hydrothermal system through time is shown schematically in Figure 41.

Flows of the A<sub>1</sub> group begin to be erupted and are deposited on the P<sub>1</sub> pyroclastic rocks. At some time during the deposition of the A<sub>1</sub> flows, the hydrothermal system begins to develop and is focused by structures which vent fluids to the surface.

The overlying lava flows act as a barrier to the system. Differing mechanical properties cause the flows to break differently under stress than the pyroclastic rocks.

Rising fluids boil in zones of fracturing of the limited permeability barrier. Release of CO<sub>2</sub> and H<sub>2</sub>S forms acid condensate which produces strong alteration in the more permeable and more reactive tuffs intercalated with the flows and below the flow groups as a whole. Flashing to steam in these zones may cause more pervasive alteration. Repeated, explosive rupture in zones of overpressuring below the water table produces sulfide-rich quartz-cemented breccias.

Eruption of flows continued during the life of the hydrothermal system. Strongly altered D<sub>1</sub> dikes represent feeders for the oldest A<sub>1</sub> flows.

D<sub>1</sub> dikes of lesser alteration represent waning of the system. The hydrothermal system becomes buried by the growing volcanic pile.

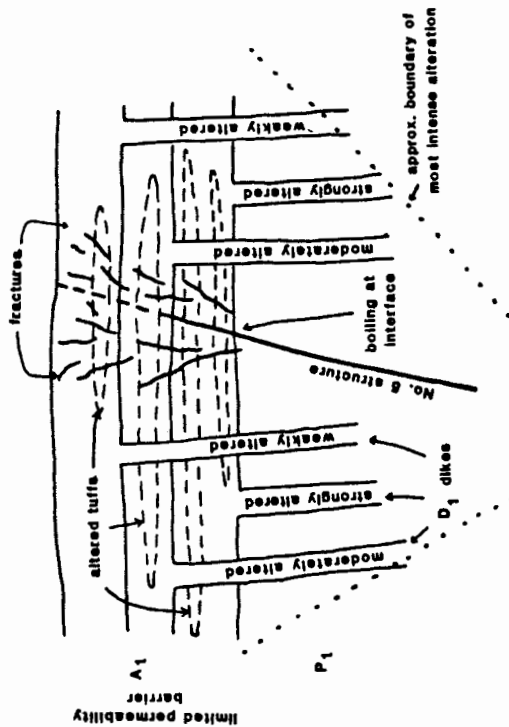
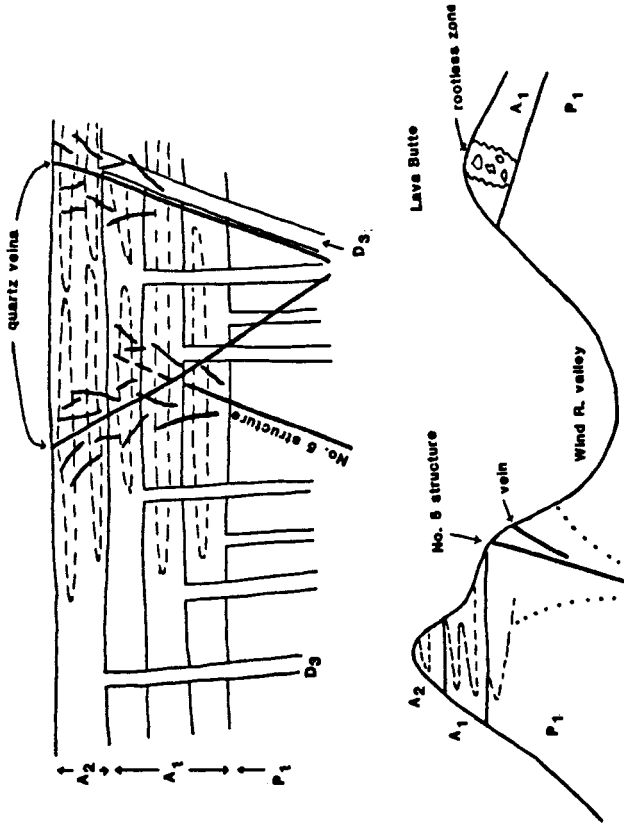


Figure 41. Development of the Wind River hydrothermal system through time.





2 A flows are deposited. Feeder dikes are emplaced along zones of structural weakness. Renewed hydrothermal activity produces the large quartz veins. Veins are frequently emplaced along zones of weakness previously intruded by dikes. Locus of boiling shifts upward relative to earlier activity, perhaps in response to changing fluid flow, water table, and paleosurface. Alteration envelopes associated with this later phase of activity overprint previous alteration in higher parts of the system which have since been removed by erosion.

Higher parts of the system over the prospect are removed by erosion. Type 2 alteration on Paradise Ridge to the west indicates previous lateral extent of alteration.

Figure 41. (continued)

## SUMMARY

The Wind River prospect shows a complex interplay between volcanic, hydrothermal, and structural activity. Relations among the A<sub>1</sub> and A<sub>2</sub> lava flows, the D<sub>1</sub>, D<sub>2</sub>, and D<sub>3</sub> dikes, and regional structural controls form the setting for the hydrothermal system developed at the prospect.

North-northeast-trending structures appear to be the most important in terms of providing foci for hydrothermal activity. Activation of these structures occurred relatively late.

There are three groups of dikes intruding the altered pyroclastic rocks at the prospect. D<sub>3</sub> dikes are chemically distinct from D<sub>1</sub> dikes. Chemical groupings within the D<sub>1</sub> dikes are related to degree of alteration of the dikes. The D<sub>1</sub>, D<sub>2</sub>, and D<sub>3</sub> dikes are chemically similar to the A<sub>1</sub> and A<sub>2</sub> lava flows. D<sub>1</sub> dikes are similar to A<sub>1</sub> flows, and D<sub>3</sub> dikes are similar to A<sub>2</sub> flows, suggesting the flows were fed by the different groups of dikes. The D<sub>3</sub> dikes would then be younger than the D<sub>1</sub> dikes.

Three types of hydrothermal alteration have been recognized in the study area, representing different lateral and vertical distances from the center of hydrothermal activity. Alteration extends up through the

flow groups capping the ridges, and therefore postdates the flows.

Type 1 alteration represents leaks off the main system where hydrothermal activity was not of sufficient duration or intensity to produce large quartz veins or mineralogically advanced alteration. Type 2 alteration represents expression of the hydrothermal system at higher elevations and off to one side of the main system. Alteration is laterally most extensive in permeable horizons. Acid leaching may have been a factor in causing this alteration. Types 1 and 2 alteration were probably structurally controlled, although poor exposures in the field make this difficult to prove. Both types of alteration have geochemical anomalies of Sb and/or As associated with them.

Alteration at the prospect is structurally controlled. Zoned alteration is controlled by the No. 5 structure. The most intense alteration is located in and near the structure. Alteration decreases in intensity away from the structure. In general, distribution of alteration metals decreases away from the structure. The large quartz veins cutting the zoned alteration produce halos of alteration metals that are superimposed on the effects of the No. 5 structure.

The quartz veins at the prospect are structurally controlled. Quartz veins frequently crosscut or are emplaced along the margins of dikes, suggesting that both dikes and veins were emplaced along the same zones of weakness. The quartz veins have brecciated or sheared margins. Quartz-cemented breccias may occur along either or both margins of the veins. The No. 2 vein in the adit shows pinch and swell along its length, and vein-margin shears and breccias, suggesting the vein lies in a fault and that movement has occurred on the structure during the

course of vein deposition.

Fluids responsible for alteration and mineralization were of relatively low temperatures and salinities. The fluids were probably of near-neutral pH, and the Au transported by S complexes. Present-day geothermal systems depositing ore-grade precipitates have waters that are near-neutral to slightly alkaline in pH. Au is much more soluble in such fluids as S complexes. As and Sb complexes cannot be ruled out, given the high concentrations of these metals in the system. Highest concentrations of Sb occur with the highest concentrations of Au, suggesting Sb may have acted as a collecting agent, causing Au to precipitate.

The fluids were high in  $\text{CO}_2$  and reducing in nature. High  $\text{CO}_2$  fluids are indicated by abundant calcite as both precipitated and replacement material. The reducing nature of the fluids is indicated by transport of Fe in the alteration of the dikes, and reduction and transport of Eu in vein margins. The solutions became oxidized in the higher parts of the system. Au distribution in the veins indicates multiple episodes of mineralization.

The Wind River hydrothermal system is not related to the episode of metallogenesis responsible for porphyry copper systems presently exposed in the Cascades. Porphyry systems in the southern Washington Cascades are typified by deposits of the St. Helens and Washougal mining districts, which represent deeper, hotter environments than that of the Wind River prospect.

Hydrothermal activity overlapped and postdated deposition of the A<sub>1</sub> and A<sub>2</sub> lava flows. Hydrothermal activity was structurally

controlled, with N-NE trending structures the most important. The lava flow groups acted as a limited permeability barrier on the system. Alteration is laterally extensive in permeable horizons within and below the flow sequences. Major fluid mixing and/or boiling activity took place in proximity to structural disruptions of the barrier. The No. 5 structure represents an earlier phase of hydrothermal activity than do the quartz veins. Extensive alteration envelopes associated with the veins may have existed in parts of the system that have since been removed by erosion. As the lava flow sequence thickened, the locus of hydrothermal activity shifted upward.

## REFERENCES

- Allen, J. E., 1932, Contributions to the structure, stratigraphy, and petrography of the lower Columbia River Gorge: MS thesis, University of Oregon, Eugene, Oregon, 96 p.
- Armstrong, R. L., 1978, Cenozoic history of the U.S. Cordillera from lat. 42° to 49°N, in, Smith, R. B., and Eaton, G. P., eds., Cenozoic tectonics and regional geophysics of the western Cordillera: Geological Society of America Memoir 152, p. 263-282.
- Armstrong, R. L., Harakol, J. E., and Hollister, V.F., 1976, Age determination of late Cenozoic porphyry copper deposits of the North American Cordillera: Institute of Mining and Metallurgy (London) Transactions, section B, v. 85, p. 239-244.
- Beeson, M. H., Moran, M.R., Anderson, J. L., and Vogt, B. F., 1982, The relationship of the Columbia River Basalt Group to the geothermal potential of the Mt. Hood area, in, Priest, G. R., and Vogt, B. F., eds., Geology and geothermal resources of the Mt. Hood area, Oregon: Oregon Department of Geology and Mineral Industries special paper 14, p. 43-46.
- Berger, B. R., and Eimon, P. I., 1982, Conceptual models of epithermal precious metal deposits: Society of Mining Engineers of AIME preprint 82-13, 14 p.
- Berri, D. A., and Korosec, M. A., 1983, Geologic and geothermal investigation of the lower Wind River valley, southwestern Washington Cascade Range: Washington Division of Geology and Earth Resources open file report no. 83-5, 48 p.
- Brooks, H. C., and Ramp, L., 1968, Gold and silver in Oregon: Oregon Department of Geology and Mineral Industries Bulletin 61, 337 p.
- Boyle, R. W., 1969, Hydrothermal transport and deposition of gold—a discussion: Economic Geology, v. 64, p. 112-115.
- Boyle, R. W., 1979, The geochemistry of gold and its deposits: Geological Survey of Canada Bulletin 280, 584 p.

- Browne, P. R. L., and Ellis, A. J., 1970, The Ohaki-Broadlands hydrothermal area, New Zealand-mineralogy and related geochemistry: *American Journal of Science*, v. 269, p. 97-131.
- Buchanan, L. J., 1981, Precious metal deposits associated with volcanic environments in the southwest: *Arizona Geological Society Digest*, v. 14, p. 237-262.
- Buckovic, W. A., 1979, The Eocene deltaic system of west-central Washington, *in*, Armentrout, J. M., Cole, M. R., and Terbest, H. eds., *Cenozoic paleogeography of the western United States, Pacific Coast Paleogeography Symposium 3*, Society of Economic Paleontologists and Mineralogists special publication, p. 147-163.
- Callaghan, E., and Buddington, A. F., 1938, Metalliferous mineral deposits in the Cascade Range in Oregon: *U. S. Geological Survey Bulletin* 893, 141 p.
- Campbell, I. H., Leshner, C. M., Coad, P., Franklin, J. M., Gorton, M. P., and Thurston, P. C., 1984, Rare earth element mobility in alteration pipes below massive Cu-Zn sulfide deposits: *Chemical Geology*, v. 45, p. 181-202.
- Chaney, R. W., 1918, The ecological significance of the Eagle Creek flora of the Columbia River Gorge: *Journal of Geology*, v. 26, p. 577-592.
- Christiansen, R. L., and Lipman, P. W., 1972, Cenozoic volcanism and plate tectonic evolution of the western United States, II. Late Cenozoic: *Philosophical Transactions of the Royal Society of London series A*, v. 271, p. 249-284.
- Church, S. E., Hammond, P. E., and Barnes, D. J., 1983a, Mineral resource potential of the Indian Heaven roadless area, Skamania Co., Washington: *U. S. Geological Survey open file report* 83-467.
- Church, S. E., Hammond, P. E., and Barnes, D. J., 1983b, Geochemical and statistical analysis of analytical results for stream sediments, rocks, ores, and waters collected from the Indian Heaven roadless area, Skamania Co., Washington: *U. S. Geological Survey open file report* 83-0234.
- Davis, G. A., 1977, Tectonic evolution of the Pacific Northwest, Precambrian to present, *in*, Washington Public Power Supply Systems P: S. A. R. for W. P. S. S. Nuclear Project 1 and 4, Amendment 23, Subappendix 2RC, Nuclear Regulatory Commission docket nos. 50-460 and 50-513, p. C1-C46.
- Davis, G. A., Monger, J. W. H., and Burchfiel, B. C., 1978, Mesozoic construction of the Cordilleran "collage", central British Columbia to central California, *in*, Mesozoic paleogeography of the western United States, *Pacific Coast Paleogeography Symposium*

2, Society of Economic Paleontologists and Mineralogists special publication, p. 33-70.

- Dickinson, W. R., 1979, Cenozoic plate tectonic setting of the Cordilleran region in the United States, in, Armentrout, J. M., Cole, M. R., and Terbest, H. eds., Cenozoic paleogeography of the western United States, Pacific Coast Paleogeography Symposium 3, Society of Economic Paleontologists and Mineralogists special publication, p. 1-13.
- Ekambaram, V., Kawabe, I., Tanaka, T., Davis, A. M., and Grossman, L., 1984, Chemical compositions of refractory inclusions in the Murchison C2 chondrite: *Geochimica et Cosmochimica Acta*, v. 48, p. 2089-2105.
- Engels, J. C., Tabor, R. W., Miller, F. K., and Obradovich, J. D., 1976, Summary of K-Ar, Rb-Sr, U-Pb, Pb alpha, and fission track ages of rocks from Washington state prior to 1975 (exclusive of Columbia Plateau basalts): U. S. Geological Survey miscellaneous field studies map MF-710.
- Ewers, G. R., and Keays, R. R., 1977, Volatile and precious metal zoning in the Broadlands geothermal field, New Zealand: *Economic Geology*, v. 72, p. 1337-1354.
- Felts, W. M., 1939a, A granodiorite stock in the Cascade Mountains of southwestern Washington: *Ohio Journal of Science*, v. 39, p. 297-316.
- Felts, W. M., 1939b, Keechelus andesitic lava flows of Washington in southward extension: *Pan-American Geologist*, v. 71, p. 294-296.
- Field, C. W., and Power, S. G., 1985, Metallization in the western Cascades, Oregon and Washington: *Geological Society of America Abstracts with Programs*, v. 17, no. 4, p. 218.
- Fiske, R. S., 1963, Subaqueous pyroclastic flows in the Ohanapecosh Formation, Washington: *Geological Society of America Bulletin*, v. 74, p. 391-406.
- Fiske, R. S., Hopson, C. A., and Waters, A. C., 1963, Geology of Mt. Rainier National Park: U. S. Geological Survey Professional Paper 444, 93 p.
- Giggenbach, W. F., 1981, Geothermal mineral equilibria: *Geochimica et Cosmochimica Acta*, v. 45, p. 393-410.
- Giggenbach, W. F., 1984, Mass transfer in hydrothermal systems—a conceptual approach: *Geochimica et Cosmochimica Acta*, v. 48, p. 2693-2711.
- Grant, A. R., 1969, Chemical and physical controls for base metal



deposition in the Cascade Range of Washington: Washington Department of Natural Resources Bulletin, v. 58, 107 p.

- Grant, A. R., 1982, Summary of economic geology data for the Glacier Peak Wildermess, Chelan, Snohomish, and Skagit Counties, Washington: U. S. Geological Survey open file report 82-0408, 41 p.
- Gresens, R. L., 1982, Early Cenozoic geology of central Washington state, II. Implications for plate tectonics and alternatives for the origin of the Chiwaukum graben: Northwest Science, v. 56, p. 259-264.
- Haas, J. L., 1971, The effect of salinity on the maximum thermal gradient of a hydrothermal system at hydrostatic pressure: Economic Geology, v. 66, p. 940-946.
- Hammond, P. E., 1974, Regional extent of the Stevens Ridge Formation in the southern Cascade Range, Washington: Geological Society of America Abstracts with Programs, v. 6, p. 188.
- Hammond, P.E., 1979, A tectonic model for the evolution of the Cascade Range, *in*, Armentrout, J. M., Cole, M. R., and Terbest, H. eds., Cenozoic paleogeography of the western United States, Pacific Coast Paleogeography Symposium 3, Society of Economic Paleontologists and Mineralogists special publication, p. 219-237.
- Hammond, P. E., 1980, Reconnaissance geologic map and cross-sections of the southern Washington Cascade Range, lat. 45° 30'-47° 15' N, long. 120° 45'-122° 22.5 W: Portland State University Department of Earth Science, 31 p.
- Hammond, P. E., Bentley, R. D., Brown, J. C., Ellingson, J. A., and Swanson, D. A., 1977, Volcanic stratigraphy and structure of the southern Cascade Range, Washington, *in*, Brown, E. H., and Ellis, R. C., eds., Geological excursions in the Pacific Northwest: Geological Society of America 1977 Annual Meeting, field trip no. 4, p. 127-169.
- Helgeson, H. C., and Garrels, R. M., 1968, Hydrothermal transport and deposition of gold: Economic Geology, v. 63, p. 622-635.
- Henley, R. W., 1973, Solubility of gold in hydrothermal chloride solutions: Chemical Geology, v. 11, p. 73-87.
- Hildreth, W., 1981, Gradients in silicic magma chambers-implications for lithospheric magmatism: Journal of Geophysical Research, v. 86, p. 10153-10192.
- Kerrich, R., and Fryer, B. J., 1979, Archean precious metal hydrothermal systems, Dome mine, Abitibi greenstone belt, II. REE and oxygen isotope relations: Canadian Journal of Earth Science, v. 16,

p. 440-458.

- Lipman, P. W., Prostka, H. J., and Christiansen, R. L., 1971, Evolving subduction zones in the western United States as interpreted from igneous rocks: *Science*, v. 174, p. 821-825.
- Lipman, P. W., Prostka, H. J., and Christiansen, R. L., 1972, Cenozoic volcanism and plate-tectonic evolution of the western United States, I. Early and middle Cenozoic: *Philosophic Transactions of the Royal Society of London series A*, v. 271, p. 217-248.
- Lowell, J. D., and Guilbert, J. M., 1970, Lateral and vertical alteration-mineralization zoning in porphyry ore deposits: *Economic Geology*, v. 65., p. 373-408.
- Ludden, J. N., Daigneault, R., Robert, F., and Taylor, R. P., 1984, Trace element mobility in alteration zones associated with Archean lode gold deposits: *Economic Geology*, v. 79, p. 1131-1141.
- Lux, D. R., 1982, K-Ar and  $^{40}\text{Ar}$ - $^{39}\text{Ar}$  ages of mid-Tertiary volcanic rocks from the western Cascade Range, Oregon: *Isochron West*, v. 33, p. 17-32.
- Misch, P., 1977, Dextral displacements at some major strike faults in the north Cascades: *Geological Association of Canada Programs with abstracts*, v. 2, p. 37.
- Moen, W. S., 1977, St. Helens and Washougal mining districts of the southern Cascades of Washington: *Washington Department of Natural Resources Information Circular no. 60*, 71 p.
- Newcomb, R. C., 1969, Effect of tectonic structure on the occurrence of groundwater in the basalt of the Columbia River Group in the Dalles area, Oregon and Washington: *U. S. Geological Survey Professional Paper 383-c*, 33 p.
- Newcomb, R. C., 1970, Tectonic structure of the main part of the basalt of the Columbia River Group, Washington, Oregon, and Idaho: *U. S. Geological Survey miscellaneous geological investigations map I-587*.
- Noble, D. C., 1972, Some observations on the Cenozoic volcano-tectonic evolution of the Great Basin, western United States: *Earth and Planetary Science Letters*, v. 17, p. 142-150.
- Peck, D. L., Griggs, A. B., Schlicher, A. G., Wells, F. G., and Dole, H. M., 1964, *Geology of the central and northern parts of the western Cascade Range in Oregon*: *U. S. Geological Survey Professional Paper 449*, 56 p.
- Polivka, D. R., 1984, Quaternary volcanology of the West Crater-Soda Peaks area, southern Washington Cascade Range: MS thesis, Portland

State University, Portland, Oregon, 78 p.

- Priest, G. R., Woller, N. M., Black, G. L., and Evans, S. H., 1982, Overview of the geology and geothermal resources of the central Oregon Cascades, *in*, Priest, G. R., and Vogt, B. F., eds., Geology and geothermal resources of the Cascades, Oregon: Oregon Department of Geology and Mineral Industries open file report O-82-7, p. 5-70.
- Raisz, E., 1945, The Olympic-Wallowa lineament: American Journal of Science, v. 243-A, p. 479-485.
- Roedder, E., 1984, Fluid inclusions: Mineralogical Society of America Reviews in Mineralogy, v. 12, 644 p.
- Rose, A. W., 1970, Zonal relations of wall rock alteration and sulfide distribution at porphyry copper deposits: Economic Geology, v. 65, p. 920-936.
- Schoen, R., and White, D. E., 1965, Hydrothermal alteration in GS-3 and GS-4 drill holes, Main Terrace, Steamboat Springs, Nevada: Economic Geology, v. 60, p. 1411-1421.
- Schoen, R., and White, D. E., 1967, Hydrothermal alteration of basaltic andesite and other rocks in drill hole GS-6, Steamboat Springs, Nevada: U. S. Geological Survey Professional Paper 575-B, p. B110-B119.
- Schoen, R., White, D. E., and Hemley, J. J., 1974, Argillization by descending acid at Steamboat Springs, Nevada: Clays and Clay Minerals, v. 22, p. 1-21.
- Schrieber, S. A., 1981, Geology of the Nelson Butte area, south-central Cascade Range, Washington: MS thesis, University of Washington, Seattle, Washington, 80 p.
- Schreiner, A., Jr., 1979, The geology and mineralization of the north part of the Washougal mining district, Skamania Co., Washington: MS thesis, Oregon State Univ., Corvallis, Oregon, 135 p.
- Shepard, R. J., 1979, Geology and mineralization of the southern Silver Star stock, Washougal mining district, Skamania County, Washington: MS thesis, Oregon State University, Corvallis, Oregon, 113 p.
- Seward, T. M., 1973, Thio complexes of gold and the transport of gold in hydrothermal ore solutions: Geochimica et Cosmochimica Acta, v. 37, p. 379-399.
- Snavely, P. D., and Wagner, H. C., 1963, Tertiary geologic history of western Oregon and Washington: Washington Division of Mines and Geology Report of Investigation 22, 25 p.

- Snyder, W. S., Dickinson, W. R., and Silberman, M. L., 1976, Tectonic implications of the space-time patterns of Cenozoic magmatism in the western United States: *Earth and Planetary Science Letters*, v. 32, p. 91-106.
- Stewart, J. H., Moore, W. J., and Zeitz, I., 1977, East-west patterns of Cenozoic igneous rocks, aeromagnetic anomalies, and mineral deposits, Nevada and Utah: *Geological Society of America Bulletin*, v. 88, p. 67-77.
- Tabor, R. W., Frizzel, V. A., Vance, J. A., and Naeser, C. W., 1984, Ages and stratigraphy of lower and middle Tertiary sedimentary and volcanic rocks of the central Cascades, Washington-application to the tectonic history of the Straight Creek fault: *Geological Society of America Bulletin*, v. 95, p. 26-44.
- Trimble, D. E., 1963, Geology of the Portland, Oregon and adjacent areas: *U. S. Geological Survey Bulletin* 1119, 119 p.
- Vance, J. A., 1982, Cenozoic stratigraphy and tectonics of the Washington Cascades: *Geological Society of America Abstracts with Programs*, v. 14, p. 241.
- Weissberg, B. G., 1969, Gold-silver ore-grade precipitates from New Zealand thermal waters: *Economic Geology*, v. 64, p. 95-108.
- Weissberg, B. G., 1970, Solubility of gold in hydrothermal alkaline sulfide solutions: *Economic Geology*, v. 65, p. 551-556.
- Wells, R. E., Engelbretson, D. C., Snavely, P. D., and Coe, R. S., 1984, Cenozoic plate motions and the volcano-tectonic evolution of western Oregon and Washington: *Tectonics*, v. 3, p. 275-294.
- White, D. E., 1974, Diverse origins of hydrothermal ore fluids: *Economic Geology*, v. 69, p. 954-973.
- White, D. E., 1981, Active geothermal systems and hydrothermal ore deposits: *Economic Geology 75th Anniversary vol.*, p. 392-423.
- Williams, I. A., 1916, The Columbia River Gorge-its geologic history interpreted from the Columbia River highway: *Oregon Bureau of Mines and Geology, Mineral Resources of Oregon* v. 2, no. 3, 130 p.
- Wise, W. S., 1961, The geology and mineralogy of the Wind River area, Washington, and the stability relations of celadonite: PhD dissertation, The Johns Hopkins University, Baltimore, Maryland, 258 p.
- Wise, W. S., 1970, Cenozoic volcanism in the Cascade Mountains of southern Washington: *Washington Division of Mines and Geology Bulletin* 60, 45 p.

## APPENDIX A

### INSTRUMENTAL NEUTRON ACTIVATION ANALYSIS

#### SAMPLE PREPARATION

Approximately 16 to 20 g of sample was first broken to chips, which were then sorted by hand under the binocular microscope to eliminate those containing abundant Fe-oxides and/or weathered surfaces. The sorted chips were crushed by hand in a tool steel mortar and pestle and sieved to -20 mesh.

One gram splits of powder were weighed to 4 decimal places on a Mettler balance and sealed in small polyvials, which were then loaded two to a larger polyvial. Standards were included in both the top and bottom layers.

Samples were irradiated in the lazy susan rack of the TRIGA Mark II reactor at Reed College in Portland, Oregon for 1.0 hr at 250 kw power. The full power flux of approximately  $2 \times 10^{12} \text{ n/cm}^2 \text{ sec}$  is generally used for geochemical samples. Samples were allowed to cool for a day or so before being transferred from the Reed reactor to Portland State University.

First counts were begun about 5 days after irradiation. Standards were counted for 3000 sec, samples for 1000 sec. Second counts were

begun about 35 days after irradiation, with standards counted for 9900 sec and samples for 3000 sec. Counting was done on a Tracor-Northern high-voltage biased, lithium-drifted germanium (Ge-Li) crystal detector maintained at operating temperatures in a Dewar flask of liquid nitrogen. Signals from the Ge-Li detector were analyzed and stored in a real-time 4096 channel digital energy spectrum analyzer. The spectral data from the minicomputer was stored on floppy disks.

Elemental abundances were calculated by comparison of the spectra of a sample to those of a standard of known concentration. Data from the Tracor-Northern system was recopied into the Portland State University Honeywell Level 66 computer and processed by the Fortran INAA2 program. This method is limited in that it can only be used for elements that are present in the standards. The final output from the Honeywell shows elemental abundances in percent oxide or ppm, as appropriate, and statistical error bounds based on one standard deviation, reflecting how narrow and sharply defined the counting peak was relative to the background.

Analytical errors may arise from estimation of thermal neutron flux, differing geometries of the samples, and the fact that the detector is not 100% efficient. Further inaccuracies will result if care is not taken in sample selection and preparation. Also, in a comparative method, the accuracy and precision of the analyses cannot be better than that for the standards used.

## CHONDRITE VALUES USED FOR NORMALIZATION OF RARE EARTH ELEMENTS

REE	PPM
La	0.2347
Ce	0.6096
Sm	0.1461
Eu	0.0550
Tb	0.0361
Yb	0.1587
Lu	0.0239

Data are from Ekambaram and others (1984).

## SAMPLES IN WHICH AG, HG, AND W WERE DETECTED

Ag	Hg	W
WRM-13A	WRM-13A	16-1
WRM-24	WRR-TD1	16-3
WRM-36	WRM-36	16-4
WRR-13	WRR-55	16-5
WRR-40	WRR-57	16-6
WRR-55	9-3	9-4
M-09	9-5	
M-046	R-036	
16-5	MF9+20	
M-08	M-08	
M-045	R-035	
PCNT2-4	PCNT2-4	
DR-VN-1		



ITAA DATA

EXISTA 1ST RUN 7D TOP 1ST COUNT

SAMPLE	SN	LJ	LA	TB	AU	AS	SB	MA	K						
WR-TAI	9.11	0.06	0.61	0.10	52.10	0.70	3.80	0.40	0.	0.	0.90	0.30	1.70	0.12	0.20
WR-TC1	7.11	0.05	0.46	0.07	34.40	0.50	3.40	0.30	0.	0.	1.30	0.20	0.96	0.	0.30
WR-TD1	4.60	0.04	0.54	0.08	23.90	0.40	3.20	0.30	0.03	0.01	1.50	0.30	1.64	0.01	0.40
WR-TE1	4.12	0.04	0.43	0.08	21.40	0.40	2.80	0.30	0.	0.	2.00	0.30	1.70	0.01	0.40
WR-TF3	3.97	0.03	0.56	0.07	19.40	0.30	3.00	0.30	0.	0.	7.30	0.90	0.06	0.	0.30
WR-TC1	6.65	0.04	0.65	0.08	47.50	0.60	3.60	0.30	0.	0.	4.20	0.50	0.95	0.	0.12
WR-TC2A	3.09	0.02	0.57	0.06	12.90	0.20	3.10	0.30	0.	0.	7.40	0.90	0.12	0.	0.20
WR-TC2B	2.38	0.02	0.42	0.05	9.24	0.18	2.60	0.20	0.	0.	8.	1.00	0.04	0.	0.
WR-TE2	6.30	0.05	0.53	0.08	28.80	0.50	3.40	0.40	0.	0.	0.80	0.20	2.91	0.01	0.20
WRBECKL	6.13	0.05	0.62	0.09	35.60	0.60	2.90	0.40	0.	0.	1.20	0.30	3.67	0.01	0.20
WRBECKD	8.18	0.06	0.63	0.10	49.60	0.70	4.50	0.50	0.	0.	0.90	0.30	3.65	0.01	0.30
WRH-1	6.01	0.04	0.61	0.09	26.10	0.40	3.60	0.40	0.	0.	1.10	0.30	2.12	0.01	0.20
WRH-8	5.82	0.05	0.55	0.09	26.00	0.50	2.90	0.40	0.	0.	0.	0.30	3.00	0.01	0.20
WRH-9	8.91	0.06	0.88	0.10	31.30	0.50	5.10	0.40	0.	0.	1.50	0.30	1.46	0.01	0.50
WRH-10	2.56	0.02	0.	0.	11.40	0.20	1.10	0.20	0.38	0.01	3.70	0.50	0.07	0.	0.40
WRH-11	2.90	0.03	0.26	0.06	11.60	0.20	1.20	0.20	0.22	0.01	5.00	0.60	0.10	0.	0.40
WRH-12	1.62	0.02	0.17	0.04	5.96	0.14	1.07	0.16	0.02	0.	5.80	0.70	0.04	0.	0.17
WRH-13A	0.	0.	0.	0.	0.11	0.02	0.	0.	10.42	0.05	20.00	2.00	0.01	0.	0.08
WRH-14	3.70	0.03	0.30	0.07	17.20	0.30	2.00	0.30	0.03	0.	2.70	0.40	0.13	0.	0.50
WRH-15	6.16	0.05	0.44	0.09	26.00	0.50	2.90	0.40	0.	0.	0.	0.	3.00	0.01	0.20
WRH-21	6.24	0.05	0.57	0.09	28.40	0.50	3.20	0.40	0.	0.	0.	0.	2.68	0.01	0.40
WRH-22	1.85	0.02	0.21	0.04	8.10	0.17	1.16	0.17	0.10	0.	8.90	1.10	0.10	0.	0.30
WRH-24	2.29	0.02	0.21	0.05	10.80	0.20	1.22	0.19	0.50	0.01	5.80	0.70	0.18	0.	0.30
WRH-25	5.62	0.05	0.54	0.10	23.50	0.50	3.30	0.40	0.	0.	0.90	0.30	2.52	0.01	0.20
WRH-35	5.95	0.05	0.58	0.10	25.30	0.50	3.40	0.40	0.	0.	0.	0.	2.43	0.01	0.40
WRH-36	0.05	0.01	0.	0.	0.12	0.03	0.	0.	7.06	0.04	23.00	3.00	0.01	0.	0.
WRH-37	4.82	0.04	0.36	0.05	20.60	0.30	2.70	0.20	0.	0.	2.70	0.40	0.10	0.	0.40
219-1	2.73	0.04	0.	0.	13.20	0.40	1.20	0.30	0.	0.	0.	0.	4.46	0.02	0.30
219-2	17.32	0.09	1.21	0.13	59.50	0.80	8.00	0.60	0.	0.	1.30	0.20	2.55	0.01	0.30
64-1(T)	5.52	0.04	0.35	0.09	25.10	0.50	2.20	0.40	0.	0.	0.	0.	2.91	0.01	0.17
201-1(T)	7.16	0.06	0.71	0.10	27.80	0.50	4.80	0.50	0.	0.	0.	0.	3.83	0.01	0.30
127-1(T)	5.46	0.04	0.52	0.09	21.40	0.40	3.20	0.40	0.	0.	0.	0.	3.40	0.01	0.30
PT124-3(T)	5.95	0.05	0.62	0.09	22.70	0.40	3.90	0.40	0.	0.	0.	0.	3.86	0.01	0.20
101-2(T)	4.41	0.04	0.37	0.08	17.20	0.40	2.50	0.40	0.	0.	0.	0.	4.24	0.02	0.30
EMT-7(T)	4.41	0.03	0.31	0.05	31.30	0.40	1.63	0.20	1.85	0.01	0.60	0.30	2.40	0.01	0.30
BCK-1(T)	6.60	0.04	0.55	0.06	26.00	0.40	3.40	0.30	0.	0.	0.	0.	3.27	0.01	0.20
ROM-(T)	4.56	0.03	0.31	0.04	28.30	0.40	1.88	0.20	0.	0.	0.	0.	3.04	0.01	0.40
PC-14(T)	3.65	0.03	0.31	0.06	25.20	0.40	2.90	0.20	0.	0.	0.37	0.10	3.77	0.01	0.40
W-1(T)	3.21	0.03	0.	0.	10.70	0.20	1.82	0.19	0.	0.	1.00	0.17	2.09	0.01	0.20

## KRISTA 1ST RUN BOTTOM 1ST COUNT

SAMPLE	SH	LJ	LA	YB	AU	AS	SB	NA	K								
WRR-1C	4.78	0.04	0.68	0.09	16.80	0.40	3.50	0.40	0.	0.	0.	2.70	0.40	3.78	0.01	1.10	0.20
WRR-2B	6.56	0.05	0.61	0.10	27.10	0.50	3.90	0.40	0.	1.70	0.40	1.60	0.30	3.18	0.01	2.40	0.30
WRR-3	5.97	0.04	0.54	0.08	20.80	0.40	3.20	0.30	0.	10.20	0.40	1.90	0.30	1.95	0.01	1.90	0.20
WRR-5	5.39	0.04	0.49	0.09	19.50	0.40	3.10	0.40	0.	0.	0.	2.40	0.30	2.89	0.01	1.17	0.19
WRR-6	5.24	0.04	0.57	0.09	19.60	0.40	3.90	0.40	0.	1.50	0.40	1.90	0.30	2.96	0.01	1.13	0.19
WRR-8	5.67	0.05	0.56	0.10	20.80	0.40	3.80	0.40	0.	12.40	0.50	1.40	0.30	2.91	0.01	1.40	0.20
WRR-12	4.08	0.04	0.35	0.06	16.00	0.30	2.20	0.30	0.	10.10	0.30	1.20	0.20	0.69	0.	3.20	0.30
WRR-13	0.06	0.01	0.	0.	0.47	0.04	0.	0.	0.26	0.60	0.07	10.60	1.30	0.04	0.	1.57	0.14
WRR-14	3.78	0.04	0.43	0.08	15.20	0.30	2.80	0.40	0.	9.00	0.40	0.	0.	2.32	0.01	4.40	0.40
WRR-23A	3.51	0.03	0.35	0.05	10.90	0.20	2.40	0.20	0.03	31.60	0.40	6.90	0.80	0.05	0.	3.90	0.40
WRR-23B	0.58	0.01	0.	0.	1.88	0.08	0.59	0.12	0.01	5.12	0.12	10.70	1.30	0.05	0.	3.40	0.30
WRR-25	7.35	0.05	0.53	0.09	35.00	0.50	4.10	0.40	0.	9.30	0.40	0.80	0.20	2.61	0.01	4.30	0.40
WRR-28	5.92	0.05	0.44	0.09	21.10	0.40	3.10	0.40	0.	13.70	0.50	1.10	0.20	2.97	0.01	1.80	0.20
WRR-31	6.87	0.05	0.41	0.09	26.30	0.40	3.60	0.40	0.	24.20	0.50	1.30	0.30	3.04	0.01	3.10	0.30
WRR-34	6.15	0.04	0.52	0.08	24.10	0.40	2.70	0.40	0.	17.00	0.50	0.90	0.20	2.31	0.01	3.30	0.40
WRR-36	4.62	0.04	0.40	0.06	16.90	0.30	2.20	0.20	0.	18.30	0.30	4.60	0.60	0.40	0.	5.20	0.50
WRR-37	1.80	0.02	0.18	0.05	6.50	0.16	1.30	0.20	0.12	23.00	0.30	6.20	0.70	0.30	0.	4.50	0.40
WRR-39	1.14	0.02	0.20	0.04	4.46	0.14	1.29	0.18	0.03	40.40	0.40	5.90	0.70	0.07	0.	3.60	0.30
WRR-40	0.05	0.01	0.	0.	0.32	0.03	0.	0.	0.90	0.74	0.06	18.00	2.00	0.02	0.	0.05	0.01
WRR-43	4.50	0.04	0.47	0.07	20.80	0.30	2.90	0.30	0.05	48.00	0.50	4.80	0.60	0.72	0.	4.50	0.40
WRR-44	5.88	0.05	0.40	0.07	26.90	0.40	2.60	0.30	0.	26.70	0.50	2.60	0.30	1.02	0.01	4.10	0.40
WRR-46	2.08	0.02	0.13	0.04	10.02	0.18	0.79	0.15	0.01	20.50	0.20	3.40	0.40	0.05	0.	2.18	0.20
WRR-49	0.	0.	0.	0.	0.	0.	0.	0.	0.16	0.	0.	46.00	5.00	0.02	0.	0.04	0.01
WRR-52	6.16	0.05	0.55	0.09	30.10	0.50	3.80	0.40	0.	22.60	0.60	2.10	0.30	3.46	0.01	2.90	0.30
WRR-53	5.04	0.05	0.47	0.08	24.00	0.40	2.90	0.40	0.04	25.70	0.50	1.80	0.30	2.43	0.01	4.00	0.40
WRR-55	0.09	0.02	0.	0.	0.54	0.04	0.	0.	20.65	0.97	0.10	31.00	4.00	0.02	0.	0.08	0.01
WRR-57	1.99	0.03	0.	0.	8.50	0.20	1.00	0.19	0.27	47.90	0.50	12.90	1.50	0.06	0.	3.50	0.30
WRR-58	6.99	0.05	0.48	0.09	30.30	0.50	4.20	0.40	0.	15.90	0.50	2.10	0.30	3.37	0.01	2.90	0.30
PC-4D	1.87	0.03	0.22	0.06	8.10	0.20	1.40	0.30	0.12	206.40	1.30	14.30	1.70	0.65	0.	0.73	0.13
64-1(B)	5.07	0.04	0.42	0.09	22.90	0.40	2.50	0.40	0.	1.20	0.30	0.	0.	2.71	0.01	0.66	0.15
201-1(B)	7.17	0.05	0.83	0.10	29.10	0.50	5.10	0.50	0.	0.	0.	0.	0.	3.90	0.01	1.70	0.30
127-1(B)	5.48	0.04	0.66	0.09	21.00	0.40	4.10	0.40	0.	0.	0.	0.	0.	3.53	0.01	1.50	0.30
PTI24-3(B)	6.00	0.05	0.62	0.09	23.30	0.50	4.00	0.40	0.	9.90	0.40	0.	0.	3.97	0.01	0.80	0.20
101-2(B)	4.42	0.04	0.34	0.08	17.50	0.40	2.90	0.40	0.	10.50	0.50	0.	0.	4.39	0.01	1.50	0.30
EMT-7(B)	4.53	0.03	0.30	0.05	32.60	0.40	1.90	0.20	1.85	80.00	0.60	1.80	0.20	2.49	0.01	3.80	0.40
BCR-1(B)	6.60	0.04	0.55	0.06	26.00	0.30	3.40	0.30	0.	0.	0.	0.	0.	3.27	0.01	1.70	0.20
BOM-1(B)	5.31	0.03	0.37	0.05	31.60	0.40	2.40	0.20	0.	0.	0.	0.	0.	3.18	0.01	4.50	0.40
PC-14(B)	3.77	0.03	0.53	0.06	25.70	0.30	3.30	0.30	0.	0.	0.	0.	0.	3.91	0.01	4.50	0.40
W-1(B)	3.25	0.02	0.35	0.04	11.01	0.19	2.10	0.20	0.	0.	0.	1.00	0.17	2.17	0.01	0.83	0.16

## KRISTA 1ST RUN 7D TOP SECOND COUNT

SAMPLE	TB	CE	EU	TB	RF	SC	FE	CO	TA	SB											
WRB-TA1	1.39	0.13	77.00	2.00	1.84	0.10	8.40	0.30	6.60	0.30	15.27	0.07	0.07	6.22	0.06	12.70	0.30	1.18	0.08	0.	0.
WRB-TCL	0.67	0.09	94.00	3.00	1.41	0.08	8.20	0.30	7.70	0.30	13.71	0.06	0.06	6.39	0.02	0.68	0.10	1.27	0.07	0.80	0.30
WRB-TDL	0.58	0.08	59.10	2.00	0.78	0.06	8.90	0.30	6.80	0.30	11.62	0.06	0.06	6.65	0.02	2.15	0.13	1.16	0.07	1.50	0.30
WRB-TFL	0.53	0.08	56.20	1.80	0.74	0.06	8.20	0.30	5.40	0.30	9.94	0.05	0.05	5.30	0.02	1.14	0.11	0.98	0.06	2.10	0.30
WRB-TFS	0.61	0.09	51.30	1.90	0.82	0.07	7.50	0.30	6.30	0.30	14.29	0.08	0.08	2.38	0.04	3.79	0.20	1.03	0.07	7.10	1.40
WRB-TG1	0.76	0.09	106.00	3.00	1.00	0.07	9.50	0.30	7.80	0.30	13.43	0.06	0.06	2.29	0.02	2.77	0.14	1.39	0.08	3.60	0.70
WRB-TG2A	0.61	0.09	57.70	2.00	0.56	0.06	7.90	0.30	6.40	0.30	13.77	0.06	0.06	1.57	0.03	4.38	0.19	1.14	0.07	7.10	1.40
WRB-TG2B	0.65	0.08	28.80	1.30	0.44	0.05	7.50	0.30	5.90	0.30	9.23	0.05	0.05	3.83	0.02	0.78	0.10	1.06	0.07	6.00	1.20
WRB-TG2	1.02	0.11	74.00	3.00	1.31	0.08	8.10	0.30	6.50	0.30	14.68	0.07	0.07	5.65	0.05	10.80	0.20	1.14	0.06	0.	0.
WRBRCCL	0.96	0.10	60.00	2.00	1.11	0.07	7.60	0.30	5.80	0.30	11.18	0.06	0.06	3.14	0.04	8.30	0.20	1.02	0.06	1.30	0.30
WRBRCED	1.00	0.12	95.00	3.00	1.58	0.09	9.00	0.40	6.50	0.30	14.04	0.08	0.08	5.93	0.07	11.40	0.30	1.11	0.07	1.30	0.40
WRM-1	0.97	0.11	64.00	2.00	1.19	0.08	8.50	0.30	6.30	0.30	16.36	0.07	0.07	6.80	0.06	13.70	0.30	1.04	0.07	1.30	0.30
WRM-8	0.93	0.11	51.00	2.00	1.57	0.09	6.70	0.30	6.00	0.30	18.48	0.08	0.08	7.33	0.06	18.60	0.40	1.04	0.08	1.20	0.30
WRM-9	1.05	0.12	89.00	3.00	1.69	0.09	9.10	0.30	9.10	0.40	15.84	0.07	0.07	5.11	0.05	5.00	0.20	1.68	0.10	1.40	0.40
WRM-10	0.35	0.05	23.10	1.00	0.36	0.04	2.96	0.14	2.34	0.13	5.29	0.03	0.03	1.56	0.01	2.86	0.12	0.41	0.03	5.00	1.00
WRM-11	0.49	0.07	30.50	1.40	0.50	0.06	3.26	0.17	2.54	0.17	8.13	0.05	0.05	2.44	0.03	6.20	0.20	0.48	0.04	6.20	1.20
WRM-12	0.31	0.05	13.90	0.90	0.28	0.04	1.65	0.12	1.70	0.13	4.58	0.04	0.04	1.79	0.03	4.52	0.17	0.32	0.04	7.90	1.60
WRM-13A	0.	0.	0.	0.	0.	0.	0.	0.	0.	0.	0.02	0.01	0.01	0.01	0.01	0.	0.	0.	0.	16.00	3.00
WRM-14	0.47	0.09	41.40	1.80	0.76	0.07	5.90	0.20	4.90	0.30	14.35	0.08	0.08	5.54	0.06	9.00	0.30	0.76	0.06	4.80	1.00
WRM-15	0.87	0.11	70.00	2.00	1.14	0.08	7.00	0.30	5.80	0.30	19.19	0.09	0.09	4.69	0.05	8.60	0.30	1.08	0.07	0.	0.
WRM-21	1.00	0.11	70.00	2.00	1.39	0.08	8.20	0.30	6.30	0.30	15.22	0.07	0.07	4.84	0.05	9.70	0.20	1.05	0.06	0.90	0.30
WRM-22	0.38	0.06	18.30	1.00	0.34	0.05	2.40	0.13	2.10	0.14	5.42	0.04	0.04	1.92	0.03	5.01	0.17	0.36	0.04	9.60	1.90
WRM-24	0.36	0.06	25.80	1.30	0.43	0.05	3.58	0.18	3.03	0.19	8.60	0.05	0.05	2.95	0.04	6.50	0.20	0.52	0.04	6.40	1.30
WRM-25	1.11	0.12	62.00	2.00	1.27	0.10	7.70	0.30	6.00	0.30	19.69	0.09	0.09	6.41	0.06	14.30	0.30	1.13	0.07	0.	0.
WRM-35	0.91	0.11	72.00	3.00	1.18	0.08	8.60	0.30	6.90	0.30	16.43	0.07	0.07	4.32	0.05	6.40	0.20	1.15	0.07	1.00	0.30
WRM-36	0.	0.	0.	0.	0.	0.	0.	0.	0.	0.	0.12	0.01	0.01	0.56	0.02	0.	0.	0.	0.	18.00	4.00
WRM-37	0.64	0.09	51.00	2.00	0.89	0.08	6.20	0.30	5.00	0.30	12.03	0.06	0.06	3.91	0.05	9.30	0.30	0.79	0.06	3.10	0.60
219-1	0.48	0.08	26.90	1.70	0.85	0.07	2.10	0.20	2.50	0.20	11.25	0.06	0.06	5.16	0.06	16.90	0.30	0.62	0.05	0.	0.
219-2	2.70	0.20	158.00	4.00	2.61	0.12	8.40	0.30	7.00	0.30	17.02	0.08	0.08	7.45	0.06	7.90	0.20	0.88	0.06	1.50	0.40
64-1(T)	0.80	0.12	57.00	2.00	1.51	0.09	4.10	0.30	4.60	0.30	25.69	0.09	0.09	8.92	0.08	29.70	0.50	1.28	0.08	0.	0.
201-1(T)	1.16	0.13	63.00	3.00	1.65	0.10	6.70	0.30	6.70	0.40	20.32	0.09	0.09	8.56	0.07	20.70	0.40	1.42	0.08	0.	0.
127-1(T)	0.83	0.11	44.00	2.00	1.35	0.08	5.60	0.30	4.80	0.30	22.13	0.10	0.10	8.05	0.07	19.30	0.40	0.93	0.06	0.	0.
PT124-3(T)	0.82	0.11	48.00	2.00	1.54	0.09	5.80	0.30	5.60	0.30	20.08	0.09	0.09	8.10	0.07	20.00	0.30	1.15	0.07	0.	0.
101-2(T)	0.52	0.10	35.00	2.00	1.37	0.08	3.40	0.30	3.90	0.30	18.73	0.08	0.08	6.86	0.07	18.10	0.30	0.83	0.06	0.	0.
BMT-7(T)	0.51	0.06	75.40	2.00	1.38	0.06	6.70	0.20	3.83	0.17	14.61	0.04	0.04	6.01	0.04	10.41	0.15	0.72	0.04	2.50	0.50
BCR-1(T)	1.00	0.09	53.90	1.80	1.94	0.08	6.00	0.20	4.70	0.20	33.00	0.09	0.09	13.40	0.06	38.00	0.40	0.91	0.05	0.	0.
BOM-(T)	0.81	0.08	76.00	2.00	1.03	0.05	16.80	0.50	4.32	0.18	10.95	0.04	0.04	4.40	0.03	11.44	0.16	1.46	0.06	0.	0.
FC-14(T)	0.53	0.05	66.90	1.80	0.56	0.03	9.40	0.30	3.25	0.14	3.21	0.02	0.02	0.84	0.01	0.32	0.03	1.01	0.05	0.20	0.07
W-1(T)	0.58	0.07	0.	0.	1.07	0.05	2.08	0.18	2.40	0.18	34.52	0.10	0.10	10.08	0.05	44.10	0.40	0.56	0.04	1.00	0.30

## KRISTA 1ST RUN 7D BOTTOM SECOND COUNT

SAMPLE	TB	CE	EU	TH	HF	SC	FZ	CD	TA	SB										
WR-1C	0.79	0.10	32.00	2.00	1.40	0.08	3.40	0.30	3.70	0.30	27.01	0.10	0.07	0.07	31.30	0.40	0.70	0.06	2.70	0.60
WR-2B	1.09	0.11	63.00	2.00	1.49	0.08	7.50	0.30	6.30	0.30	16.63	0.07	7.25	0.07	15.90	0.30	1.14	0.08	1.40	0.40
WR-3	1.04	0.11	40.00	1.80	1.30	0.07	4.80	0.30	5.00	0.30	16.86	0.08	4.80	0.05	8.20	0.20	0.89	0.06	2.20	0.50
WR-5	0.86	0.11	39.00	2.00	1.34	0.08	4.80	0.30	4.90	0.30	24.92	0.09	8.88	0.07	24.90	0.40	0.94	0.07	2.20	0.50
WR-6	0.69	0.10	36.00	2.00	1.31	0.08	4.50	0.30	4.70	0.30	24.82	0.09	8.91	0.08	25.10	0.40	0.80	0.06	2.20	0.50
WR-8	0.88	0.12	48.00	2.00	1.45	0.09	4.80	0.30	5.20	0.30	25.41	0.11	8.94	0.09	25.40	0.40	0.94	0.08	2.40	0.60
WR-12	0.63	0.09	18.40	1.70	0.86	0.06	3.20	0.20	2.80	0.20	15.42	0.07	5.45	0.06	11.40	0.30	0.44	0.05	1.80	0.40
WR-13	0.	0.	0.	0.	0.	0.	0.	0.	0.	0.	0.36	0.01	0.19	0.01	0.55	0.07	0.	0.	9.90	1.80
WR-14	0.64	0.10	8.10	1.70	1.10	0.06	4.90	0.30	4.70	0.30	22.88	0.10	10.32	0.08	19.60	0.40	0.90	0.06	1.20	0.40
WR-23A	0.57	0.08	19.70	1.50	0.58	0.06	5.00	0.30	3.80	0.30	13.85	0.07	5.99	0.06	11.90	0.30	0.62	0.05	8.80	1.70
WR-23B	0.11	0.03	5.00	0.60	0.11	0.03	0.41	0.07	0.31	0.07	1.90	0.02	0.72	0.02	1.34	0.10	0.	0.	10.50	2.00
WR-25	0.88	0.12	48.00	2.00	1.45	0.09	4.80	0.30	5.20	0.30	25.41	0.11	8.94	0.09	25.40	0.40	0.92	0.06	0.	0.
WR-28	0.82	0.11	37.00	2.00	1.63	0.09	4.40	0.30	4.50	0.30	20.40	0.09	7.48	0.07	19.50	0.40	1.10	0.07	0.	0.
WR-31	0.92	0.12	41.00	2.00	1.97	0.09	4.10	0.30	4.80	0.30	22.79	0.10	9.83	0.08	21.80	0.40	1.06	0.07	1.50	0.40
WR-34	0.75	0.10	47.00	2.00	1.81	0.09	4.00	0.30	4.50	0.30	18.82	0.08	7.97	0.07	17.90	0.30	1.05	0.07	0.80	0.30
WR-36	0.64	0.09	23.40	1.60	1.04	0.07	3.40	0.20	3.40	0.30	14.43	0.08	6.16	0.06	16.00	0.30	0.82	0.06	5.50	1.10
WR-37	0.37	0.07	12.40	1.10	0.53	0.05	2.51	0.16	2.53	0.17	8.80	0.06	4.19	0.05	13.20	0.30	0.50	0.04	7.90	1.50
WR-39	0.30	0.06	11.90	1.00	0.14	0.04	3.70	0.19	2.99	0.18	7.02	0.04	1.11	0.03	0.97	0.11	0.68	0.04	8.40	1.60
WR-40	0.	0.	0.	0.	0.	0.	0.	0.	0.	0.	0.23	0.01	0.13	0.01	0.47	0.08	0.	0.	18.00	3.00
WR-43	0.76	0.08	52.80	1.90	0.88	0.06	7.80	0.30	5.00	0.20	11.12	0.06	3.92	0.04	5.00	0.19	0.79	0.06	6.60	1.20
WR-44	0.71	0.11	22.20	1.90	1.21	0.08	4.00	0.30	4.40	0.30	18.85	0.08	8.76	0.08	26.80	0.50	1.11	0.07	2.40	0.50
WR-46	0.23	0.05	16.40	1.00	0.33	0.04	1.59	0.12	1.65	0.13	5.64	0.04	2.15	0.03	9.70	0.20	0.37	0.03	5.10	1.00
WR-49	0.	0.	0.	0.	0.	0.	0.	0.	0.	0.	0.02	0.	0.07	0.01	0.	0.	0.	0.	46.00	8.00
WR-52	1.24	0.12	76.00	3.00	1.41	0.08	10.60	0.40	6.80	0.30	15.00	0.07	5.68	0.06	14.30	0.30	1.05	0.06	2.30	0.50
WR-53	0.87	0.10	60.00	2.00	1.23	0.07	10.40	0.40	7.00	0.30	13.52	0.07	4.06	0.05	11.60	0.30	1.08	0.07	2.10	0.50
WR-55	0.	0.	0.	0.	0.	0.	0.	0.	0.	0.	0.06	0.01	0.12	0.01	0.	0.	0.	0.	31.00	6.00
WR-57	0.34	0.06	11.40	1.10	0.31	0.05	2.71	0.17	1.73	0.15	4.39	0.04	1.86	0.03	3.44	0.16	0.29	0.03	17.00	3.00
WR-58	0.92	0.11	74.00	3.00	1.19	0.08	10.10	0.40	6.50	0.30	15.96	0.07	6.26	0.07	14.60	0.30	0.93	0.06	2.20	0.50
PC-4D	0.28	0.07	4.50	1.10	0.47	0.04	2.86	0.20	2.96	0.19	6.98	0.04	6.17	0.06	5.18	0.18	0.46	0.04	22.00	4.00
64-1(B)	0.56	0.10	54.00	2.00	1.50	0.08	4.50	0.30	4.70	0.30	25.68	0.09	9.07	0.07	29.30	0.40	1.19	0.07	0.	0.
201-1(B)	1.30	0.12	64.00	2.00	1.61	0.08	6.80	0.30	6.50	0.30	20.17	0.09	8.60	0.07	21.10	0.40	1.18	0.07	0.	0.
127-1(B)	0.80	0.10	45.00	2.00	1.34	0.08	5.60	0.30	5.20	0.30	22.09	0.10	7.94	0.07	20.10	0.40	0.89	0.06	0.	0.
PT124-3(B)	0.80	0.10	48.00	2.00	1.39	0.09	5.70	0.30	5.20	0.30	19.90	0.09	8.24	0.07	20.90	0.40	1.05	0.07	0.	0.
101-2(B)	0.62	0.09	35.20	1.90	1.32	0.08	3.50	0.30	3.90	0.30	18.06	0.08	6.83	0.07	18.10	0.30	0.71	0.05	0.	0.
EMT-7(B)	0.54	0.05	75.40	2.00	1.42	0.05	7.00	0.20	4.06	0.17	14.77	0.04	6.20	0.04	10.44	0.16	0.68	0.04	2.50	0.50
BCR-1(B)	1.00	0.08	53.90	1.80	1.94	0.07	6.00	0.20	4.70	0.20	33.00	0.09	13.40	0.06	38.00	0.40	0.91	0.05	0.	0.
BCR-2(B)	0.72	0.06	87.00	2.00	1.12	0.05	11.20	0.30	3.90	0.16	10.70	0.04	4.59	0.03	12.65	0.13	1.62	0.07	0.	0.
FC-14(B)	0.57	0.05	68.30	1.80	0.51	0.03	9.70	0.30	3.22	0.13	3.24	0.02	0.86	0.01	0.29	0.03	0.94	0.04	0.26	0.08
W-1(B)	0.49	0.06	0.	0.	1.03	0.05	2.22	0.17	2.21	0.17	34.40	0.10	10.11	0.05	43.20	0.40	0.49	0.04	1.00	0.30



KRISTA 2ND RUN 7J BOTTOM 1ST COUNT

SAMPLE	SM	LA	LU	YB	AU	AS	SB	MA	K					
BCR-1(B)	6.60	0.06	26.00	0.30	0.55	0.06	3.40	0.30	0.	0.	0.	0.01	1.70	0.30
BQM-(B)	4.68	0.05	31.30	0.40	0.39	0.05	2.70	0.30	0.	0.	0.	0.	3.04	0.01
FC-14(B)	3.55	0.04	24.80	0.30	0.54	0.06	3.30	0.30	0.	0.	0.	0.	3.80	0.01
FMT-7(B)	4.68	0.04	33.60	0.40	0.31	0.05	1.90	0.30	1.85	0.02	80.00	0.60	2.53	0.01
BQM-(B)2	3.11	0.03	43.80	0.50	0.32	0.04	2.40	0.20	0.	0.	0.	0.	3.14	0.01
FC-14(B)2	3.51	0.05	24.50	0.40	0.51	0.05	3.30	0.30	0.	0.	0.	0.12	3.74	0.01
ARHCO-1(B)	11.29	0.08	48.70	0.50	0.70	0.06	5.00	0.40	0.	0.	0.	0.	3.31	0.01
M-01	7.10	0.08	24.80	0.50	0.65	0.09	4.80	0.60	0.	9.30	0.50	0.54	2.83	0.01
M-04	7.32	0.07	28.90	0.50	0.64	0.09	4.20	0.40	0.	16.40	0.60	0.96	2.41	0.01
M-06	1.04	0.02	4.33	0.13	0.	0.	0.	0.	0.49	0.01	77.40	0.50	0.04	0.
M-08	0.	0.	0.12	0.03	0.	0.	0.	0.	16.65	0.16	2.25	0.13	17.10	0.50
M-010	1.53	0.02	6.41	0.18	0.14	0.04	0.73	0.17	0.	0.	21.50	0.30	2.68	0.09
M-012	5.95	0.07	20.50	0.50	0.46	0.09	3.40	0.50	0.	0.	46.30	0.70	1.65	0.13
M-043	6.23	0.07	28.90	0.50	0.53	0.09	4.00	0.50	0.	11.80	0.50	0.72	2.13	0.01
M-045	0.12	0.02	0.38	0.04	0.	0.	0.	0.	26.00	0.20	0.66	0.10	7.30	0.20
M-047	6.11	0.06	23.10	0.40	0.52	0.07	3.50	0.30	0.	0.	22.10	0.30	2.70	0.10
M-049	2.57	0.04	8.20	0.20	0.22	0.05	1.40	0.20	0.74	0.02	9.40	0.30	2.07	0.08
R-033	4.92	0.07	18.70	0.40	0.47	0.09	3.00	0.50	0.	0.	5.10	0.50	0.60	0.10
R-035	3.28	0.04	13.90	0.30	0.24	0.04	1.41	0.20	0.16	0.01	9.30	0.20	2.56	0.09
R-026	5.15	0.07	23.10	0.40	0.46	0.08	3.50	0.40	0.	0.	3.90	0.40	0.32	0.09
MF21-40	4.86	0.07	19.60	0.40	0.62	0.09	4.00	0.60	0.	0.	10.70	0.50	1.39	0.11
MF21-20	6.08	0.07	27.70	0.50	0.55	0.09	3.90	0.50	0.	0.	33.40	0.60	1.47	0.13
MF22-20	6.38	0.09	26.00	0.50	0.61	0.09	4.40	0.50	0.	0.	6.30	0.50	1.20	0.10
MF15-20	6.12	0.07	27.70	0.50	0.42	0.08	4.00	0.50	0.	0.	3.30	0.50	0.56	0.11
MF24-40	5.53	0.07	20.40	0.40	0.38	0.09	2.40	0.40	0.	0.	16.10	0.60	2.62	0.13
R-023	5.87	0.08	27.40	0.50	0.40	0.08	3.80	0.50	0.	0.	3.20	0.40	0.	0.
R-022	3.86	0.06	16.80	0.40	0.61	0.09	4.00	0.40	0.	0.	38.60	0.60	1.61	0.10
6401-5	5.61	0.09	36.80	0.60	0.54	0.09	3.50	0.60	0.	0.	1.30	0.50	0.80	0.10
6401-5E	5.54	0.08	26.80	0.50	0.51	0.09	4.20	0.50	0.	0.	2.60	0.60	0.42	0.10
6401-6	4.98	0.06	30.10	0.50	0.39	0.06	3.00	0.30	0.	0.	0.90	0.20	0.	0.
PCNT2-4	1.51	0.03	8.35	0.18	0.24	0.06	0.80	0.20	0.35	0.01	52.70	0.50	23.80	0.70
DR-VN-1	0.39	0.02	1.79	0.08	0.	0.	0.	0.	4.58	0.05	4.96	0.15	7.30	0.20
CC102-F	0.75	0.01	1.98	0.09	0.10	0.03	0.	0.	0.	0.	14.60	0.20	4.75	0.15
PCNT2-5	6.49	0.08	29.20	0.50	0.44	0.09	3.70	0.50	0.	0.	0.	0.	0.	0.
NB-3	7.48	0.09	27.10	0.50	0.70	0.09	4.60	0.50	0.	0.	0.	0.	0.	0.
203-1	8.78	0.09	36.00	0.60	0.68	0.09	5.20	0.50	0.	0.	2.30	0.60	0.82	0.10
FC152A-3	7.19	0.08	28.60	0.50	0.55	0.10	4.20	0.50	0.	0.	0.	0.	0.	0.
6401-5B	6.01	0.09	25.90	0.50	0.45	0.08	3.80	0.50	0.	0.	0.	0.	0.27	0.10
WRH-1A1	6.48	0.08	25.90	0.50	0.46	0.08	3.90	0.40	0.	0.	0.	0.	0.	0.

ERISTA 2ND RUN 7J TOP 2ND COUNT

SAMPLE	TA	TB	CE	ED	HF	TH	SC	FE	CO	SB
BGR-1(T)	0.91	1.00	54.00	1.94	0.07	6.00	33.00	13.40	38.00	0.30
BGR-1(T)	1.08	0.14	77.00	1.08	0.05	13.60	11.93	4.92	11.92	0.16
FC-14(T)	1.07	0.08	46.10	0.54	0.03	9.00	3.15	0.80	0.31	0.04
ENT-7(T)	0.63	0.06	51.90	1.31	0.05	6.00	13.81	5.60	9.32	0.14
BGR-1(T)2	1.11	0.09	68.00	1.08	0.05	12.60	11.18	4.62	10.72	0.15
AGV-1	1.11	0.12	72.00	1.66	0.08	6.20	12.78	6.82	15.70	0.30
ARHCO-1(T)	1.32	1.24	83.00	3.98	0.13	6.30	25.72	12.40	27.60	0.30
M-03	1.18	0.14	53.00	1.91	0.09	5.40	20.50	7.70	11.60	0.30
M-05	0.45	0.07	20.30	1.10	0.44	3.40	6.64	2.34	5.70	0.20
M-07	0.26	0.05	12.80	1.20	0.33	1.40	3.96	1.46	3.60	0.50
M-09	0.	0.	0.	0.	0.	0.	0.04	0.01	0.	16.00
M-011	1.04	0.12	34.00	1.13	0.08	6.40	20.75	6.92	18.70	0.30
M-042	0.96	0.10	45.60	1.10	0.07	6.40	14.80	5.65	11.20	0.30
M-044	0.40	0.06	18.20	1.00	0.31	2.66	5.30	1.93	4.63	0.70
M-046	0.	0.	0.	0.	0.	0.	0.14	0.01	0.	9.80
M-048	0.60	0.11	24.60	0.99	0.07	2.60	20.42	7.79	22.90	0.40
16-1	1.02	0.10	40.10	1.60	0.08	6.40	13.18	0.36	0.35	0.10
16-3	0.98	0.10	53.40	1.90	1.24	6.90	20.19	0.31	0.57	0.30
16-4	1.03	0.11	29.10	1.60	0.65	6.40	31.11	0.25	0.91	0.14
16-5	1.18	0.11	27.40	1.30	0.49	7.70	13.02	0.44	1.30	0.13
16-6	1.00	0.12	31.70	1.40	0.83	8.80	14.11	0.77	0.69	0.11
9-1	1.05	0.10	55.10	1.90	0.95	7.40	10.43	1.05	1.50	0.12
9-3	0.92	0.10	40.90	1.60	1.01	6.10	12.14	0.75	1.17	0.12
9-4	0.97	0.10	29.30	1.40	0.73	5.40	12.86	0.69	1.13	0.13
9-5	0.	0.	0.	0.	0.	0.	0.36	0.01	0.	21.10
9-6	0.81	0.09	33.00	1.40	0.59	5.70	10.42	0.52	1.07	0.12
IR-1	1.42	0.13	53.20	2.00	1.77	7.60	13.99	4.19	3.86	0.16
WRH-42	0.95	0.11	43.00	1.14	0.08	4.40	17.52	6.55	18.30	0.30
R-031	0.86	0.10	28.60	1.40	0.59	6.30	11.35	2.07	3.15	0.16
CCL-7A	0.77	0.09	45.20	1.90	1.37	6.00	11.34	4.19	6.30	0.19
R-019	0.97	0.10	52.00	1.21	0.08	7.50	12.93	5.27	9.10	0.20
R-025	1.05	0.11	56.00	1.29	0.08	7.50	15.44	4.75	11.10	0.20
R-036	1.12	0.12	52.00	3.00	1.01	7.50	17.33	5.27	14.70	0.30
84-CC-1	0.97	0.10	48.00	1.23	0.07	7.10	13.81	5.42	8.50	0.20
HF17-55	0.82	0.10	49.00	1.02	0.07	6.60	16.48	5.26	12.70	0.30
HF9-20	0.74	0.10	41.00	1.13	0.07	7.00	17.75	5.83	15.50	0.30
R-037	0.55	0.07	20.20	1.10	0.44	3.70	8.68	0.79	0.65	0.10
LB-12-CZ	0.	0.	1.60	0.08	0.30	0.09	0.82	0.20	0.01	0.50
LB12CLAST	0.79	0.09	28.30	1.40	1.13	5.06	11.59	3.33	7.02	0.20

KRISTA 2ND RUN 7J BOTTOM SECOND COURT

SAMPLE	TA	TB	TU	TE	TF	SC	FE	CO	SB									
BCE-1(B)	0.91	1.00	0.13	1.94	0.07	53.90	1.40	6.00	0.20	4.70	0.20	33.00	0.09	13.40	0.06	38.00	0.30	0.
BQH-(B)	1.33	1.16	0.12	1.06	0.04	64.20	1.40	19.00	0.60	4.90	0.20	2.00	0.	4.58	0.03	11.29	0.15	0.
FC-14(B)	0.99	0.08	0.70	0.55	0.03	57.20	1.00	9.70	0.30	3.27	0.14	3.19	0.02	0.84	0.01	0.48	0.03	0.18
EW-7(B)	0.65	0.07	0.73	1.30	0.05	45.70	1.60	7.10	0.20	4.00	0.30	15.27	0.05	6.24	0.04	10.58	0.15	2.00
BQH-(B)2	1.19	0.11	0.70	1.09	0.05	72.50	1.70	11.50	0.40	4.06	0.19	11.09	0.04	4.71	0.03	11.42	0.16	0.
FC-14(B)2	0.90	0.07	0.70	0.58	0.03	41.90	0.90	9.10	0.30	3.00	0.13	3.08	0.02	0.81	0.01	0.30	0.03	0.24
ARCOX-1(B)	1.18	0.13	1.30	1.16	0.13	86.00	2.00	6.50	0.30	9.50	0.40	27.37	0.08	13.27	0.07	15.82	0.12	0.
M-01	1.22	0.14	1.21	1.93	0.10	52.30	1.90	5.90	0.40	6.80	0.40	24.33	0.09	7.87	0.06	13.50	0.30	1.10
M-04	1.30	0.13	1.35	1.50	0.08	53.50	1.80	6.50	0.30	6.40	0.30	22.55	0.08	8.30	0.06	12.60	0.30	1.40
M-06	0.09	0.03	0.13	0.04	0.03	7.10	0.50	0.98	0.12	0.75	0.10	2.41	0.03	0.66	0.02	1.96	0.11	8.30
M-08	0.	0.	0.	0.	0.	0.	0.	0.	0.	0.	0.	0.04	0.01	0.13	0.01	0.	0.	35.00
M-010	0.21	0.04	0.08	0.29	0.04	11.30	0.80	1.80	0.14	1.33	0.14	4.42	0.04	1.46	0.03	2.65	0.15	4.60
M-012	0.93	1.07	0.14	1.65	0.09	44.00	2.00	6.80	0.40	4.70	0.40	22.64	0.10	7.35	0.06	21.20	0.40	1.30
M-043	1.15	1.23	0.19	1.26	0.08	60.00	2.00	8.00	0.30	6.50	0.30	15.77	0.07	5.94	0.06	11.00	0.30	1.20
M-045	0.	0.	0.	0.	0.	0.	0.	0.	0.	0.	0.	0.06	0.01	0.06	0.01	0.	0.	14.70
M-047	1.04	1.13	1.02	1.10	0.09	40.20	1.60	7.00	0.30	6.10	0.40	17.97	0.08	4.96	0.05	11.90	0.30	4.30
M-049	0.35	0.08	0.38	0.60	0.06	14.40	1.60	1.70	0.20	1.80	0.20	12.35	0.06	4.35	0.04	12.60	0.30	3.80
R-033	1.00	0.13	0.81	1.14	0.08	38.60	1.90	4.80	0.30	4.60	0.40	22.57	0.10	8.18	0.07	22.80	0.40	0.
R-035	0.43	0.07	0.41	0.09	0.70	23.30	1.00	2.62	0.19	2.20	0.20	7.26	0.05	0.21	0.02	0.40	0.09	4.80
MF21-40	1.16	0.13	1.02	1.14	0.07	47.00	2.00	8.70	0.40	6.80	0.40	16.66	0.07	7.67	0.06	12.70	0.30	2.00
MF21-20	0.96	0.12	0.94	1.15	0.08	53.00	2.00	8.40	0.40	6.40	0.30	13.11	0.07	7.25	0.06	9.60	0.30	1.40
MF22-20	1.08	1.12	1.09	1.15	0.07	56.50	1.90	8.20	0.30	6.70	0.40	15.46	0.07	6.11	0.06	10.90	0.30	2.30
R-026	0.77	0.10	0.98	1.33	0.07	42.10	1.50	6.70	0.30	5.10	0.30	12.97	0.07	4.36	0.05	8.10	0.20	0.70
MF15-20	1.05	0.14	1.00	1.44	0.09	50.00	2.00	7.60	0.40	5.90	0.40	18.75	0.08	6.55	0.06	14.10	0.30	0.
MF24-40	1.17	0.15	1.06	1.62	0.09	42.80	2.00	4.10	0.30	4.60	0.30	21.09	0.09	8.85	0.07	30.70	0.50	4.20
R-023	0.87	0.12	1.04	1.16	0.07	50.90	2.00	6.90	0.40	5.30	0.40	18.79	0.08	6.34	0.06	14.50	0.30	0.
R-022	0.86	0.11	0.94	1.33	0.07	37.30	1.50	6.40	0.40	5.10	0.30	14.58	0.08	6.26	0.04	7.00	0.20	2.10
6401-5B	1.20	0.15	1.08	1.17	0.10	48.00	2.00	6.90	0.40	5.50	0.40	20.68	0.09	7.51	0.06	17.30	0.30	1.10
FC152A-3	1.13	0.12	1.12	1.57	0.08	51.30	1.90	6.80	0.40	6.40	0.30	17.46	0.08	7.00	0.06	12.70	0.30	0.
RB-3	1.56	0.17	1.12	1.58	0.09	53.00	2.00	7.20	0.40	6.70	0.40	19.51	0.09	7.94	0.07	17.30	0.30	0.
PORTZ-5	1.02	0.12	1.08	1.20	0.08	56.10	2.00	9.20	0.40	6.70	0.30	13.71	0.07	6.15	0.06	11.40	0.30	0.
203-1	1.17	0.13	1.56	1.78	0.09	61.00	2.00	7.60	0.40	7.40	0.40	13.95	0.07	6.56	0.06	9.80	0.20	1.20
WRB-1A1	1.28	0.15	1.08	1.66	0.09	48.20	1.90	5.00	0.30	5.70	0.30	19.86	0.09	8.27	0.07	18.70	0.30	0.
6401-5	1.17	0.12	1.06	1.14	0.07	65.00	1.80	14.00	0.50	6.40	0.30	8.23	0.05	1.87	0.03	4.27	0.17	1.70
6401-5E	1.44	0.14	1.09	1.37	0.09	58.10	1.90	9.10	0.40	7.20	0.40	19.78	0.09	4.66	0.05	22.30	0.40	0.
6401-6	1.27	0.12	0.94	0.86	0.08	49.00	1.80	9.90	0.40	7.50	0.40	22.42	0.10	0.38	0.02	0.	0.	0.
PORTZ-4	0.36	0.10	0.	0.22	0.06	17.80	1.60	2.50	0.20	2.60	0.20	4.79	0.04	12.98	0.07	4.30	0.20	44.00
DR-VN-1	0.08	0.03	0.10	0.	0.	3.50	0.50	0.44	0.09	0.38	0.08	0.91	0.02	0.36	0.01	0.55	0.08	13.80
CC10Z-F	0.	0.	0.10	0.04	0.03	5.40	0.50	0.77	0.10	0.57	0.10	1.61	0.02	0.60	0.02	1.00	0.09	9.20